HUMAN HEALTH

ENVIRONMENTAL HEALTH

SINGLE PARTICLE ICP-MS

Single Particle ICP-MS Compendium

PerkinElmer®
For the Better

INTRODUCTION

Nanomaterial-enabled products (ENPs) are entering the market at an exponential rate, spanning from health care and sports equipment to electronics, cosmetics, energy, agriculture and food products. Nanotechnology is a truly enabling technology, with enormous potential for innovation.

Advancing this market with socio-economical responsibilities requires sophisticated analytical techniques that allow reliable and reproducible characterization of nanomaterials (NMs). Characterization of nanoparticles in complex matrices, such as biological, environmental and chemical can be extremely diverse and dynamic in nature.

Faced with these challenges, Single Particle Inductively Coupled Plasma Mass Spectrometry (SP-ICP-MS) has emerged as an exciting new technique, enabling the detection and quantification of metallic nanomaterials at trace and ultra-trace levels.

Table of Contents

WHITE PAPER

Weighing the Benefits and Risks of Nanotechnology

Author:

Chady Stephan

PerkinElmer, Inc.
Waltham, MA

Nanotechnology through the Ages

There is a famous artifact at the British Museum known as The Lycurgus Cup. Fashioned from gold and silver nanoparticles mixed with glass by Roman craftsmen in the 4th century, its shifting colors of green to red reflect one of the earliest known examples of nanotechnology at work. It is far from unique. From the gold chloride nanoparticles that give the stained glass windows of Europe's medieval cathedrals their magnificent hue to the carbon nanotubes behind the razor-sharp edges of the legendary Damascus swords of the 13th century, manmade nanotechnology has played a significant role in human history for thousands of years.[1]

The Scale of Things

It was not until the 20th century that scientists could actually see inorganic nanoparticles (NPs) for the first time. Thanks to electron and atomic force microscopy, mass and infrared spectrometry, and other advanced technologies, scientists and engineers can now not only detect nanoparticles and study their interactions, they can essentially manipulate them to build entirely new nanoparticles.[2]

To fully appreciate what that means requires a clear definition and a better sense of scale. In short, nanomaterials are chemical structures with at least one dimension of 1 to 100 nanometers (one-billionth of a meter).[3] For comparison's sake, a strand of human hair is 80,000 nanometers wide and a single grain of rice measures 5 million nanometers long. If a nanoparticle was the size of a baseball, a typical red cell would be about the size of the entire stadium.

Yes, nanomaterials are infinitesimal, but do not let their size fool you. Their surface area actually increases at the nanoparticle scale to infuse these miniature building blocks with unique magnetic, mechanical, structural, optical, and electrical properties that are different from the same chemical at a larger size. Some scientists believe that these properties, known as quantum mechanical effects, hold the promise of revolutionary discoveries yet to come. Others are concerned they may unleash a flood tide of human and environmental health issues.[5]

PerkinElmer®
For the Better

The Potential for Good and Bad

Some nanotechnology wonders, and at least one possible nightmarish discovery, are already upon us. Touching all of the physical sciences, molecular engineers and scientists are able to build nanostructures from "Buckyballs" to nanotubes to leverage the quantum effects that occur when matter is organized at nanoscale.[6] Those results now play an important role in advancing technology, manufacturing, medicine, and consumer products, all without much in the way of regulatory barriers.[7] Engineered nanomaterials are currently employed in the fight against cancer and other diseases, such as Ebola.[8] They are also used in a host of industrial and consumer products, from flash memory chips and stronger materials for the automotive industry to anti-bacterial clothing, kitchenware, and toothpaste. Nanoparticles are even finding their way into the foods we eat to keep them looking and tasting fresh.[9]

While the initial benefits of nanotechnology are undeniable, there are mounting concerns over the potential dangers nanomaterials may pose to human and environmental health. Especially in an unregulated environment that one bioethicist describes as the "Wild West,"[10] some scientists worry that the media might misinterpret an aspect of nanomaterial research and trigger a public outcry against the technology in general, much like what has happened with GMO products.[11]

The Silver Nanoparticle Debate

In many respects, the proverbial "smoking gun" may well have already surfaced in the form of silver nanoparticles. A traditional remedy against infections, silver's alleged curative powers are now marketed as nanoparticle additives to a host of consumer antimicrobial products from socks that fight odors to stuffed animals for children that fend off germs.[12] At the same time, research studies show conclusively the toxicity of nanosilver on cells. The latest is a report from the Max Planck Institute in Germany. It concludes that silver nanoparticles are highly toxic once inside cells.[13] How they actually get there is provoking another heated debate. Ingesting colloidal silver as a medicinal is certainly one possibility. Absorption through the skin is another popular, if persistent, myth, along with a variety of other plausible and fanciful theories.[14]

Whatever the cause, an increasing number of scientists wonder if modern society is promoting the virtues of nanosilver without fully appreciating its potential risks to human and environmental health.[15] Still others argue that poor testing standards by nanotoxicology labs have led to misleading information. Worse still, the press has been quick to link such findings to the use of silver nanoparticles in general. For all of the wrong reasons, they argue, silver nanoparticles have become the red herrings of a potential nanotechnology scare fueled more by hearsay than hard science.[16]

The Guiding Hand of Government

The French Agency for Food, Environmental, and Occupational Health and Safety (ANSES) recently admitted as much. Despite all of "the research that has been carried out to examine the potential health and environmental effects of silver nanoparticles, … [it] is still insufficient to allow the health risks to be assessed," ANSES reported. In light of its findings, ANSES is currently recommending "that the use of silver nanoparticles (production, processing, and utilization) be limited to applications whose advantages have been clearly demonstrated, and whose benefits to human health outweigh the risks for the environment."[17]

The EU, meanwhile, enacted legislation in late 2014 requiring food manufacturers to list all nanomaterials used in ingredients of what are classified as "novel foods." The full impact of that law will not be realized until 2016, when manufacturers need to meet health and safety requirements for all of their nanomaterial additives or pull these novel foods off the market.[18]

In the U.S., the Environmental Protection Agency (EPA) also recently issued its current thoughts on silver nanoparticles. It came in the form of a 23-page response to a seven-year-old petition from a number of activist groups requesting federal regulation of nanosilver.

In brief, the EPA noted that it would now require companies using nanosilver for antimicrobial purposes to register their products as pesticides, even if there is no pesticide claim made. It mandates that all new products containing nanosilver to control microbes will be subject to a battery of tests to review their health and safety impacts before they are made available to the public. Much like the French, however, the EPA refused to take actions against all nanosilver products currently on the market, as requested by the petitioners. The reason? There is a lack of factual evidence proving that silver nanoparticles are solely used because of their antimicrobial properties, which would place them under EPA regulation as pesticides.[19]

The U.S. Food and Drug Administration (FDA), meanwhile, does not even have regulatory definitions for "nanotechnology," "nanomaterial," or "nanoscale." Until recently, the FDA says that it considered these as engineering terms.[20] That position is slowly changing.

In June 2014, the FDA updated its final guidance for the nanotechnology industry. While it took no categorical stand on the safety or danger of nanotechnology, it made clear that the FDA would be proactive in making its future decisions about nanomaterials on a case-by-case basis. For the nanotechnology industry, that means more documented research and third-party oversight are needed. According to the FDA's own guidance, manufacturers "should consider potential implications for regulatory status, safety, effectiveness, or public health impact that may arise with the application of nanotechnology in FDA-regulated products."[21]

The FDA also put manufacturers on notice that any significant product changes that introduce intentionally manipulated nano-materials would be subject to additional safety and regulatory screenings of foods intended for animal and/or human consumption.[22] As strong as these guidelines appear, the FDA echoed the EPA and ANSES in calling for more research on the physical, chemical, and biological effects of nanomaterials on both human health and the environment.[23]

Characterizing Nanoparticles

There is a growing body of evidence showing that there are significant differences between some nanomaterials and their non-nanoscale counterparts. What those differences portend raises many new questions about their potential to cause harm to human health and the environment. For decades, the bulk of nanotechnology research has been left to various business sectors with little in the way of shared scientific methodology or regulatory oversight. While that process has led to some astonishing advances in our ability to manipulate the basic building blocks of life, some scientists, environmentalists, and regulators wonder if we have overlooked the risks.[24]

Government agencies are now taking the first significant steps to develop the proper scientific methodologies needed to analyze the unique properties and effects of nanomaterials during their production, while they are in use, and what happens to them when they are recycled or discarded. According to the EPA and other agencies, those testing methods need to evaluate the chemical makeup of nanosubstances to identify and depict their composition down to the elemental level.[25]

For inorganic nanomaterials, among the most advanced analytical instruments for precise nanoparticle characterization, structure analysis, counting, and sizing is the award-winning PerkinElmer NexION® 350 ICP-MS single particle analyzer.[26] In tandem with PerkinElmer's Syngistix™ Nano Application Module software interface, this dedicated system accurately characterizes nanoparticles with a data-acquisition speed that is 10 times faster than any other SP-ICP-MS system, so nothing is missed.

As a global leader in nanomaterial analysis, PerkinElmer also offers an array of analytical instrumentation that provides rapid, clear analysis of even the most challenging organic, carbonaceous, and hybrid nanomaterials. These include among others:

- The LAMBDA™ 1050 UV/Vis/NIR spectrometer, with its wide range of accessories, is the instrument of choice for many applications from detecting carbon nanotube defects and impurities to analyzing nanoparticles in cosmetics.
- PerkinElmer's TG-IR-GC/MS evolved gas analysis system, combining a TGA or STA analyzer with an FT-IR spectrometer and a GC/MS, lets you uncover results and insights not otherwise possible through individual techniques. This hyphenated system is ideal for testing carbonaceous and hybrid nanomaterials, QA/QC applications, and polymer analysis.
- The AxION® DSA/TOF system is among the most reliable rapid screening analyzers in the industry with high mass accuracy. It can analyze nanoscale organic layers used in engineering surfaces, biosensing, nano-medicines, and smart materials with minimal sample preparation.

As new oversight methods are developed to deal with current and future generations of nanomaterials, scientists, engineers, and government regulatory agencies will continue to rely on the analytical instrumentation and expertise of PerkinElmer instruments where sound science has been making a difference in our world for over 75 years.

PerkinElmer Solutions for Nanometrology

References

1. http://www.nano.gov/timeline
2. http://pubs.acs.org/cen/coverstory/83/8348atoms.html. See also, http://www.physics.utoronto.ca/physics-at-uoft/history/the-electron-microscope/the-electron-microscope-a-personal-recollection; http://www.nano.gov/nanotech-101/special
3. http://www.epa.gov/oppt/nano/nano-fact-sheet.html#Q1
4. http://htwins.net/scale2/. See also, http://grist.org/food/nanoparticles-in-your-food-youre-already-eating-them/
5. http://www.rsc.org/chemistryworld/2015/04/nanoparticle-toxicology. See also, http://grist.org/food/nanoparticles-in-your-food-youre-already-eating-them; and http://www.understandingnano.com/introduction.html
6. http://www.azom.com/article.aspx?ArticleID=3499. See also, http://scifun.chem.wisc.edu/chemweek/buckball/buckball.html
7. http://www.fda.gov/RegulatoryInformation/Guidances/ucm257698.htm#intro
8. http://www.cnn.com/2015/03/25/tech/webster-nanoparticles-cancer-mci/index.html
9. http://grist.org/food/nanoparticles-in-your-food-youre-already-eating-them/. See also, http://www.nanotechproject.org/cpi/browse/categories/
10. http://nano.cancer.gov/learn/now/safety.asp. See also, http://www.thefactsabout.co.uk/information-on-nanomaterials-and-cosmetic-products./content/1/h. See also, http://www.bioethics.net/2009/04/the-wild-west-of-nanotechnology/; http://www.alzheimersweekly.com/2014/03/nanosilver-warning.html
11. http://grist.org/food/nanoparticles-in-your-food-youre-already-eating-them/
12. http://well.blogs.nytimes.com/2014/05/23/silver-too-small-to-see-but-everywhere-you-look/?_r=0
13. http://www.jnanobiotechnology.com/content/12/1/59
14. http://www.rsc.org/chemistryworld/2015/04/nanoparticle-toxicology
15. http://articles.chicagotribune.com/2014-02-16/health/ct-nanosilver-met-20140216_1_consumer-products-other-antibiotic-drugs-germs
16. http://www.rsc.org/chemistryworld/2015/04/nanoparticle-toxicology
17. http://nanotech.lawbc.com/2015/03/articles/international/eu-member-state/french-agency-publishes-opinion-on-silver-nanoparticles/
18. http://europa.eu/rapid/press-release_IP-14-2560_en.htm
19. http://www.lexology.com/library/detail.aspx?g=be827f22-52af-4aea-a3b6-b3c15164dfd3
20. http://www.fda.gov/RegulatoryInformation/Guidances/ucm257698.htm#intro
21. http://www.fda.gov/NewsEvents/Newsroom/PressAnnouncements/ucm402499.htm
22. http://www.fda.gov/Food/GuidanceRegulation/GuidanceDocumentsRegulatoryInformation/IngredientsAdditivesGRASPackaging/ucm300661.htm#IIIE
23. Ibid
24. http://www.pewtrusts.org/en/research-and-analysis/reports/2009/04/28/oversight-of-next-generation-nanotechnology
25. http://www.epa.gov/oppt/nano/nano-fact-sheet.html#Q1
26. http://www.selectscience.net/products/nexion-350-icp-ms-spectrometers/?prodID=85431

PerkinElmer, Inc.
940 Winter Street
Waltham, MA 02451 USA
P: (800) 762-4000 or
(+1) 203-925-4602
www.perkinelmer.com

PerkinElmer®

For a complete listing of our global offices, visit www.perkinelmer.com/ContactUs

012252_01 PKI

WHITE PAPER

Single Particle Inductively Coupled Plasma Mass Spectrometry: Understanding How and Why

Authors

Chady Stephan

Ken Neubauer

PerkinElmer, Inc.
Shelton, CT

Introduction

Nanotechnology is an emerging and rapidly growing field whose dynamics and prospects pose many great challenges to scientists and engineers. Nanoparticles are being used in many materials and products, including coatings (on plastic, glass and clothing), sunscreen, antimicrobial bandages and clothing, MRI contrast agents, biomedical elemental tags and fuel additives, only to name few. However, rapid, simultaneous characterization of their elemental composition, number of particles, size, and size distribution is challenging. For inorganic nanoparticles, the technique best suited to provide the above-mentioned characteristics is inductively coupled plasma mass spectrometry (ICP-MS) operated in so-called single particle mode. Analyzing single nanoparticles with ICP-MS requires a different approach than measuring dissolved elements. This work describes the theory behind single-particle ICP-MS measurements, drawing comparisons and differences with analyzing dissolved elements.

Understanding Single Particle ICP-MS Analysis

Effectively detecting and measuring single, individual nanoparticles with ICP-MS requires operating the instrumentation in a different manner than when analyzing dissolved samples. Figure 1 shows traces from both dissolved and single nanoparticle analyses. In Figure 1a, a steady state signal results from measuring dissolved elements; the output when detecting single particles is quite different, as illustrated for 60 nm silver particles in Figure 1b. Each spike in Figure 1b represents a particle. The differences in the way these data are acquired are the key to understanding single particle analysis. The easiest way to gain this understanding is to review and compare the processes involved when both dissolved elements and particles are measured.

Dissolved Analyses with ICP-MS

When dissolved elements are measured, aerosols enter the plasma, where the droplets are desolvated and ionized. The resulting ions enter the quadrupole to be sorted by their mass-to-charge ratios (m/z). The quadrupole spends a certain amount of time at each m/z before moving to the next m/z; the time spent analyzing each m/z is called "dwell time". After each dwell time measurement, a certain amount of time is spent for the electronics to stabilize before the next measurement is performed. This stabilization time is called "settling time", i.e. overhead and processing time. When analyzing dissolved elements, the resulting signal is essentially a steady-state signal, as shown in Figure 2a. However, considering the dwell and settling times, a significant amount of the signal is not measured due to the settling time of the electronics, a critical aspect when analyzing nanoparticles (Figure 2b).

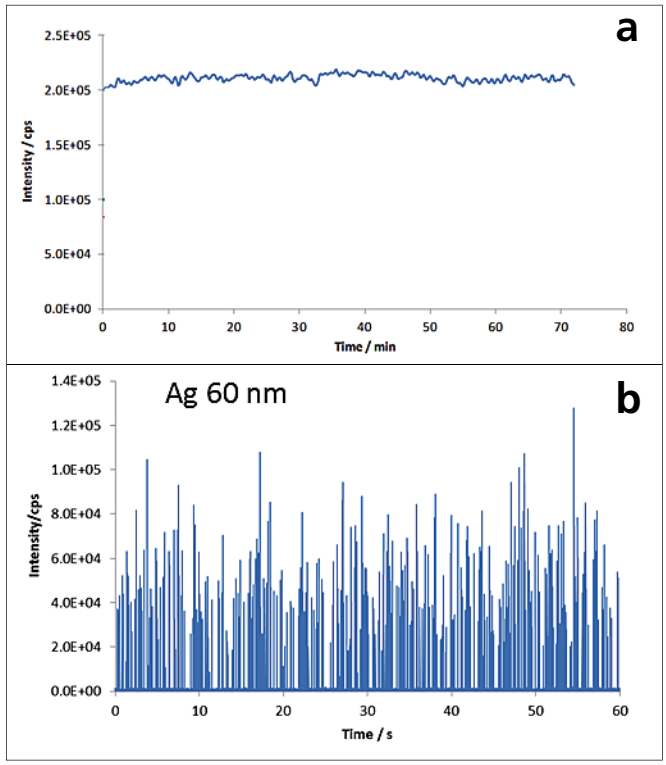

Figure 1. a) A continuous signal from measuring a dissolved analyte; b) A signal from measuring 60 nm silver nanoparticles.

PerkinElmer®
For the Better

For dissolved ions, the part of the signal which is missed is not critical since the elements are dissolved and produce a continuous signal.

Single Particle Analyses with ICP-MS

Particles present in an aqueous solution are introduced to the plasma the same way as dissolved solutions. As the droplets are desolvated in the plasma, the resulting particles are ionized producing a burst of ions (one ion cloud per particle). The ions then pass into the quadrupole. However, using conventional ICP-MS data collection, alternating between dwell time and settling time, ion clouds are not always detected. If, for example, the ion cloud happens to fall within the dwell time window, it will be detected. Otherwise, if it passes into the quadrupole or reaches the detector during the settling time, it will not be detected, leading to an inaccurate counting efficiency. Figure 3a shows that an ion cloud from a single particle (the "Signal" peak) can be missed if it falls outside of the dwell time window. When the ion cloud from a single particle falls within the dwell time window, it is detected, as represented in Figure 3b. When multiple particles are detected in rapid succession, the resulting signal is a series of peaks, each one originating from a particle, as shown in Figure 3c.

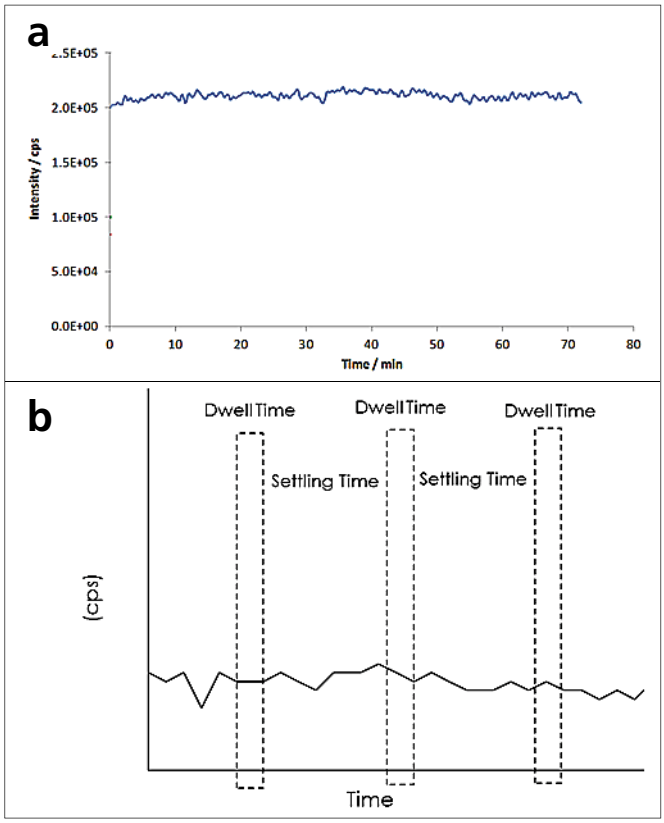

Figure 2. a) A continuous signal from measuring a dissolved element; b) A continuous signal, with the dwell and settling times overlaid – data is only collected during the dwell time.

The Timing Parameters of Single Particle ICP-MS

Figure 4 is a representation of the timing parameters involved in ICP-MS analysis. The three axes represent signal intensity, mass (m/z), and time. With conventional/dissolved analyses, the mass and intensity axes are the most important: resulting spectra are plots of m/z vs. intensity. The time axis is important when considering how fast the quadrupole can move from mass-to-mass – this parameter is called "quadrupole scan speed". The quadrupole scan speed is important when measuring multiple elements in a transient signal, such as for laser ablation and multielement speciation analyses.

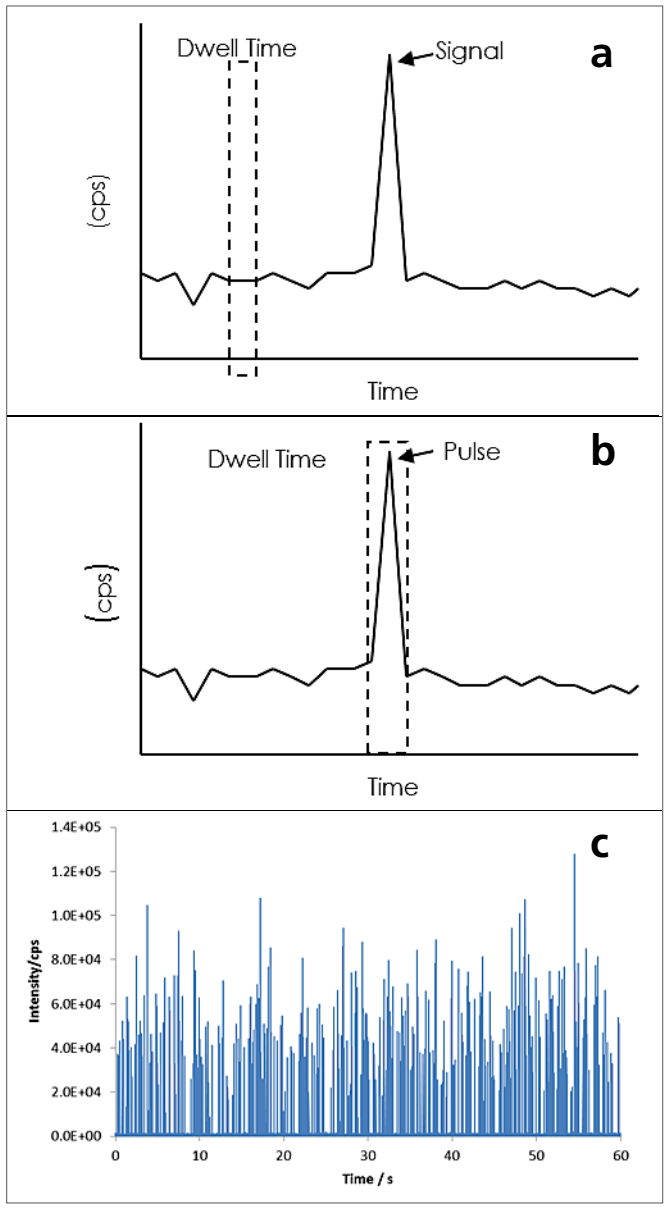

Figure 3. a) Signal from a single nanoparticle falling outside of the dwell time/measurement window, and, therefore, not detected; b) Signal from a single nanoparticle falling within the dwell time/measurement window, and, therefore, detected; c) Signals from multiple nanoparticles falling within dwell time/measurement windows and detected.

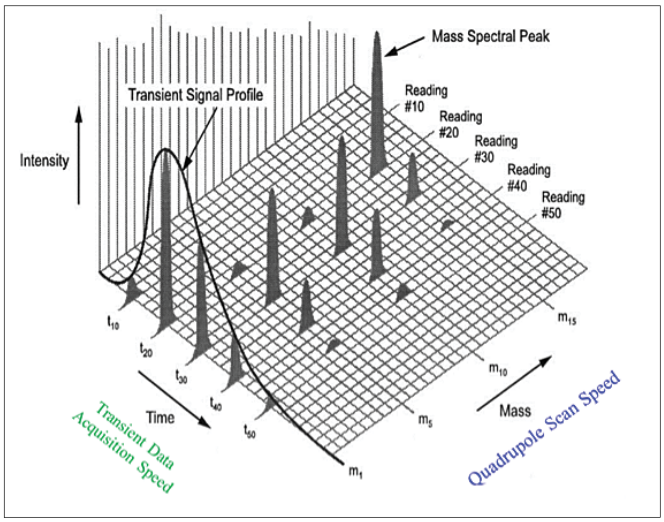

Figure 4. The timing parameters of ICP-MS analyses.

When measuring transient signals for a single m/z, the time axis becomes important, since enough data points must be acquired to define the peak. For example, with HPLC/ICP-MS, usually 4-10 points/second are enough to define a peak. Comparing HPLC peaks to single particle signals, the ion packets from each particle are typically 1000 times narrower than peaks produced by HPLC. Therefore, data must be acquired significantly faster for single particle analysis. Since only a single mass is being measured for single particle analysis, the quadrupole scan speed is not important, and the time axis becomes the "transient data acquisition speed", which encompasses both the dwell and settling times. The faster the transient data acquisition speed, the better suited the system is for single particle analysis.

In single particle ICP-MS, transient data acquisition speed consists of two parameters: dwell time (reading time) and settling time (overhead and processing time). It is very important that the ICP-MS is able to acquire signals at a dwell time that is shorter than the particle transient time, thus avoiding false signals generated from partial particle integration, particle coincidence and agglomerates/aggregates. The shorter the settling time, the less chance there is of missing a particle. Figure 5 demonstrates the importance of settling time using a constant 100 µs dwell time and a constant time window. In Figure 5a, there are only two 100 µs windows to detect particles; the rest of the time is overhead, where data cannot be acquired. In this case, there are only about 100 measurements made in one second. Therefore, most of the time is wasted. Figure 5b is the same time scale, but with a settling time of 100 µs. Therefore, more time is spent measuring and looking for nanoparticles – about 5000 measurements in one second. However, still half of the time is wasted. Figure 5c represents the ideal situation with no settling time. This allows for 10,000 measurements per second, with no wasted time: all the time is spent looking for particles, the ideal situation for single particle ICP-MS.

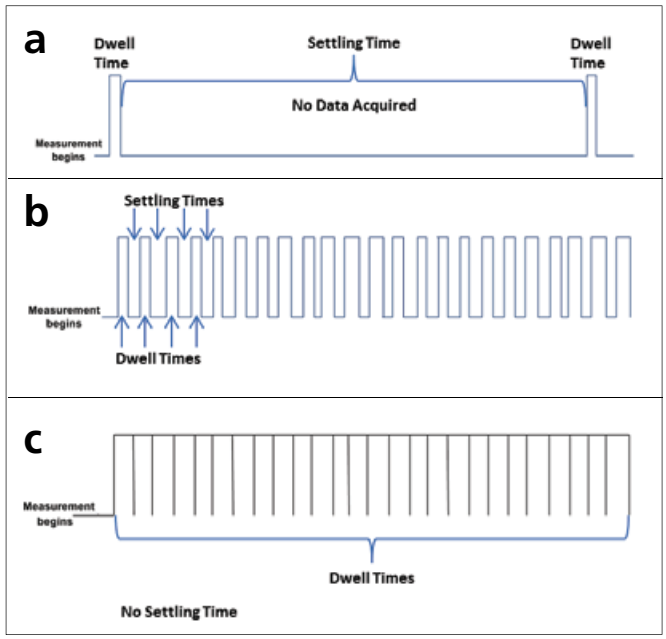

Figure 5. Effect of settling time and dwell time on ICP-MS measurements: a) Settling time is much longer than the dwell time; b) Settling time is equal to the dwell time; c) Settling time is eliminated.

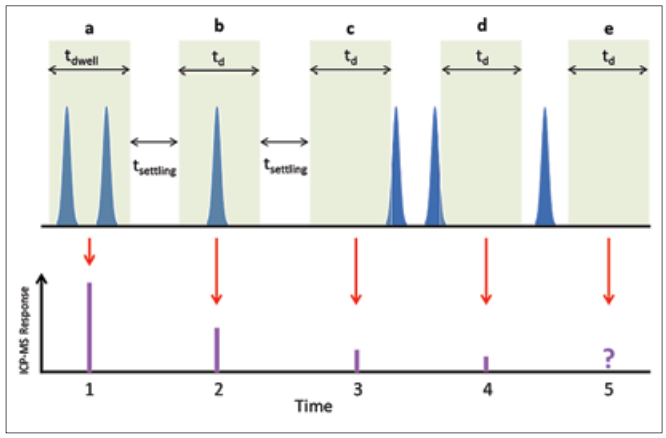

Figure 6. Effect of dwell and settling times on single nanoparticle measurements: a) Two particles detected; b) One particle detected; c) The leading edge of one particle detected; d) The trailing edge of one particle detected; e) No particles detected.

Multiple Measurements per Particle: The Ideal Situation

To understand the importance of fast sampling time for single particle measurements, consider the representation in Figure 6. In this figure, the upper portion represents pulses from single particles as they relate to dwell and settling times, while the lower portion shows the corresponding mass spectrometer response (intensity vs. time). In Figure 6a, two particles are detected in a single dwell time window, leading to a response twice as large as if one particle were detected, not a desirable situation and easily encountered if the instrument dwell time is longer than the nanoparticle transient pulse. In Figure 6b,

a single particle is detected in the dwell time window – the ideal situation, if fast continuous data acquisition was not available. The resulting signal is half the size of Figure 6a. Figures 6c and 6d represent undesirable situations where only a part of the ion pulse from particles is detected, leading to small signals, thus inaccurate particle sizing. Figure 6e represents the most undesirable situation, where the particle falls outside of the dwell time window and is not detected. These examples demonstrate the importance of having fast continuous data acquisition ability, where data is collected continuously without any settling time, ensuring accurate particle counting - every particle entering the plasma will be counted.

Another benefit of fast continuous data acquisition is that multiple points can be measured from a single particle, thus eliminating the chances that particles are missed or that only partial ion clouds from particles are detected. Figure 7 shows how this can be accomplished. In Figure 7a, the signal from a single particle is measured multiple times. The signal from each time slice is plotted, which defines the peak. When multiple particles are detected, the resulting peaks are a series of time slices, as shown in Figure 7b.

Figures 8a and 8b show how typical single particle responses can be converted into peaks which define a single particle. In Figure 8a, data was collected in fast continuous mode (no settling time)

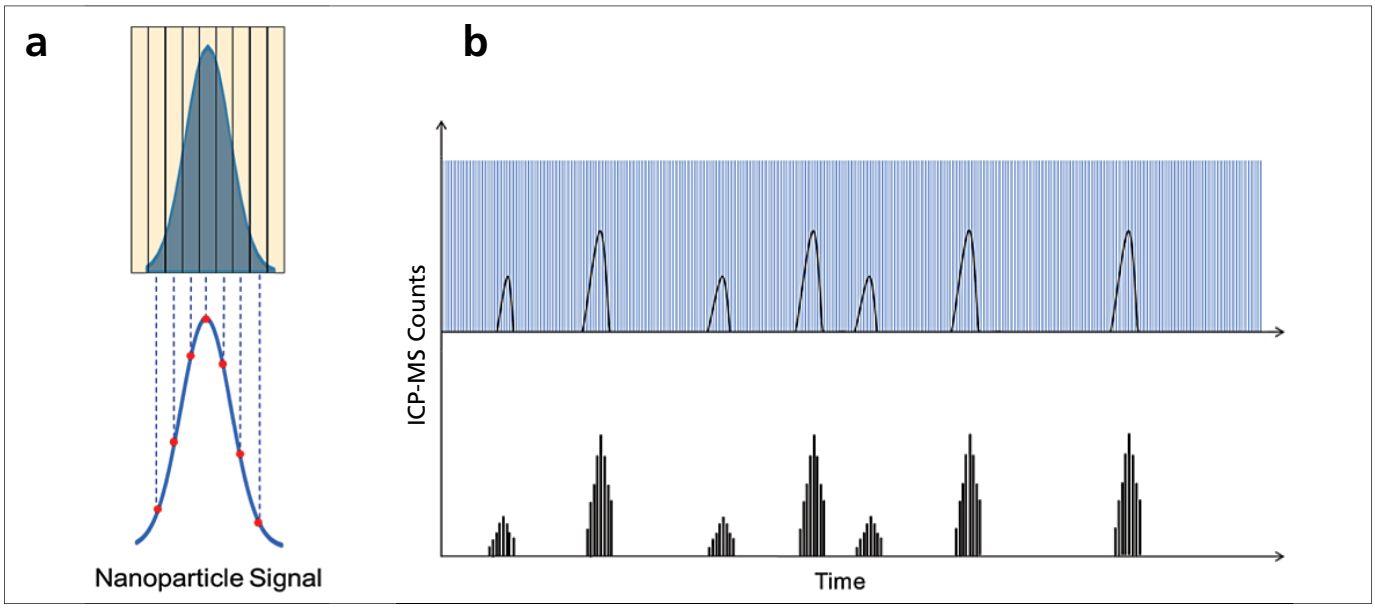

Figure 7. Effect of measuring multiple measurements per particle: a) For a single particle and b) For multiple particles detected in series.

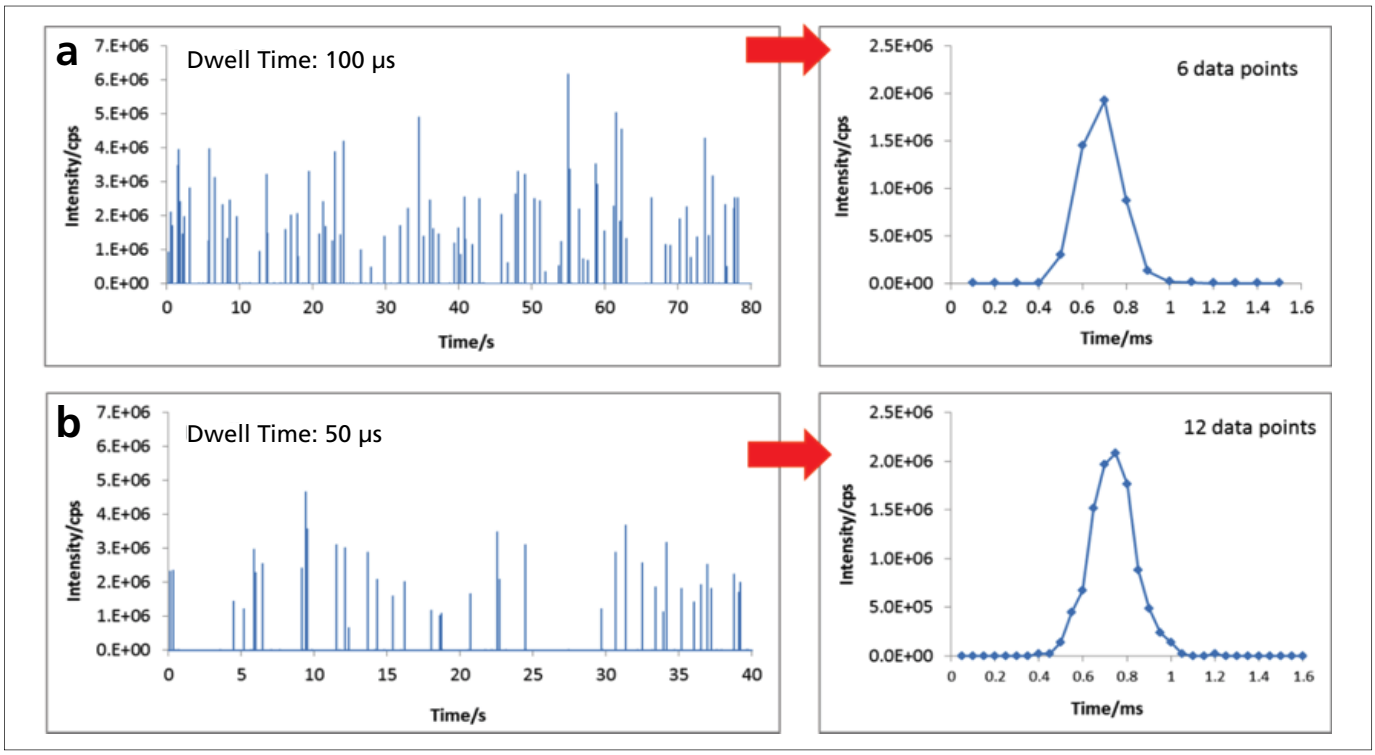

Figure 8. Ability to acquire multiple measurements per particle: a) 6 data points per particle; b) 12 data points per particle.

with a dwell time of 100 µs. When the intensities from the first 1.6 seconds are plotted, it is seen that 6 points define a peak. In Figure 8b, the dwell time was reduced to 50 µs, which leads to twice as many data points being acquired. As a result, the peak shape is defined by 12 points, leading to a different peak shape. These examples demonstrate the benefit of sampling multiple data points per particle.

Summary

As has been shown, measuring single particles with ICP-MS is quite different than measuring dissolved species. The most important factor when measuring single particles is the speed at which data can be acquired: since particle ionization events are on the order of microseconds, rapid data acquisition and elimination of the settling time between measurements are crucial. Continuous measurement allows multiple readings per particle ionization event, which results in more accurate size determinations. For single particle ICP-MS analysis, continuous data acquisition at a dwell time smaller than or equal to 100 µs is the most important instrumental requirement for precise nanoparticle counting and sizing.

PerkinElmer, Inc.
940 Winter Street
Waltham, MA 02451 USA
P: (800) 762-4000 or
(+1) 203-925-4602
www.perkinelmer.com

011649_01

APPLICATION NOTE

ICP - Mass Spectrometry

Authors:

Yongbo Dan
Honglan Shi
Xinhua Liang

Missouri University of
Science & Technology

Chady Stephan

PerkinElmer, Inc.
Shelton, CT

Measurement of Titanium Dioxide Nanoparticles in Sunscreen using Single Particle ICP-MS

Introduction

Titanium dioxide (TiO_2) nanoparticles are commonly used in sunscreens as part of the formulation to block the sun's harmful UV rays. As the use of nanoparticles in consumer products has increased, concern has risen as to the health and environmental effects of nanoparticles. Since sunscreens contact skin and wash off in water, the TiO_2 nanoparticles can find their way into biological and environmental systems. As a result, there is a need to measure both the size and size distribution of these nanoparticles in sunscreens so as to assess their impact on human health and the environment.

PerkinElmer®
For the Better

Traditionally, nanoparticle size characteristics have been determined by several methods, including field flow fractionation (FFF), dynamic light scattering, and microscopy, among others. Recently, single particle inductively coupled plasma mass spectrometry (SP-ICP-MS) has been gaining attention as a way to both measure and characterize nanoparticles. Advantages of SP-ICP-MS include speed and the amount of information which can be gained from the analysis.

This work will focus on characterizing TiO_2 nanoparticles in sunscreens using SP-ICP-MS with a simple sample preparation.

Experimental

Sample Preparation

Sunscreen products were purchased at a local store and had the label information shown in Table 1. For each sample, 15 mL of sunscreen was added to a 50 mL container and mixed for three minutes to create a homogeneous sample. Next, 0.2 g of each homogenized sample was transferred to another container, followed by addition of 200 mL 1% Triton-X solution. These solutions were sonicated until all aggregates appeared to be broken up (5-10 minutes). After sonication, serial dilutions were performed on the samples with deionized water to produce particle concentrations of 100,000 – 200,000 particles/mL (as measured during analysis).

Transport efficiency determination was performed with gold nanoparticles (50, 80, 100 nm, nanoComposix, San Diego, California, U.S.A.) which were prepared by dilution in deionized water to a final nominal concentration of 100,000 particles/mL. All standards were sonicated for five minutes prior to analysis to ensure that any agglomerated particles were dispersed. Forty nanometer TiO_2 (US Research Nanomaterials Houston, Texas, U.S.A.) spikes were added to various samples to verify the accuracy of the TiO_2 size measurements.

Calibration standards for titanium consisted of 2, 5, and 10 ppb standards prepared in deionized water from a 1000 mg/L titanium standard (PerkinElmer, Shelton, Connecticut, U.S.A.).

Table 1. Label Information for Sunscreen Products.

Sunscreen	SPF	TiO_2 Content (%)
1	60+	4.9
2	50	6
3	45	0
4	50	6
5	45+	5.1

Instrument Conditions

All analyses were performed on a PerkinElmer NexION® 350D ICP-MS using the Syngistix™ Nano Application Software Module. Tables 2 and 3 show the instrumental and method parameters, respectively. When using the Syngistix Nano Application Module, the quadrupole settling time is automatically eliminated, thus ensuring that no particles are missed. The combination of elimination of quadrupole settling time and short dwell time results in the collection of multiple data points for each particle.

Table 2. NexION 350D ICP-MS Instrument Parameters.

Parameter	Value
Nebulizer	Glass concentric
Spray chamber	Glass cyclonic
Sample uptake rate	0.26-0.28 mL/min
RF power	1600W
Analysis mode	Standard
Quadrupole settling time	0 µs

Table 3. Method Parameters.

Parameter	Value
Analyte	Ti48
Dwell time	100 µs
Data acquisition time	100 sec
Density	4.23 g/cm^3
Ti mass fraction	60%

Results and Discussion

To characterize the Ti background of the system and reagents, a blank solution consisting of only the reagents (i.e. Triton X-100 in deionized water) was analyzed, with the resulting signal shown in Figure 1. While a few signal spikes are seen, the majority of the Ti background is below two counts, which demonstrates the cleanliness of the system.

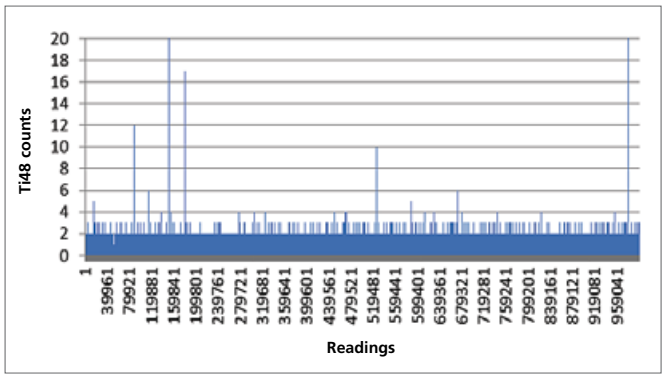

Figure 1. Ti background signal for blank.

To determine the ability to see TiO_2 particles in a sunscreen matrix, the sunscreen without any TiO_2 particles was analyzed. Figure 2A shows the TiO_2 particle signal from a sunscreen which does not contain TiO_2 (according to its label). Aside from a few spikes, the background is equivalent to the blank (Figure 1).

Next, this sunscreen solution was spiked with 40 nm TiO_2 particles at a concentration of 6.65 µg/L; the resulting signal is shown in Figure 2B. Since each spike represents a particle, it is evident that TiO_2 particles can easily be seen in a sunscreen matrix.

Furthermore, the most frequent size particle was 37.7 µm, demonstrating the accuracy of the measurement.

Figure 3 shows the TiO_2 particle size distribution for a 20,000 times-diluted sunscreen (Sunscreen 5).

With the ability to accurately measure TiO_2 particles in sunscreen established, other sunscreen samples were analyzed three times; the results are shown in Table 4.

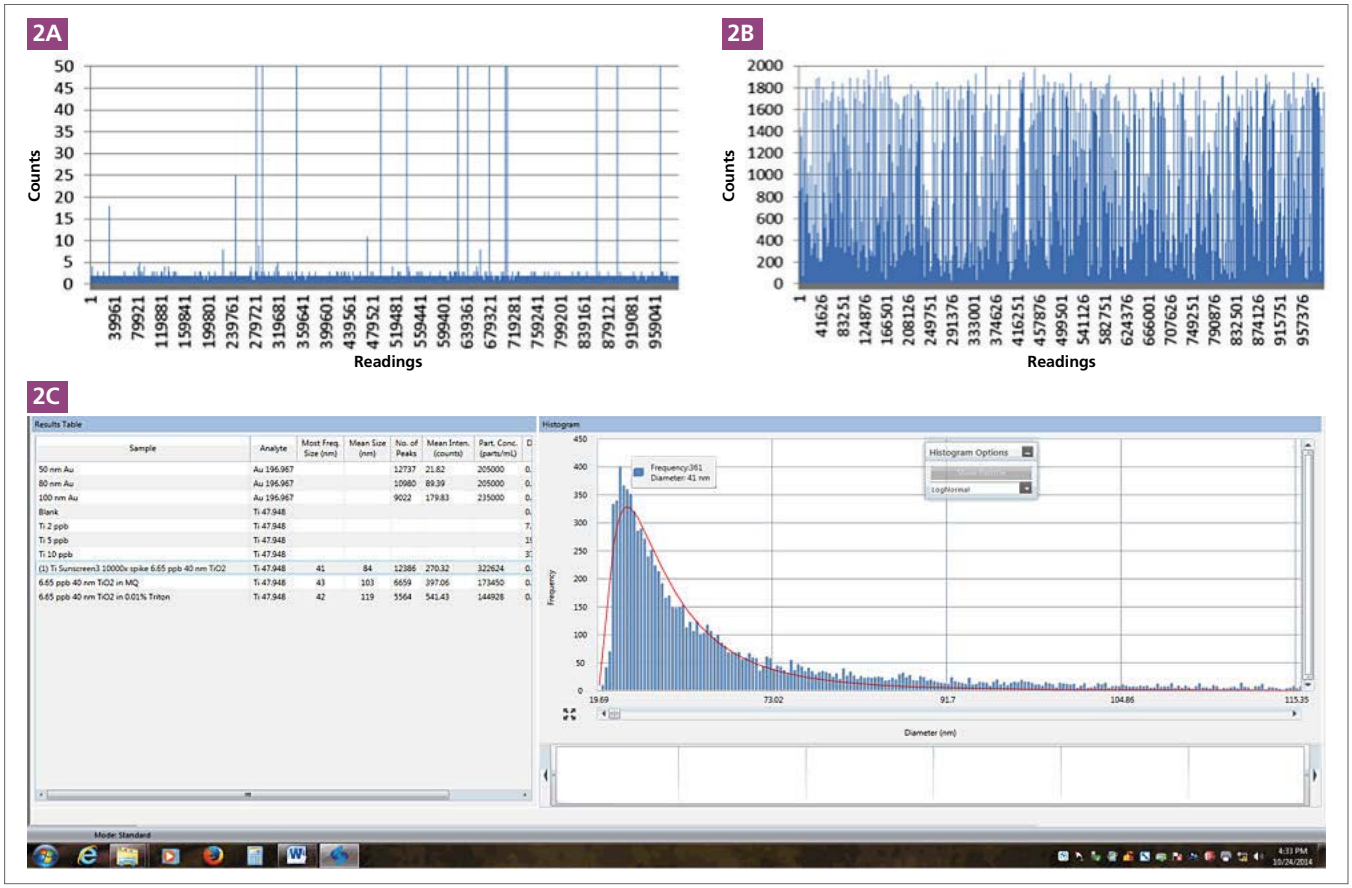

Figure 2. TiO_2 signals from a sunscreen which does not contain TiO_2 (2A), and spiked with 40 nm TiO_2 (2B) particles. The screen shot shows the processed data of spiking 40 nm TiO_2 into a sunscreen which does not contain any TiO_2 nanoparticles (2C).

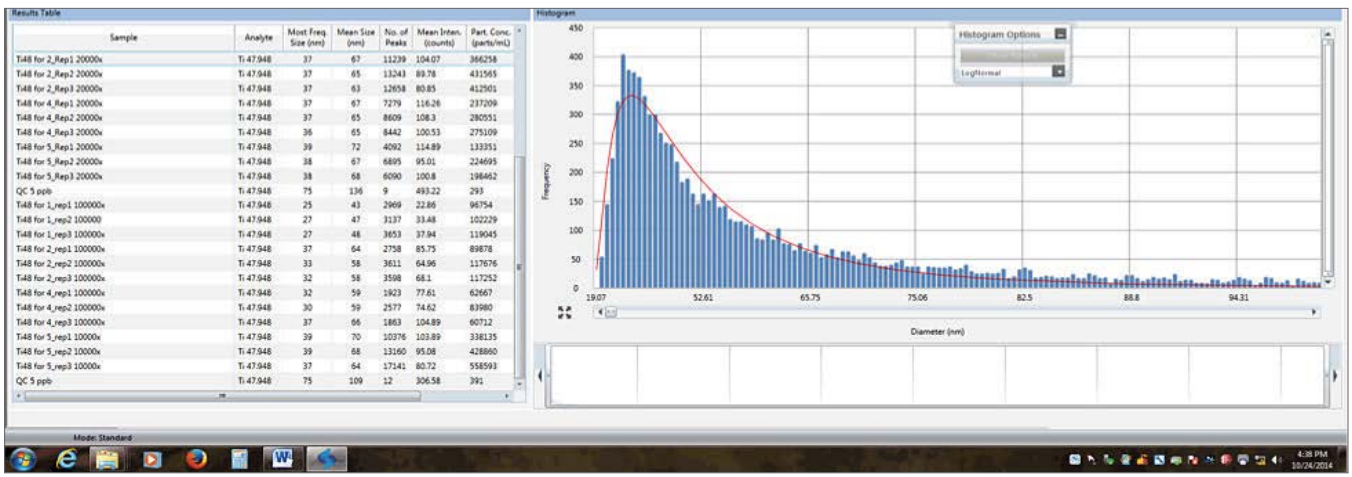

Figure 3. Processed data for 20,000 times-diluted sunscreen which contains TiO_2 nanoparticles.

Table 4. TiO_2 Nanoparticle Analysis in Commercial Sunscreens.

Sunscreen	Dilution Factor	Most Frequent Size (nm)	Particle Size Distribution (nm)	Particle Concentration (particles/mL)
1	100,000	32	24 – 58	102,229
2	100,000	34	24 – 64	117,252
3*	100,000	-	-	-
4	100,000	33	24 – 61	63,000
5	20,000	42	28 – 67	198,462

*This sunscreen contains no nanoparticles, as shown in Table 1.

These results indicate that the sunscreens had TiO_2 nanoparticles ranging from 24 – 67 nm, with similar size distributions in each. However, Sunscreen 5 is clearly different from the others: the smaller dilution factor required to obtain less than 200,000 particles/mL indicates that fewer TiO_2 particles are present in this sample than the others.

Conclusion

This work has demonstrated the ability to measure TiO_2 nanoparticles in commercial sunscreen samples. Using both the NexION 350 ICP-MS and the Syngistix Nano Application Software Module, the analysis is simple and rapid, yet can clearly differentiate the TiO_2 content among different samples.

Consumables Used

Component	Description	Part Number
Titanium standard	1000 ppm, 125 mL	N9303806
Sample uptake tubing	0.38 mm id (green/orange), flared, 2-stop	N0777042
Drain tubing	1.30 mm id (gray/gray), Santoprene, 2-stop	N0777444

PerkinElmer, Inc.
940 Winter Street
Waltham, MA 02451 USA
P: (800) 762-4000 or
(+1) 203-925-4602
www.perkinelmer.com

PerkinElmer®

011990_01 PKI

APPLICATION NOTE

ICP - Mass Spectrometry

Author:

Chady Stephan

PerkinElmer, Inc.
Shelton, CT

Analysis of Iron Nanoparticles in Organic Solvents Used in the Semiconductor Industry Using Single Particle ICP-MS in Reaction Mode

Introduction

Metallic contamination in semiconductor products adversely affects device performance. As line widths on chips decrease, the allowable levels of metal contamination also decrease. The most commonly occurring forms of metal contamination are either transition metals or alkaline elements. Transition metals tend to diffuse through the semiconductor material and aggregate on the surface in various oxide forms. Among the transition metals, iron (Fe) is, by far, the most common contaminant.

Single particle ICP-MS (SP-ICP-MS) has proven to be a popular technique for the analysis of nanoparticles due to its ability to detect, count, and size individual particles at very low particle concentrations down to limits between 100 and 1000 particles/mL, depending on the introduction system being used. Along with the particulate information, SP-ICP-MS will provide the user with the dissolved concentration without prior separation[1]. Many available publications have demonstrated the ability of SP-ICP-MS to measure and characterize nanoparticles in a wide variety of matrices[2-5], including chemical mechanical planarization slurries[6].

PerkinElmer®
For the Better

Iron ($^{56}Fe^+$) is known to exhibit plasma-based interferences, more specifically $^{40}Ar^{16}O^+$. Dynamic Reaction Cell™ (DRC) technology, along with the use of ammonia as a reactive gas, is the most efficient way to remove the ArO^+ interference on the most abundant isotope of Fe ($^{56}Fe^+$), which is required to achieve the lowest Fe-nanoparticle size detection limits[7].

This work will demonstrate the ability to measure and characterize Fe nanoparticles and iron oxides in semiconductor solvents using SP-ICP-MS in Reaction mode.

Experimental

Reagents and Sample Preparation

Iron oxide (Fe_2O_3) – PVP capped nanoparticles of 20 nm ± 5 nm were purchased from nanoComposix™ (San Diego, California, USA) and used as a quality control (QC) sample. Transport efficiency was determined using 60 nm gold (Au) nanoparticles prepared in each analyzed solvent at a concentration of 50,000 particles/mL (Note: transport efficiency is independent of particle size). Dissolved Fe standards (100, 200, and 300 ppt) were prepared in 1% nitric acid and a certain % of isopropyl alcohol (IPA). Nitric acid was necessary to keep iron from precipitating, while IPA was added to compensate for the difference in both the ionization potential and transport efficiency between the aqueous standards and the solvents (i.e. samples) being analyzed. The level of added IPA was assessed based on the sample matrices being analyzed. All nanoparticle solutions were sonicated for 10 minutes prior to analysis.

Samples included tetramethylammonium hydroxide (TMAH) and mixture of 90% cyclohexane / 10% propylene glycol monomethyl ether (PGME).

Instrumental Conditions

All analyses were performed on a PerkinElmer NexION® 350S ICP-MS using the Syngistix™ Nano Application Software Module (Version 1.1). Instrumental conditions are shown in Table 1. The sample introduction conditions varied slightly depending on which solvent was analyzed, with oxygen added after the spray chamber to prevent carbon deposition on the cones. All other components and parameters remained constant.

Table 1. NexION 350S ICP-MS Instrumental Parameters.

Parameter	Value
Nebulizer	PFA, self-aspirating
Sample Uptake Rate	0.112 mL/min (TMAH) 0.515 mL/min (cyclohexane, PGME)
Spray Chamber	PC3
Spray Chamber Temperature	+2 °C
Oxygen Flow	0.05 L/min
Injector	0.85 mm ID, quartz
RF Power	1600W
Analyte	Fe at m/z 56
Reaction Gas	NH_3
RPq	0.65 (TMAH, cyclohexane, PGME)
Dwell Time	50 µs
Analysis Time	60 s

Results and Discussion

Before organic solvents were analyzed, the performance of the instrument for Fe nanoparticles in aqueous solutions was evaluated. Since the interference on $^{56}Fe^+$ (ArO^+) is present whether aqueous or organic solvents are analyzed, the optimum NH_3 flow was established by running 20 nm Fe_2O_3 nanoparticles at various NH_3 flows. The resulting mean intensity counts from the nanoparticles and the dissolved intensity counts were recorded, and the signal-to-background (S/B) ratios calculated. Figure 1 shows a plot of the ammonia optimization, indicating an optimal ammonia flow of 0.5-0.6 mL/min (S/B = 260), demonstrating the effectiveness of ammonia in removing the ArO^+ interference while retaining Fe^+ sensitivity. All analyses were done with an NH_3 flow of 0.55 mL/min.

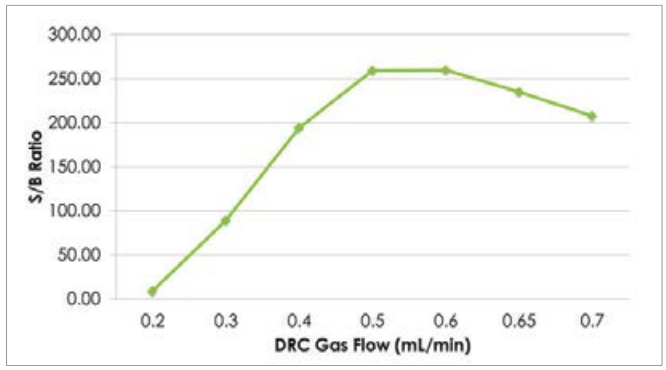

Figure 1. Ammonia flow optimization for 20 nm Fe_2O_3 nanoparticles in water.

With the optimum ammonia flow established, the feasibility of analyzing Fe nanoparticles was determined by analyzing 20 nm Fe_2O_3 nanoparticles in water. Figure 2 shows the particle size distributions at a concentration of 50,000 particles/mL. As shown in Table 2, the average measured sizes (20 nm) agree with the certificate values (20 ± 5 nm), validating that Fe-containing nanoparticles can be accurately measured using SP-ICP-MS in Reaction mode using ammonia as a reactive gas. In addition, the precision of the measurements is less than 3%.

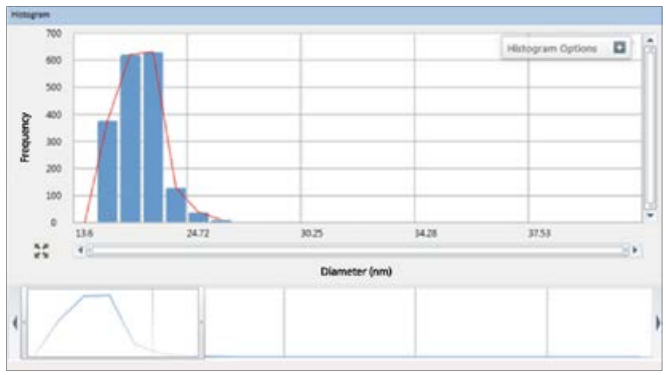

Figure 2. Size distribution of 20 nm Fe_2O_3 prepared in water.

Table 2. Accuracy and Precision of 20 nm Fe_2O_3 Nanoparticle Analysis at m/z 56.

Replicate	Most Frequent Size (nm)	Mean Size (nm)	Particle Conc. (part/mL)
20 nm Fe_2O_3 - 1	19.6	20.2	50801
20 nm Fe_2O_3 - 2	20.6	20.3	51075
20 nm Fe_2O_3 - 3	19.6	20.1	50862
20 nm Fe_2O_3 - 4	20.1	20.7	50926
Average	*20.0*	*20.3*	*50916*
Std. Dev.	*0.47*	*0.28*	*117*
RSD	*2.35%*	*1.36%*	*0.23%*

To determine size detection limits for Fe nanoparticles, deionized water blanks were analyzed which did not contain any Fe nanoparticles. The resulting background noise corresponds to 13 nm particles. Table 3 shows the detection limits from three analyses, along with the counts of dissolved Fe determined in the same analysis. The low intensity for dissolved iron demonstrates that ArO^+ is eliminated in Reaction mode and that there is very little Fe contamination in the sample. The reproducibility of the results indicates that these are real detection limits and not the result of random signals.

Table 3. Size Detection Limits for Iron Nanoparticles in Water.

Replicate	Most Frequent Size (nm)	Mean Size (nm)	Dissolved Intensity (counts)
1	13.7	13.7	0.14
2	13.0	13.4	0.14
3	12.9	12.9	0.14
Average	*13.2*	*13.3*	*0.14*
Std. Dev.	*0.44*	*0.40*	*< 0.01*
RSD	*3.30%*	*3.03%*	*< 0.01*

With feasibility established, the methodology was applied to the solvents for Fe-containing nanoparticles. To determine the background, a mixture of deionized water and 10% PGME was analyzed. The resulting real-time scan appears in Figure 3, which shows no Fe-containing nanoparticles being detected.

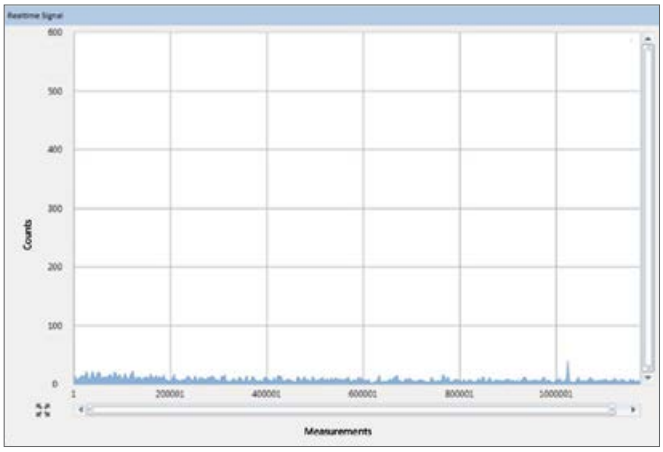

Figure 3. Real-time display from the analysis of 10% PGME in deionized water showing that no Fe-containing nanoparticles are detected.

The cyclohexane (90% cyclohexane + 10% PGME) mixture was then analyzed, and the real-time display showed numerous Fe-containing nanoparticles, as seen as spikes in Figure 4. These nanoparticles must originate from the cyclohexane as the 10% mixture of PGME did not show any nanoparticles (Figure 3). This result proves that Fe-containing nanoparticles can be detected in organic solvents.

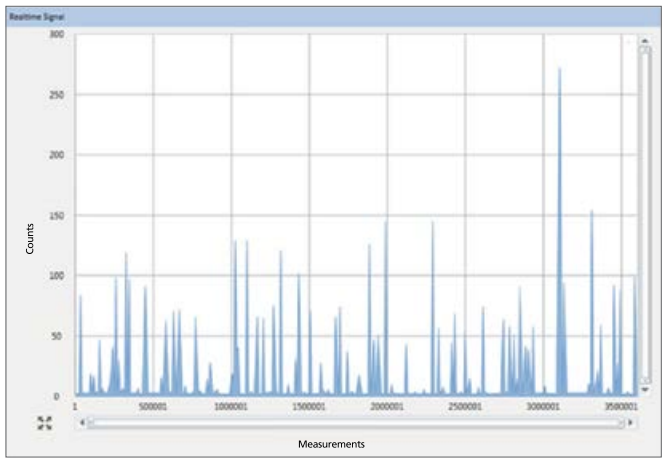

Figure 4. Real-time display from the analysis of 90% cyclohexane + 10% PGME showing Fe-containing nanoparticles.

The corresponding particle size and concentration results from three analyses of the sample appear in Table 4 and demonstrate the consistency of the methodology, both for the measured size and particle concentration, even at very low particle concentrations.

Table 4. Fe Particle Size and Concentration from the Analysis of 90% Cyclohexane and 10% PGME.

Sample	Most Frequent Size (nm)	Mean Size (nm)	Particle Concentration (particles/mL)
1	59.0	92.8	2971
2	60.7	89.8	2929
3	63.0	89.7	2935
Average	*60.9*	*90.8*	*2945*
Std. Dev.	*2.01*	*1.76*	*22.7*
RSD	*3.30%*	*1.94*	*0.77*

The calculated particle size depends on both the density of the particles and the particle composition (mass fraction of iron). Table 5 shows the same results as in Table 4, but under two different assumptions: that the particles are pure Fe and that they are stainless steel particles. As the data shows, the sizes vary slightly.

Table 5. Fe Nanoparticle Size in 90% Cyclohexane/10% PGME under Two Different Assumptions.

Composition	Sample	Most Frequent Size (nm)	Mean Size (nm)
Metallic Fe	1	59.0	92.8
Density = 7.87 g/cm³	2	60.7	89.8
Fe Mass Fraction: 100%	3	63.0	89.7
Stainless Steel	1	67.0	105
Density = 7.70 g/cm³	2	68.8	102
Fe Mass Fraction: 70%	3	71.5	94.9

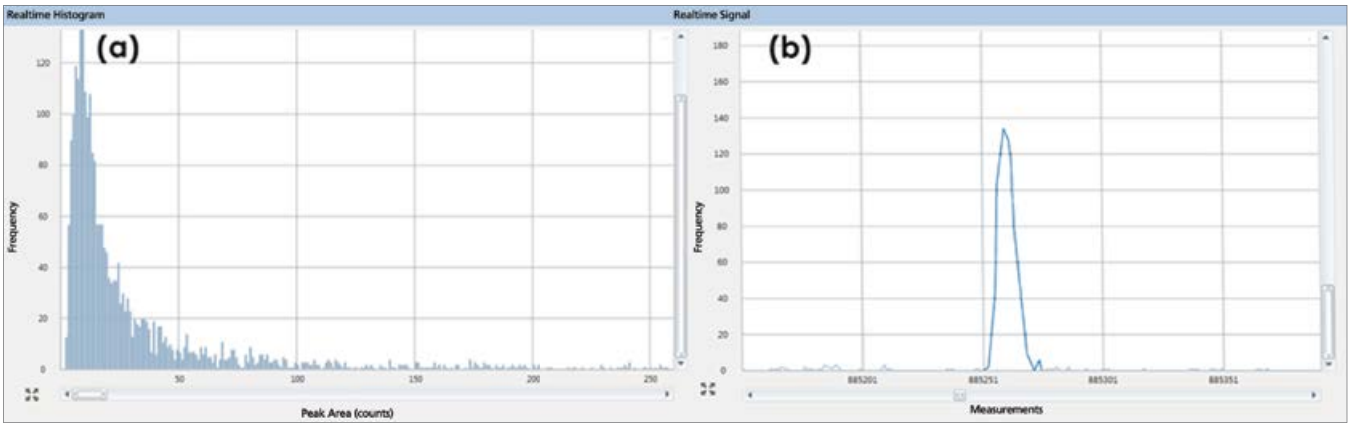

Figure 5. Fe-containing nanoparticle in TMAH. (a) Particle size distribution. (b) Real-time signal from a single Fe-containing nanoparticle.

Next, TMAH diluted ten times with deionized water was analyzed, with the results appearing in Figure 5 and Table 6. Figure 5a shows the particle size distribution on the left, while the signal from a single Fe nanoparticle appears in Figure 5b. (The x-axis in Figure 5b is zoomed significantly to show the single peak.) As with the cyclohexane, the results are consistent over three replicate analyses, both for particle size and concentration. Table 6 shows the results from three analyses of the sample, which again demonstrate the consistency of the methodology, both for particle size and concentration.

To determine if these nanoparticles originate from stainless steel, the sample was run again, this time monitoring chromium (Cr). As the real-time trace in Figure 6 shows, no particles are present, which means that these Fe-containing nanoparticles are not stainless steel. Based on TMAH chemistry, it is suspected that these are $Fe(OH)_2$ particles.

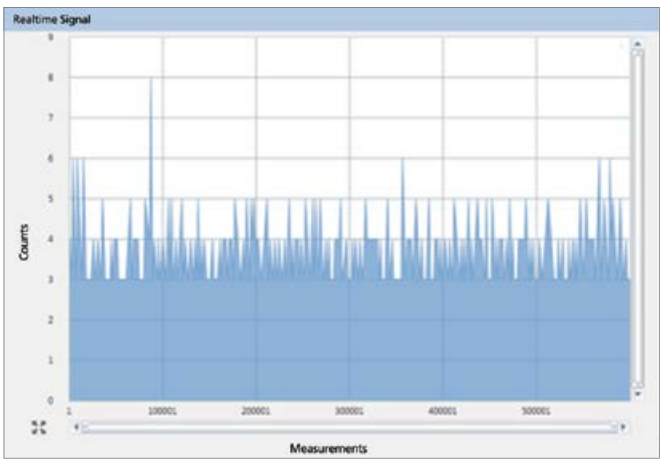

Figure 6. Real-time signal for Cr-containing nanoparticles in TMAH. Since no Cr-containing particles are detected, the Fe-containing particles detected in Figure 5 cannot be from stainless steel.

Assuming that $Fe(OH)_2$ particles are present in the TMAH, the total iron concentration being measured can be calculated based on the density of $Fe(OH)_2$, (3.4 g/cm^3), the Fe mass fraction (70%), the particle size, and particle concentration. Table 7 displays the data for three replicate analyses of the TMAH, which shows that the total concentration of iron (converted from the particle concentration and assuming particles are clusters of $Fe(OH)_2$) is being detected with great precision.

Table 7 displays the data for three replicate analyses of the TMAH and shows the total concentration of iron detected after conversion from the particle concentration and assuming particles are clusters of $Fe(OH)_2$.

Table 6. Fe Nanoparticle Size and Concentrations in TMAH.

Sample	Most Frequent Size (nm)	Particle Conc. (particles/mL)	Dissolved Intensity (counts)
1	27.6	43809	0.11
2	26.6	43253	0.08
3	26.9	42617	0.08
Average	*27.0*	*43226*	*0.09*
Std. Dev.	*0.513*	*596*	*0.02*
RSD	*1.90%*	*1.38%*	*19.2%*

Table 7. Mass Conversion of Fe from $Fe(OH)_2$ to total Fe.

Sample	Mean Size (nm)	Particle Conc. (part/mL)	Mass of individual $Fe(OH)_2$ particle (g)	Fe Concentration (ppt)
1	41.6	43809	1.28E-16	3.92
2	41.0	43253	1.23E-16	3.71
3	40.0	42617	1.14E-16	3.40
Average	*40.9*	*43226*	*0.00*	*3.68*
Std. Dev.	*0.80*	*596*	*7.09E-18*	*0.262*
RSD	*1.98%*	*1.38%*	*5.83%*	*7.11%*

Conclusion

This work has demonstrated the ability of SP-ICP-MS in Reaction mode to detect Fe-containing nanoparticles in organic solvents. By using ammonia in Reaction mode on the NexION 350, the ArO^+ interference on the main isotope of Fe (m/z 56) is completely eliminated, allowing the size and concentration of Fe-containing nanoparticles to be accurately determined. Reaction mode was used instead of Collision mode since the latter cannot eliminate the ArO^+ interference without causing a significant sensitivity loss for iron, which would prevent the Fe-containing nanoparticles from being seen. In Reaction mode, Fe nanoparticle detection limits of 13 nm were established, and particles were accurately counted and sized at concentrations as low as 3000 particles/mL in organic solvents. Future work will focus on other nanoparticles which will benefit from Reaction mode.

Consumables Used

Component	Part Number
60 nm Spherical Au Nanoparticles	N8142303 (25 mL)
PerkinElmer Pure-Grade Standard, 1000 ppm	N9303771 (125 mL) N9300126 (500 mL)
Sample Tubes	B0193233 (15 mL) B0193234 (50 mL)

References

1. Stephan, C., Neubauer, K. "Single Particle Inductively Coupled Plasma Mass Spectrometry: Understanding How and Why", PerkinElmer white paper, 2014.
2. Hadioui, M., Wilkinson, K., Stephan, C. "Assessing the Fate fo Silver Nanoparticles in Surface Water using Single Particle ICP-MS", PerkinElmer application note, 2014.
3. Donovan, A.R., Shi, H., Adams, C., Stephan, C. "Rapid Analysis of Silver, Gold, and Titanium Dioxide Nanoparticles in Drinking Water by Single Particle ICP-MS", PerkinElmer application note, 2015.
4. Neubauer, K., Stephan, C., Kobayashi, K. "Analysis of SiO_2 Nanoparticles in Standard Mode with Single Particle ICP-MS", PerkinElmer application note, 2015.
5. Gray, E., Higgins, C.P., Ranville, J.F. "Analysis of Nanoparticles in Biological Tissues using SP-ICP-MS", PerkinElmer application note, 2014.
6. Davidowski, L., Stephan, C. "The Characterization of Nanoparticle Element Oxide Slurries Use in Chemical-Mechanical Planarization by Single Particle ICP-MS", PerkinElmer application note, 2014.
7. Ong, K. "Determination of Impurities in Organic Solvents used in the Semiconductor Industry with the NexION 300/350S ICP-MS", PerkinElmer application note, 2012-2014.

PerkinElmer, Inc.
940 Winter Street
Waltham, MA 02451 USA
P: (800) 762-4000 or
(+1) 203-925-4602
www.perkinelmer.com

PerkinElmer®

For a complete listing of our global offices, visit www.perkinelmer.com/ContactUs

012407A_01 PKI

APPLICATION NOTE

ICP - Mass Spectrometry

Authors:

Lee Davidowski

Chady Stephan

PerkinElmer, Inc.
Shelton, CT

The Characterization of Nanoparticle Element Oxide Slurries Used in Chemical-Mechanical Planarization by Single Particle ICP-MS

Introduction

This study outlines the quantitation and characterization of element oxide nanoparticles (Al_2O_3, and CeO_2) commonly used in the nanoelectronics and semiconductor fabrication industry for the chemical-mechanical planarization (CMP) of semiconductor surfaces. CMP is a process of smoothing surfaces with the combination of chemical and mechanical forces in preparation for photolithography. The process uses various element oxide slurries and pressure to chemically and mechanically polish the silicon wafers during the manufacturing of semiconductor devices. In an effort to reduce size of the electronic device and improve the yield of the manufacturing process, CMP slurries consisting of nanoparticles are now in use.

PerkinElmer®
For the Better

The characterization of the size distribution of CMP slurry nanoparticles, as well as the identification of larger particles, is an important aspect for the quality control of the photolithography process as they can impact the eminence of the silicon wafers. One of the most promising techniques for analyzing metallic nanoparticles is ICP-MS run in single particle mode (SP-ICP-MS). Due to its ability to measure both the dissolved concentrations of analytes and individual nanoparticles, an ICP-MS which is capable of measuring single particles is an ideal instrument for both types of analyses in the semiconductor industry.

Because of its sensitivity, flexibility, and analysis speed, SP-ICP-MS is gaining popularity for detecting and measuring inorganic-based nanoparticles. With this technique, nanoparticles are introduced into an ICP and completely ionized, with the resulting ions being detected by a mass spectrometer. The intensity of the signal is related to the particle size; thus SP-ICP-MS provides the user with particle concentration (particles/mL), size and size distribution.

In order to ensure that only a single particle is measured at a time, the sample has to be diluted to achieve temporal resolution between particles. The mass spectrometer must be capable of making extremely rapid measurements to ensure nanoparticle detection as the transient signal of a 50 nm nanoparticle can vary on average between 300 and 500 µs, depending on the instrument's operating conditions and ion optics design (Figures 1 and 2).

The kind of speed required for SP-ICP-MS is called "transient data acquisition speed", which is the number of data points the instrument can acquire for a single mass per second. The greater the transient data acquisition speed the instrument provides, the better it is for SP-ICP-MS. The PerkinElmer NexION® 350 ICP-MS operating in single particle mode is able to acquire data continuously, with the elimination of settling times, giving it the ability to acquire as much as 100,000 data points/second.

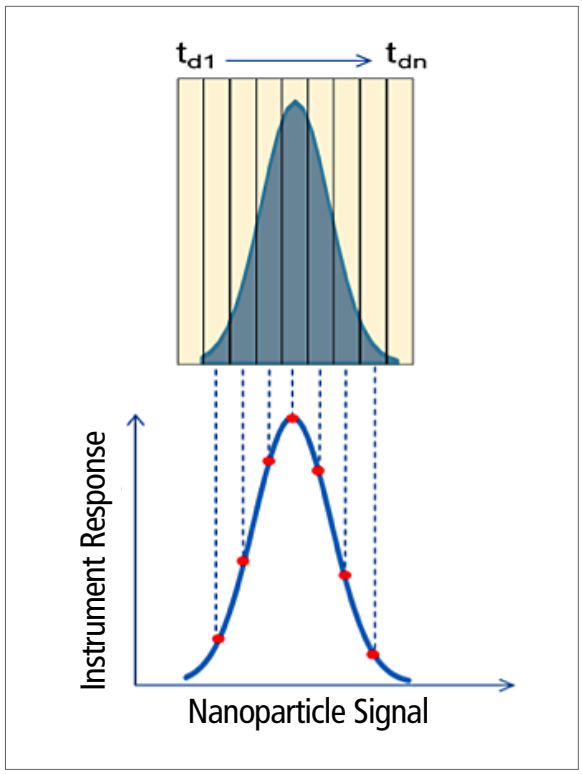

Figure 1. Acquiring data faster than the transient signal allows surface area integration of nanoparticle signal.

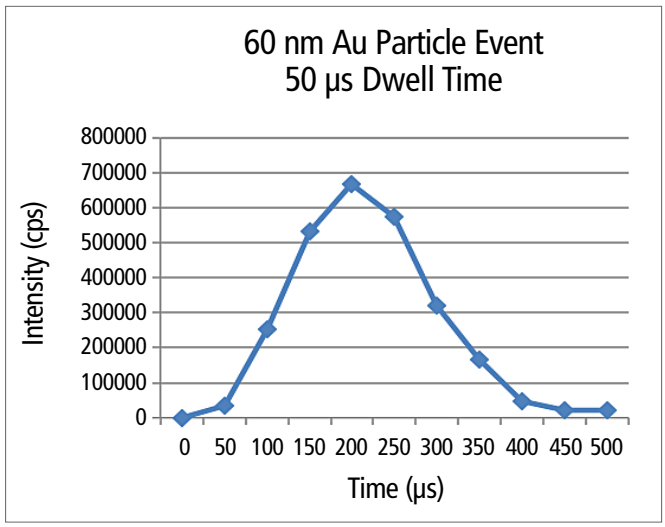

Figure 2. Signal of one gold 60 nm particle acquired using the NexION 350 ICP-MS operating in single particle mode (50 µs dwell time and no settling).

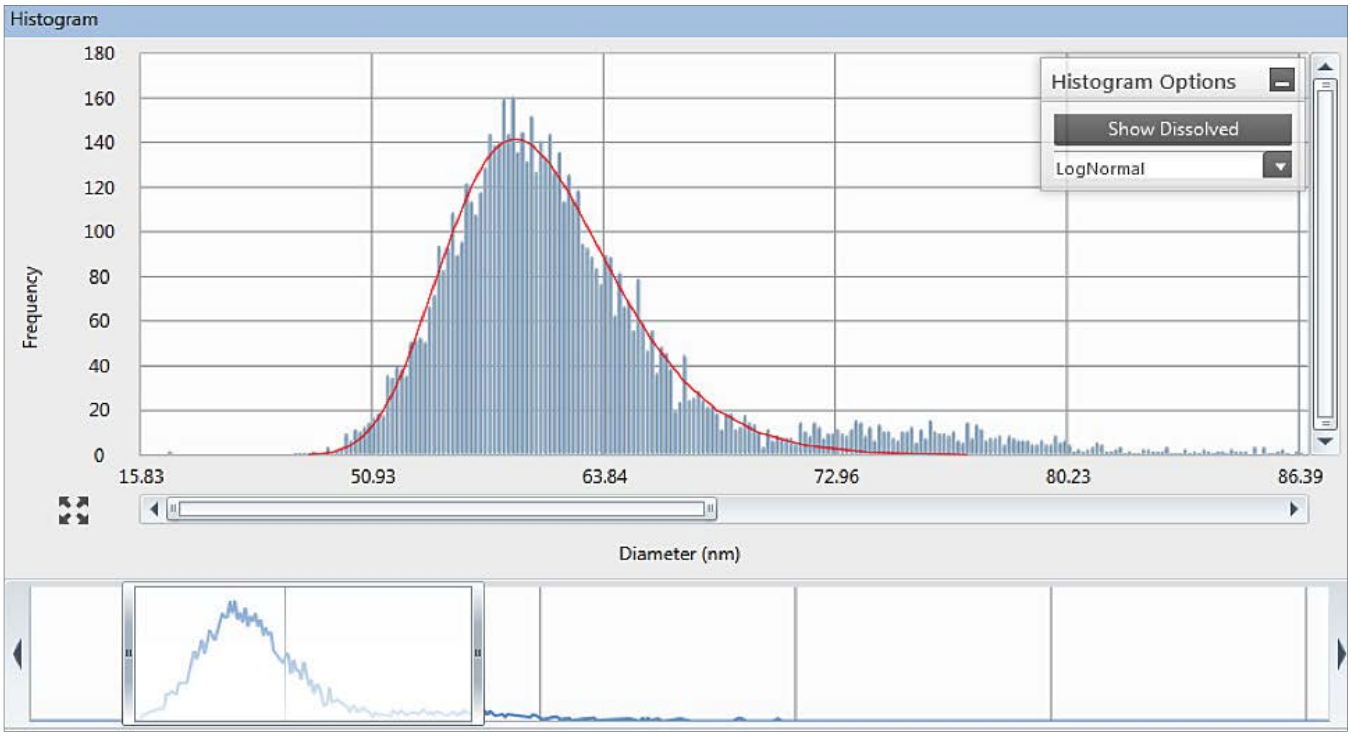

Figure 3. NIST SRM 8013 Gold 60 nm SP-ICP-MS size distribution graph.

Experimental

Sample Preparation

In preparation for SP-ICP-MS analysis, the sample slurries were ultrasonicated for 5 minutes and simply diluted in laboratory pure Type I water prior to analysis. Dilutions were calculated so that the final analysis sample liquid contained approximately 200,000 particles/mL. For most CMP slurries, this amounted to a dilution of between 10^6 and 10^7.

Instrumental

The instrument used in this work was a NexION 350D ICP-MS (PerkinElmer Inc., Shelton, CT, USA) – instrumental parameters and conditions are given in Table 1. Calibration curves for the elements were built from PerkinElmer Pure commercially available NIST traceable standards (PerkinElmer Inc., Shelton, CT). One blank and four calibration points were used. The system transport efficiency was calculated using two Ted Pella, Inc. (Redding, CA, USA) gold nanoparticle standards (50 and 80 nm) and validated using the NIST SRM 8013 (60 nm). Unlike conventional quadrupole ICP-MS systems, the NexION 350 in single particle mode completely eliminates the quadrupole settling time. The elimination of quadrupole electronics settling time provides for a truly continuous stream of data from the ICP-MS detector. By capturing data continuously and rapidly, the NexION ICP-MS does not miss any of the single particle events, resulting in precise particle counting and a greater number of events per period of time spent analyzing each sample.

Table 1. Instrumental Parameters and Conditions for SP-ICP-MS.

Parameter	Value
Instrument	NexION 350D ICP-MS
Nebulizer	PFA Concentric
Spray Chamber	Cyclonic
Torch and Injector	Quartz Torch and Alumina 2.0 mm ID injector
Power (W)	1600
Plasma Gas (L/min)	15
Aux Gas (L/min)	1.2
Neb Gas (L/min)	1.02
Sample Uptake Rate (mL/min)	0.25
Sample Tubing	Orange/Green
Dwell Time (µs)	100
Sampling Time (s)	60

Method Validation

Instrument validation was performed using the NIST SRM 8013 Gold Nanoparticles Nominal 60 nm Diameter as a quality control (QC). The size distribution of the NIST SRM 8013 Gold Nanoparticles is displayed in Figure 3. The graph shows good nano scale agreement with the certified value 60 nm. The Ted Pella gold nanoparticles are used to calibrate the instrument as well as establish the transport efficiency of the nebulized nanoparticle suspensions into the plasma; the NIST 8013 is used as a QC check on the calibration.

Results – CeO_2

Both slurry samples contain a wide distribution of CeO_2 nanoparticles. The normalized frequency graph for Slurry #1 (Figure 4) shows sizes that fluctuate from 12 nm to 42 nm with a mean size distribution of 22.3 nm. The cumulative graph shows that 80% of the measured nanoparticles are 30 nm or less with a prevalent amount of 12 nm particles (at 20%) and the majority of the nanoparticles in the 20-30 nm range. The normalized frequency graph for Slurry #2 CeO_2 (Figure 5) shows sizes that fluctuate from 22 nm to 76 nm with a mean size distribution of 47.8 nm. 80% of the measured nanoparticles are below 62 nm. There was also an elevated background signal which indicated that some of the Ce was dissolved into solution. The results for both slurry samples are summarized in Table 2.

Results – Al_2O_3

Like the CeO_2 samples, both Al_2O_3 slurries contain a distribution of nanoparticles. The normalized frequency graph for Slurry #3 (Figure 6) shows sizes that range from 28 nm to 58 nm with a mean size distribution of 44.4 nm. The cumulative graph shows that about 80% of the particles are less than 54 nm with 50% below 48 nm. There appear to be two dominant sizes: the first at 28-38 nm (27%) and the second around 50 nm.

The normalized frequency graph for Slurry #4 (Figure 6) shows that this slurry sample has an even distribution of sizes from 22 nm to 46 nm with a mean size of 32.5 nm. The cumulative graph shows that 80% of the particles are 38 nm and less. The results for both Al_2O_3 slurries are summarized in Table 3.

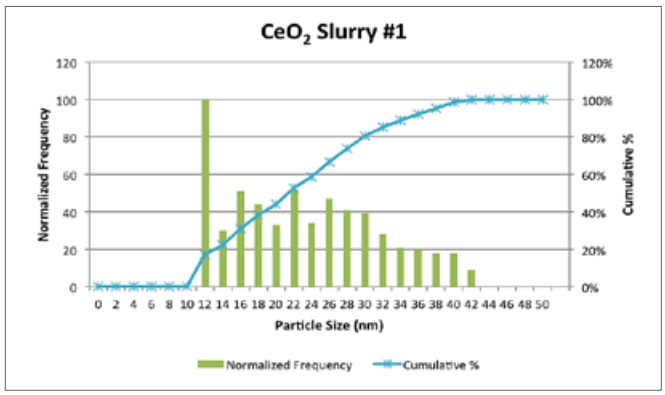

Figure 4. Slurry #1 normalized frequency particle size distribution graph.

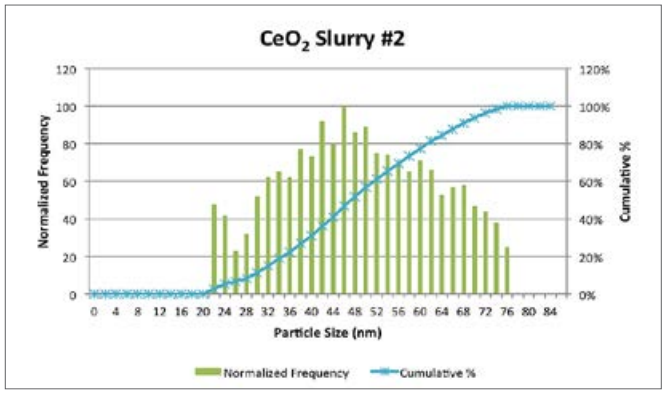

Figure 5. Slurry #2 normalized frequency particle size distribution graph.

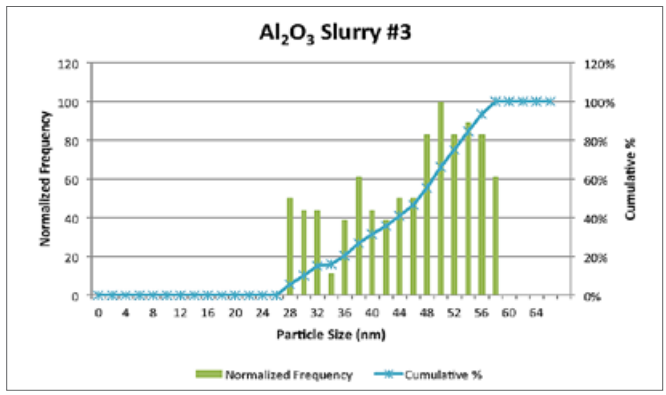

Figure 6. Slurry #3 normalized frequency particle size distribution graph.

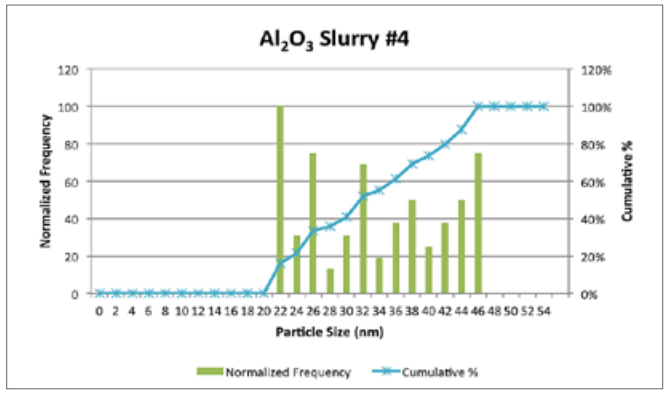

Figure 7. Slurry #4 normalized frequency particle size distribution graph.

Table 2. Results for CeO_2 Slurry Samples

Sample ID	Mean Size (nm)	Median Size (nm)	Particle Conc. (particles/mL)	Dissolved Conc. (ppb)
CeO_2 Slurry #1	22.3	21.4	196821	<0.01
CeO_2 Slurry #2	47.8	47.3	267029	0.13

Table 3. Results for Al_2O_3 Slurry Samples

Sample ID	Mean Size (nm)	Median Size (nm)	Particle Conc. (particles/mL)	Dissolved Conc. (ppb)
Al_2O_3 Slurry #3	44.4	47.2	122536	<0.02
Al_2O_3 Slurry #4	32.5	31.8	148960	<0.02

Conclusions

This work has shown how the NexION 350D ICP-MS in single particle mode was used to successfully characterize two types of element oxide nanoparticles. Results were given for mean and median particle size, particle concentration, as well as graphs of the size distribution and cumulative percentage of particles versus size. The acquisition of this data was achieved in a single, rapid analysis of the slurry samples tested.

PerkinElmer, Inc.
940 Winter Street
Waltham, MA 02451 USA
P: (800) 762-4000 or
(+1) 203-925-4602
www.perkinelmer.com

011617_01

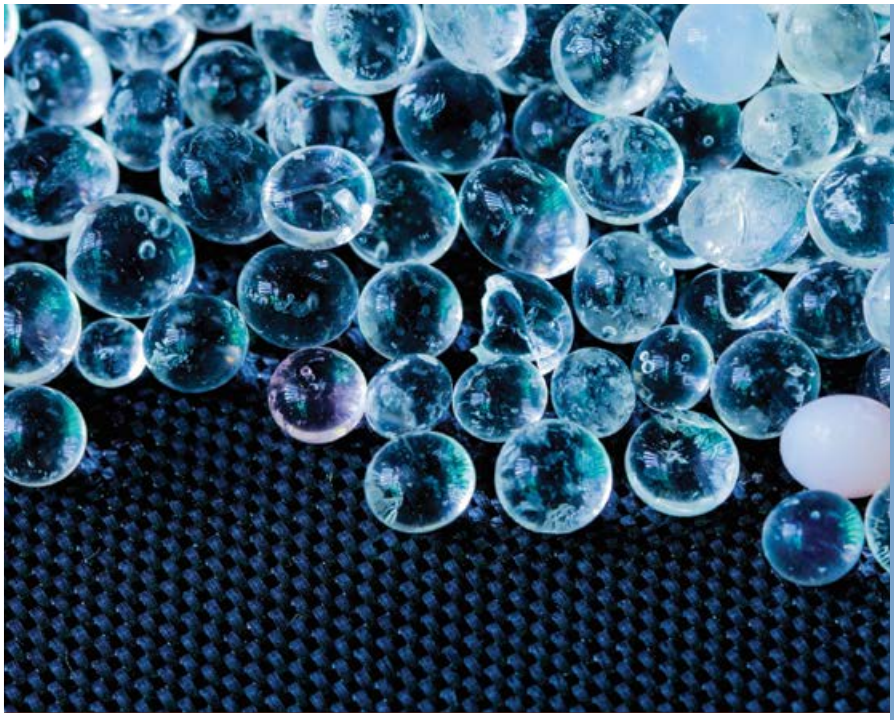

APPLICATION NOTE

ICP - Mass Spectrometry

Authors:

Kenneth Neubauer

Chady Stephan

Kyoko Kobayashi

PerkinElmer, Inc.
Shelton, CT

Analysis of SiO_2 Nanoparticles in Standard Mode with Single Particle ICP-MS

Introduction

With the development of nanotechnology and the increased use of nanoparticles in numerous products and processes, the need to characterize nanoparticles has also grown. Nanoparticles come in a wide variety of compositions, depending on their uses, with silica dioxide (SiO_2) nanoparticles being used in many areas, including paint, strengthening of materials, and semiconductor processes, among others. For successful implementation and incorporation into products, the size and size distribution of the SiO_2 particles must be characterized.

Nanoparticle-size analysis has traditionally been accomplished by a variety of techniques, including, but not limited to, microscopy, light scattering, small angle x-ray scattering (SAXS) and field flow fractionation (FFF). While all the techniques work well with some advantages and disadvantages, they all are limited by low sample throughput, which inhibits their ability to characterize large numbers of particles. In addition, the above mentioned techniques, except microscopy, do not provide information on individual particle composition, nor direct particle counting.

PerkinElmer®
For the Better

To meet these limitations, single particle ICP-MS (SP-ICP-MS) has been developed[1, 2]. This technique allows for the rapid analysis of nanoparticles, measuring thousands of particles in less than a minute, while providing individual particle information on particle size, particle size distribution, particle concentration, dissolved concentration of the element, and agglomeration.

Measuring silica (Si) with ICP-MS is challenging due to the presence of $^{14}N_2^+$ and $^{12}C^{16}O^+$, which form in the plasma and have the same m/z as the most abundant Si isotope ($^{28}Si \approx 92\%$ abundance). As a result, the background at m/z 28 is very high, which inhibits low-level Si determination and can make detection of SiO_2 nanoparticles difficult. However, as measurement time decreases, the background signal will also decrease since fewer counts will be accumulated during an individual dwell time, yet the number of ions produced from ionizing a particle remains constant. As a result, the ions are measured over more time slices. Therefore, shorter dwell time should improve particle size detection limit for analytes suffering from elevated background (i.e. SiO_2, Fe, Se, etc.).

This work will explore the ability of SP-ICP-MS to detect, measure, and characterize SiO_2 nanoparticles using dwell times as low as 25 µs.

Experimental

Sample Preparation

Known SiO_2 nanoparticle standards of various sizes were purchased from nanoComposix™ (San Diego, California, USA). Sample preparation involved sonicating the solutions for ten minutes to loosen up any agglomerated particles, followed by dilutions with deionized water to yield final concentrations of 100,000 – 200,000 particles/mL. The final solutions were sonicated again prior to analysis.

Dissolved calibration curves were made by serial dilutions of a 1000 mg/L dissolved silica standard. The silica concentrations of the dissolved standards were 2, 5, 10, and 20 µg/L Si. Particle calibration curves were made from the SiO_2 nanoparticle standards (180, 200 nm) at concentrations of about 100,000 particles/mL.

Analysis and Instrumentation

All analyses were performed on a PerkinElmer NexION® 350D ICP-MS operating in Standard mode, using the Nano Application Module (Part No. N8140309) within Syngistix™ for ICP-MS software. Instrumental parameters appear in Table 1 and were optimized to give the highest Si signal while maintaining the lowest possible background due to silica leaching from the torch.

Table 1. NexION 350D ICP-MS Instrumental Parameters.

Parameter	Value
Sample Uptake Rate	0.33 mL/min
Nebulizer	Glass Concentric
Spray Chamber	Baffled Glass Cyclonic
RF Power	1000 W
Analyte	Si^+ at m/z 28
Mode	Standard
Analysis Time	60 seconds per sample

Results and Discussion

The difficulty in analyzing Si with ICP-MS is the high background at m/z 28 (the most abundant isotope of Si) due to CO^+ and N_2^+. However, when using SP-ICP-MS, very short dwell times are used, and counts are monitored instead of counts per second. As a result, backgrounds are much lower in SP-ICP-MS analyses than in conventional ICP-MS analyses. Figure 1 shows the background at m/z 28 when measuring deionized water in Standard mode with SP-ICP-MS. The background is only 15 counts when measured with 100 µs dwell time, much lower than would be seen with conventional ICP-MS analyses. This low background allows SiO_2 nanoparticles to be detected as the Si signal produced from the ionization of SiO_2 nanoparticles should be greater than 15 counts, based on previous work with other metallic-oxide nanoparticles[3, 4].

Figure 2 shows the unprocessed signal from 200 nm SiO_2 particles in deionized water. Each spike represents the signal from a SiO_2 particle, signifying that 200 nm SiO_2 particles are easily seen in Standard mode with SP-ICP-MS. The results indicate that the mean particle size detected is 208 nm, which agrees with the size on the certificate (198.5 ± 10.5 nm, as determined by transmission electron microscopy).

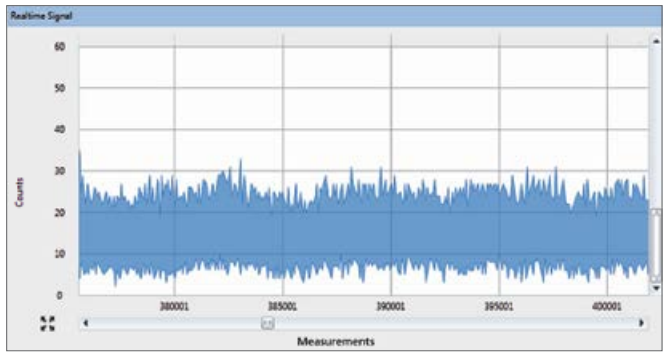

Figure 1. Unprocessed signal of deionized water at m/z 28 with a dwell time of 100 µs using SP-ICP-MS in Standard mode.

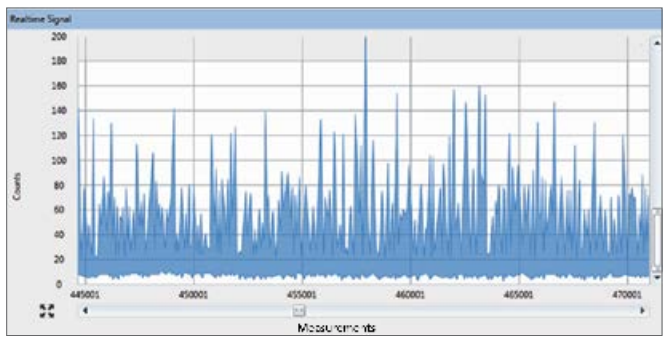

Figure 2. Unprocessed signal of 200 nm SiO_2 particles deionized water at m/z 28 with a dwell time of 100 µs using SP-ICP-MS in Standard mode.

Because counts are being measured, shorter dwell times result in lower backgrounds, although the analyte intensity will also be lower. Table 2 shows the effect of dwell time on the signal-to-background (S/B) ratio at m/z 28 for deionized water and a 10 ppb dissolved silica standard. These data demonstrate the importance of using short dwell times. With a dwell time typically used for aqueous analysis (i.e. 50 ms), the S/B ratio is less than 1. However, with dwell times of 100 µs or less, the S/B ratio becomes greater than 1, demonstrating the importance of short dwell times for nanoparticle work. As the dwell time is reduced further, the Si sensitivity decreases, yet the signal-to-background ratio remains constant, which implies that shorter dwell times should allow smaller SiO_2 particles to be detected.

Table 2. Effect of Dwell Time on Si Signal to Background (S/B) at m/z 28.

Dwell Time (µs)	Background (counts)	10 ppb Si (counts)	S/B
50,000	20,000	10,000	0.5
100	21	42	2.0
50	10	21	2.1
25	5	10	2.0

The basis for this deduction is that while shorter dwell times result in lower background signals, individual particle mass is constant, and once ionized in the plasma, the number of ions formed is constant and is not a function of the dwell time when surface area integration is applied.

Figure 3 provides a representation of this concept. In this figure, each vertical line represents a time slice, and the red dots with the plus signs represent ions. The number of ions detected in each time slice is shown below each time slice. The circled clusters of ions represent the ions produced from a single nanoparticle; the other ions represent the background. In Figure 3a, assume that each slice represents a dwell time of 600 µs. Over 4800 µs (i.e. 8 dwells of 600 µs each), three particles are detected, each producing 16 ions. The average background signal is 6 ions, for a S/B of 2.67. Since particles arrive at random times in the plasma, their ion cloud is not always fully captured in a single dwell time window if the dwell time used is larger than the particle transit time.

In Figure 3b, each slice represents a dwell time of 300 µs, resulting in 16 dwell times over the same 4800 µs time window. Because of the shorter time, the number of background ions is halved: an average of 3 ions per dwell time. However, the number of ions from each particle remains constant: 16. Because of the shorter dwell time, however, the number of ions from each particle may be spread out over 2 dwell times, averaging 13 ions per dwell time. The resulting S/B is 4.3, higher than with the 600 µs dwell time.

In Figure 3c, the dwell time is reduced to 100 µs, meaning that there are 48 measurements over the same 4800 µs time window. With this timing, the average background signal drops to 1 ion per dwell time. A particle still produces 16 ions, but these are now spread out over several measurement windows to yield about 5 ions per dwell time window. The resulting S/B is 5. This example demonstrates how shorter dwell times can allow smaller particles to be detected.

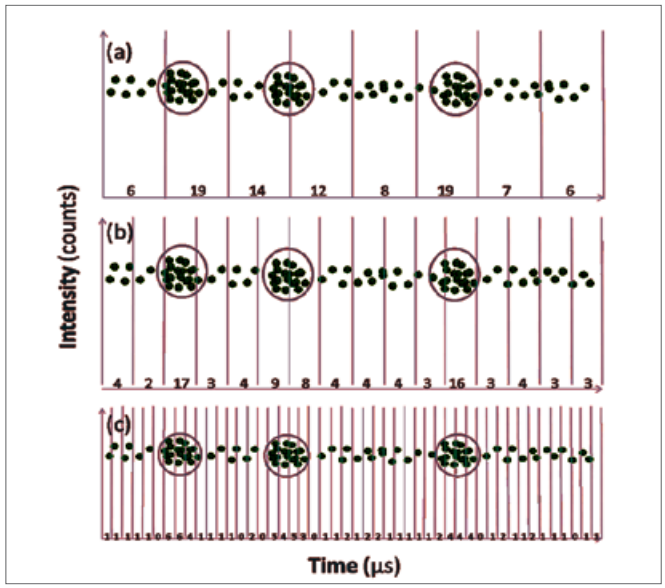

Figure 3. Representation of the effect of dwell time on particle and background detection. Dwell times: (a) 600 µs; (b) 300 µs; (c) 100 µs. Each red dot represents an ion. The circled dots represent the ions from a single nanoparticle (3 particles detected in each representation); other dots represent the background signal.

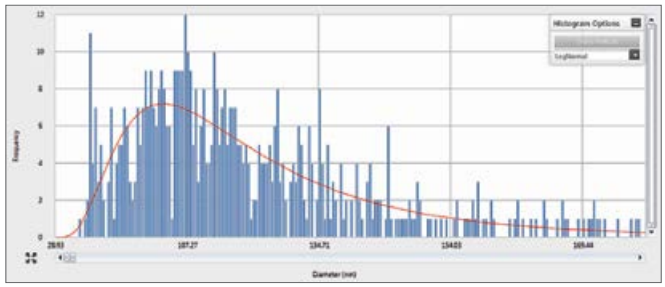

Figure 4. Particle size distribution for 100 nm SiO_2 particles measured with a 25 µs dwell time.

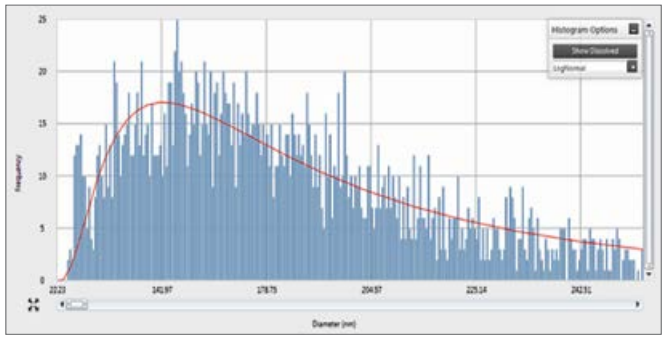

Figure 5. Particle size distribution for 140 nm SiO_2 measured with a 25 µs dwell time.

Table 3. Size Measurements of 140 and 100 nm SiO_2 Nanoparticles.

SiO_2 Standards (nm)	Most Frequent Size (nm)	Mean Size	Certificate*
100 nm	100	103	101.7 ± 4.5
140 nm	143	143	142.4 ± 8.3

** as determined by transmission electron microscopy*

With this philosophy in mind, smaller SiO_2 particles were analyzed at a shorter dwell time: 25 µs. Figures 4 and 5 show the particle size distributions of 100 nm and 140 nm SiO_2 particles, respectively. The measured sizes and comparison to the certificate values appear in Table 3 and demonstrate that SiO_2 particles as small as 100 nm can be accurately characterized in Standard mode.

Conclusion

This work has demonstrated the ability to measure SiO_2 nanoparticles in Standard mode by SP-ICP-MS. The key advantage of the NexION 350 ICP-MS single particle analyzer is its speed of analysis and the short dwell times which reduce the background on Si, allowing 100 nm SiO_2 particles to be measured in Standard mode.

Future work will focus on characterizing smaller SiO_2 particles using Reaction mode to further reduce the background. Initial studies have shown promise, but more extensive work is required to fully characterize the analysis.

References

1. *"Single Particle Inductively Coupled Plasma Mass Spectrometry: Understanding How and Why",* PerkinElmer White Paper, 2014.
2. Hineman, A., Stephan, C., *J. Anal. At. Spectrom,* 2014, 29, 1252-1257.
3. *"Measurement of Titanium Dioxide Nanoparticles in Sunscreen Using Single Particle ICP-MS",* PerkinElmer Application Note, 2015.
4. *"The Characterization of Nanoparticle Element Oxide Slurries Used in Chemical-Mechanical Planarization by Single Particle ICP-MS",* PerkinElmer Application Note, 2014.

Consumables Used

Component	Part Number
Sample Uptake Tubing, 0.38 mm id (Green/Orange) Flared PVC 2-stop Peristaltic Pump Tubing	N0777042
Drain Tubing, 1.30 mm id (Gray/Gray) Santoprene 2-Stop Peristaltic Pump Tubing	N0777444
Autosampler Tubes	B0193233 (15 mL) B0193234 (50 mL)

PerkinElmer, Inc.
940 Winter Street
Waltham, MA 02451 USA
P: (800) 762-4000 or
(+1) 203-925-4602
www.perkinelmer.com

PerkinElmer®

012251_01 PKI

APPLICATION NOTE

ICP - Mass Spectrometry

Authors

Chady Stephan, Ph.D.

Aaron Hineman

PerkinElmer, Inc.
Woodbridge, Ontario CAN

Analysis of NIST Gold Nanoparticles Reference Materials Using the NexION 350 ICP-MS in Single Particle Mode

Introduction

Engineered nanomaterials (ENs) refer to the process of producing and/or controlling materials that have at least one dimension in the size range of 1 to 100 nm. They often possess different properties compared to bulk materials of the same composition, making them of great interest to a broad spectrum of industrial and commercial applications.

Recent studies have shown that some nanoparticles may be harmful to humans. A 2009 study in the Journal of Nanoparticle Research showed that zinc oxide nanoparticles were toxic to human lung cells in lab tests even at low concentrations (Weisheng et al., 2009).[1] Other studies have shown that tiny silver particles (15 nanometers) killed liver and brain cells in laboratory rats. At the nano scale, particles are more chemically reactive and bioactive, allowing them to easily penetrate organs and cells (Braydich-Stolle *et. al.*, 2005).[2]

PerkinElmer®
For the Better

To better understand the impact of nanoparticles, several key characteristics need to be assessed, such as concentration, composition, particle size, shape and other surface characteristics (Figure 1). Given these requirements, several analytical instruments must be used to characterize the material. Table 1 lists the key characteristics and many of the current analytical technologies that can be applied.

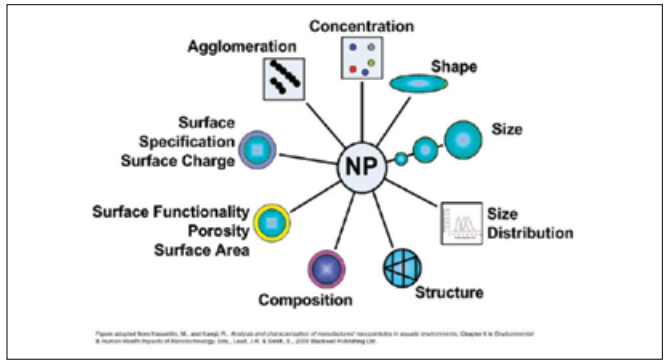

Figure 1. Key parameters to characterize nanomaterials (Hasselhov, 2009).[3]

Table 1. Nanomaterial characteristics and applicable analytical technologies.

Analytical Technique		Nanomaterial Characteristic								
		Concentration	Particle Size	Particle Size Distribution	Surface Charge	Surface Area	Shape	Agglomeration	Structure	Composition
Inductively Coupled Plasma-Mass Spectrometry	ICP-MS	●								●
Single Particle ICP-MS	SP-ICP-MS	●	●	●				●		●
Field Flow Fractionation + ICP-MS	FFF-ICP-MS	●	●				●	●		●
Liquid Chromatography/Mass Spectrometry	LC/MS	●								●
Optical Spectroscopy - UV/Vis	UV/Vis	●								●
Fluorescence Spectroscopy	FL	●	●					●		●
Turbidity			●	●				●		
Scanning Electron Microscopy	SEM		●	●			●	●	●	
Transmission Electron Microscopy (+EDX)	TEM		●	●		●	●	●	●	●
Atomic Force Microscopy	AFM		●	●	●	●	●	●		
Confocal Microscopy			●	●			●	●	●	
Field Flow Fractionation	FFF		●	●			●	●		
Dynamic Light Scattering	DLS		●	●			●	●		
Static Light Scattering	SLS		●				●	●		
Laser-Induced Plasma Spectroscopy	LIPS		●							
Dialysis			●	●						
Electrophoresis and Capillary Electrophoresis			●	●	●					
Ultrafiltration			●	●						
Centrifugation			●	●				●		
Filtration			●	●						
Nanoparticle Tracking Analysis	NTA		●	●				●		
Hydrodynamic Chromatography	HDC		●	●						
Laser-Induced Breakdown Detection	LIBD		●	●				●		
Size Exclusion Chromatography	SEC		●	●						
Selected Area Electron Diffraction	SAED		●	●					●	
Zeta Potential by DLS					●					
Molecular Gas Absorption (BET)					●	●				
X-ray Photoelectron Spectroscopy	XPS				●	●				●
X-ray Diffraction	XRD								●	
Thermogravimetric Analysis	TGA									●
Quartz Microbalances										●
Differential Scanning Calorimetry	DSC									●
Dynamic Mechanical Analysis	DMA									●
Fourier Transform-Infrared Spectroscopy	FT-IR									●
FT-IR Imaging									●	●
Raman Spectroscopy									●	●
TGA Coupled with Gas Chromatography/Mass Spectrometry	TGA-GC/MS									●
Electron Energy Loss Spectroscopy	EELS (+EDX)									●

Inductively coupled plasma mass spectrometry (ICP-MS) is one of the leading analytical techniques capable of measuring and assessing many of these key characteristics of metal-containing particles[4]. Low detection limits are critical in determining small concentrations of particles in a liquid sample as well as examining the characteristics of individual particles. Additionally, flexibility of instrumental parameters, such as dwell time and speed of the electronics, can influence the quality of data collected. This work explores the capability of the NexION® 350 ICP-MS to measure the key characteristics of manufactured metal nanoparticles.

Experimental

All work was performed using a NexION 350 ICP-MS (PerkinElmer, Shelton, CT, U.S.) operated in single particle mode using the Syngistix™ Nano Application Module. Single particle mode analysis (SP-ICP-MS) allows the differentiation between the dissolved and nanoparticle analyte, measuring nanoparticle size, size distribution and assessing agglomeration. Coupled to a size-separation technique (i.e. field flow fractionation [FFF] or liquid chromatography [LC]), ICP-MS is capable of addressing size, size distribution, surface charge and surface functionality.

The NexION 350 ICP-MS is capable of data acquisition speeds of 100,000 points/sec using dwell times as short as 10 µs and eliminating electronic settling time. Combined with a unique ion path design (Triple Cone Interface [TCI] and Quadrupole Ion Deflector [QID]), the NexION 350 ICP-MS, in SP-ICP-MS mode is crucial in assessing nanoparticle fate, transformation and transportation in different matrices (i.e. environmental, biological, food, etc.).

Gold nanoparticle standard reference materials (NIST 8011, 8012 and 8013 – NIST®, Gaithersburg, MD, U.S.) were used for all analyses.

The gold particles were suspended in a solution of deionized (DI) water at a concentration of 250,000 particles/mL. In order to avoid dissolution of the gold nanoparticles, acid was not added.

Table 2. NexION 350 ICP-MS operational conditions.

Parameter	Value
Instrument	NexION 350D ICP-MS
Nebulizer	Concentric
Spray Chamber	Baffled Cyclonic
Torch and Injector	Glass Torch and Glass Injector
Power (W)	1600
Plasma Gas (L/min)	17
Aux Gas (L/min)	1
Neb Gas (L/min)	1.03
Sample Uptake Rate (mL/min)	0.3
Sample Tubing (Standard)	Orange/Green
Dwell Time (µs)	100

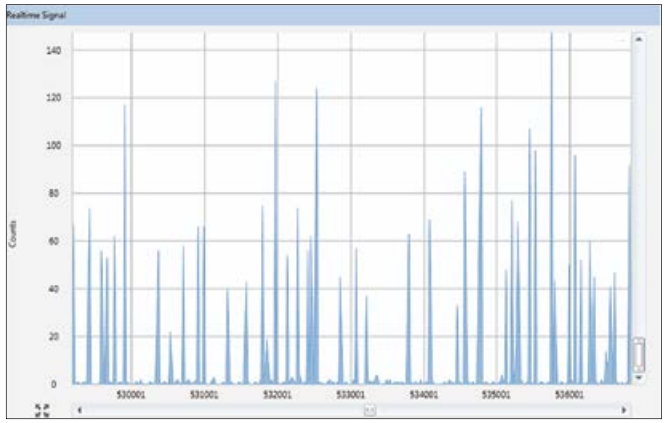

Figure 2. Generic signal when measuring nanoparticles in single particle ICP-MS mode. Each peak results from the ionization of a single nanoparticle.

All data was collected and processed using the Syngistix Nano Application Module. Gold was measured at m/z 197 (its only isotope) using a 100 µs dwell time with no settling time.

Results

Figure 2 shows part of the acquisition of 60 nm gold nanoparticles (NIST 8013), where each peak represents the instrumental response for an individual particle.

Particle size can be validated two ways with the Syngistix Nano Application Module: using calibrations from particle standards and calibrations with dissolved standards, the latter requiring the transport efficiency of the system be determined. Figure 3 shows the intensity distribution for three different size gold nanoparticles: 10, 30, and 60 nm (NIST 8011, 8012, 8013, respectively). These distributions demonstrate the NexION's ability to accurately detect, count, and measure nanoparticles of various sizes.

The intensity of the pulses generated by a single nanoparticle is a function of the number of atoms in the nanoparticle, and hence its size. Figure 4 shows the plot of the mean intensity versus the mass of the nanoparticle for the different NIST SRMs (10, 30, 60 nm gold nanoparticles).

One of the unique features of the Syngistix Nano Application Module is its ability to investigate nanoparticle size distribution and precisely quantify each distribution, thus providing accurate particle counting. To evaluate this function, nanoparticle solutions were prepared at different nanoparticle concentrations in DI water by mixing various concentrations of nanoparticles from both NIST 8012 and 8013 (i.e. 30 and 60 nm particles). Figure 5 displays the size distributions as shown in the Syngistix Nano Application Module. The reason that the intensities of the peaks are different is that the particles were present at different concentrations in the mixture: the 30 nm particles (NIST 8012) were at a concentration of 250,000 particles/mL, while the 60 nm particles (NIST 8013) were at 100,000 particles/mL.

To further test the power of the NexION 350 ICP-MS coupled with Syngistix Nano Application Module, four solutions containing different relative amounts of 30 and 60 nm gold nanoparticles (NIST 8012 and 8013) were prepared and measured. Figure 6 compares the actual particle concentrations (i.e. the particle concentrations used to prepare the standards) with the measured particle concentrations for both the 30 and 60 nm particles in all four solutions. The strong agreement between the actual and the measured concentrations demonstrates the accuracy of the measurements.

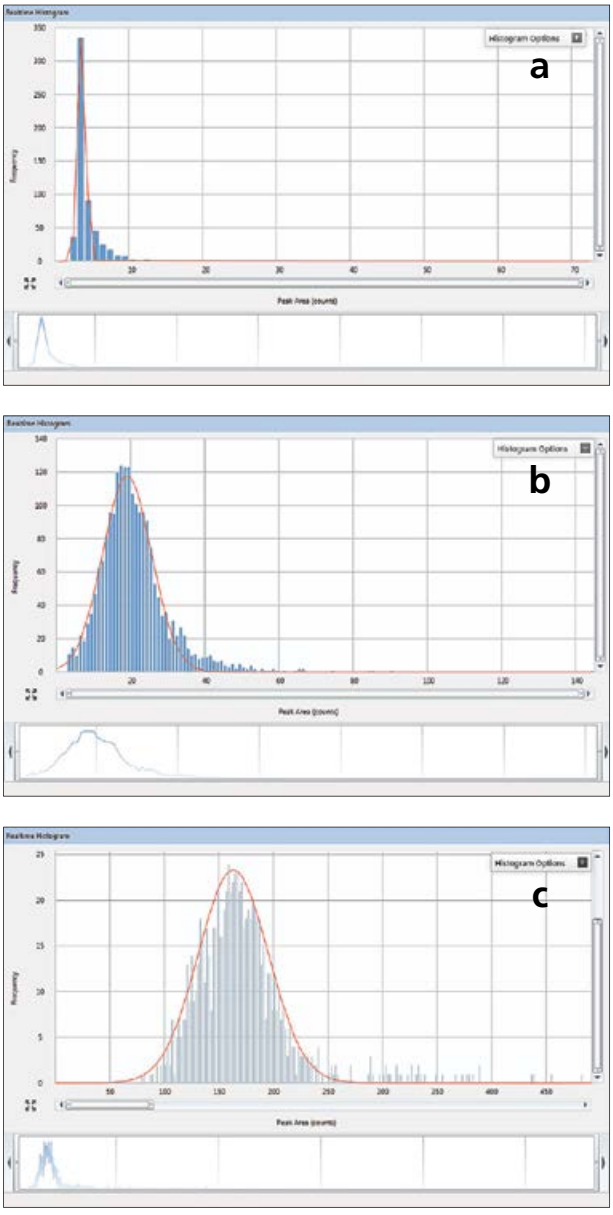

Figure 3. Intensity distributions of three different size gold nanoparticles: (a) 10 nm (NIST 8011); (b) 30 nm (NIST 8012); (c) 60 nm (NIST 8013).

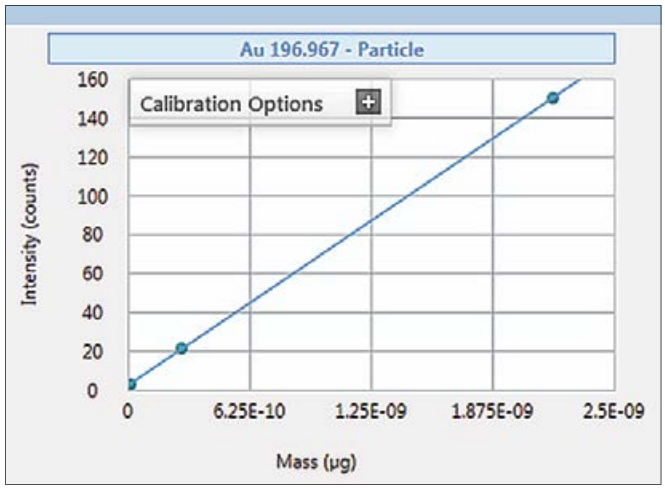

Figure 4. Plot of intensity vs. mass of gold nanoparticles (10, 30, 60 nm) as determined with the Nano Application Module in Syngistix for ICP-MS Software.

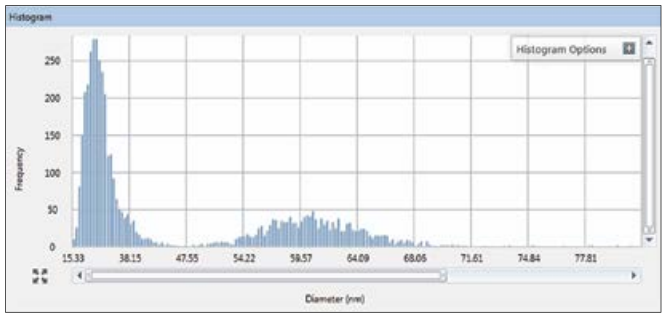

Figure 5. Size distribution as displayed in the Syngistix Nano Application Module for a mixture of 30 and 60 nm gold nanoparticles. The difference in the size of the peaks is due to the different concentrations of each nanoparticle in the mixture.

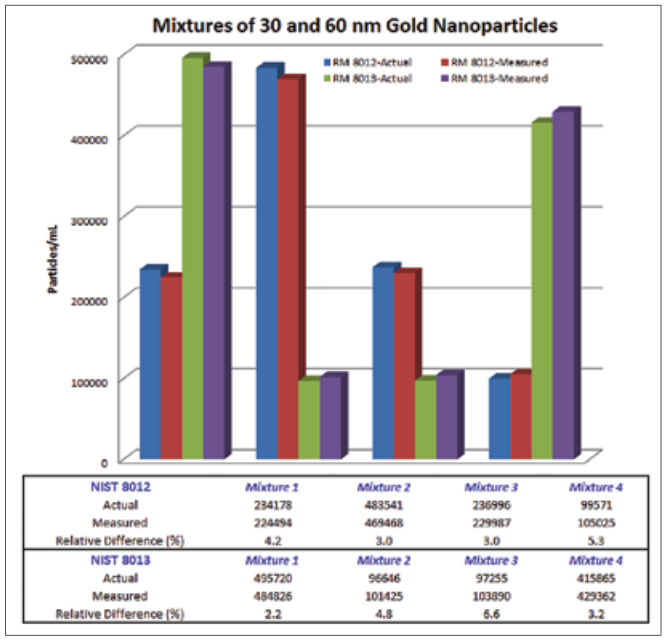

NIST 8012	Mixture 1	Mixture 2	Mixture 3	Mixture 4
Actual	234178	483541	236996	99571
Measured	224494	469468	229987	105025
Relative Difference (%)	4.2	3.0	3.0	5.3
NIST 8013	**Mixture 1**	**Mixture 2**	**Mixture 3**	**Mixture 4**
Actual	495720	96646	97255	415865
Measured	484826	101425	103890	429362
Relative Difference (%)	2.2	4.8	6.6	3.2

Figure 6. Analysis of four gold nanoparticle solutions comparing the actual and measured concentrations of both 30 and 60 nm particles. The blue (30 nm) and green (60 nm) bars represent the actual particle concentrations. The red (30 nm) and purple (60 nm) bars represent the measured particle concentrations.

Conclusion

ICP-MS is rapidly becoming the elemental measurement technique of choice for assessing the manufacturing accuracy and environmental lifecycle of engineered nanoparticles. When measuring dissolved elements, an ICP-MS system provides accurate composition and concentration measurements. Modern instruments, with ultra-fast electronics that enable the fastest data rates to capture nanoscale events, can provide advantages in the collection of more data per unit of time with greater precision.

The PerkinElmer NexION 350 ICP-MS, with Syngistix Nano Application Module operating in single particle mode, combines fast, accurate data acquisition with powerful data analysis capabilities, allowing metal and metal-containing nanoparticles to be characterized. Nanoparticle properties, which can be determined with this combination of hardware and software, include differentiation between dissolved and particulate signals, measurement of particle size and size distribution as well as exploration of agglomeration. This capability allows the characterization of nanoparticles used in food and consumer products, as well as the ability to explore the fate, transformation and effects of manufactured nanomaterials in the environment[5].

References

1. Weisheng Lin, Yi Xu, Chuan-Chin Huang, Yinfa Ma, Katie B. Shannon, Da-Ren Chen and Yue-Wern Huang, "Toxicity of nano- and micro-sized ZnO particles in human lung epithelial cells", Journal of Nanoparticle Research, 2009, Volume 11, Number 1, pp 25-39.
2. Laura Braydich-Stolle, Saber Hussain, John J. Schlager and Marie-Claude Hofmann, "In Vitro Cytotoxicity of Nanoparticles in Mammalian Germline Stem Cells", Toxicological Sciences, 2005, Volume 88, Issue 2, pp 412-419.
3. Hasselhov, M., Kaegl, R., "Analysis and Characterization of Manufactured Nanomaterials in Aquatic Environment", Chapter 6 of Environmental and Human Health Impacts of Nanomaterials, Eds. Lead, J. and Smith, E,. Blackwell Publishing Ltd.
4. Salamon, A.W. and *et. al*., "Nanotechnology and Engineering Nanoparticles – A Primer", PerkinElmer, 2010.
5. E.M. Heithmar and S.A. Pergantis "Characterizing Concentrations and Size Distributions of Metal-Containing Nanoparticles in Waste Water (APM 272)", U.S. Environmental Protection Agency, Office of Research and Development, Washington, DC 20460.

PerkinElmer, Inc.
940 Winter Street
Waltham, MA 02451 USA
P: (800) 762-4000 or
(+1) 203-925-4602
www.perkinelmer.com

PerkinElmer®

For a complete listing of our global offices, visit www.perkinelmer.com/ContactUs

010402A_01

APPLICATION NOTE

ICP – Mass Spectrometry

Authors:

Ariel R. Donovan[1,2], Honglan Shi[1,2], Craig Adams[2,3], Chady Stephan[4]

[1] Department of Chemistry and Environmental Resource Center, Missouri University of Science and Technology

[2] Center for Single Nanoparticle, Single Cell, and Single Molecule Monitoring (CS^{3}M)

[3] Department of Civil and Environmental Engineering, Utah State University

[4] PerkinElmer, Inc.

Rapid Analysis of Silver, Gold, and Titanium Dioxide Nanoparticles in Drinking Water by Single Particle ICP-MS

Introduction

As the use of nanoparticles (NPs) in industrial processes and consumer products has increased, so has the likelihood that they will appear in the environment, both through the discharge of industrial waste and from discarded consumer products. Although the concentration of NPs is expected to be low in environmental systems, their impact on human health is unknown. Therefore, the need exists to determine NPs in drinking water systems.

Because of its unique ability for rapid, sensitive and element-specific analysis, single particle ICP-MS (SP-ICP-MS) is an ideal tool for measuring NPs in drinking water systems. This work will highlight the efficiency of drinking water treatment systems in removing silver (Ag), gold (Au), and titanium dioxide (TiO_2) nanoparticles using SP-ICP-MS as the sole analytical technique.

PerkinElmer®
For the Better

Experimental

Chemicals and Materials

Au and Ag nanoparticles were purchased from nanoComposix™ Inc. (San Diego, California, USA), and TiO_2 nanoparticles were acquired from US Research Nanomaterials, Inc. (Houston, Texas, USA). Table 1 shows the sizes and characteristics of the NPs used in this study. Intermediate suspensions were prepared in ultra-high purity water to disperse any agglomerated particle clusters.

Table 1. Nanoparticle Characteristics.

Material	Diameters (nm)	Characteristics
Gold (Au)	50, 80, 100	Capped with citrate
Silver (Ag)	40, 70, 100	Capped with citrate
Titanium dioxide (TiO_2)	100, 160	Uncapped

Water samples studied include ultra-pure water, source water (surface water from Missouri River), and the corresponding drinking water (post- treatment) from three water treatment plants.

Instrumental Conditions

All analyses were performed on a PerkinElmer NexION® 300D/350D ICP-MS using Syngistix™ software with the Syngistix Nano Application Module (PerkinElmer Part No. N8140309). Table 2 shows the instrumental and method parameters used. The sample uptake rate was measured gravimetrically, and the transport efficiency was determined with Au nanoparticles.

All measurements were made against external calibration curves in the Syngistix Nano Application Module. For the dissolved concentrations, calibration standards were made from serial dilutions of single-element stock solutions. Particle calibration standards were made by diluting the appropriate particles to concentrations of approximately 10^5 particles/mL or less to minimize the probability that multiple particles arrive at the plasma at the same time.

Table 2. Instrument and Method Parameters for Single Particle ICP-MS Analysis of Au, Ag, and TiO_2 in Single Particle Mode.

Instrument Parameter	Operation Setting		
Nebulizer	Concentric		
Spray Chamber	Cyclonic		
Cones	Platinum		
RF Power (W)	1400		
Nebulizer Gas Flow (L/min)	1.02-1.06		
RPq	0.5		
Sample Uptake Rate (mL/min)	0.26-0.29		
Dwell Time (µs)	100		
Sample Time (s)	100		
Transport Efficiency (%)	7.5-8.5		
Method Parameters	**Au**	**Ag**	**Ti**
Isotope (amu)	196.967	106.905	46.9518
Density (g/cm^3)	19.3	10.49	4.23
Mass Fraction (%)	100	100	60
Ionization Efficiency (%)	100	100	100

Results and Discussion

Detection Limits

Both the dissolved and particle size detection limits in surface water are shown in Table 3 and were determined by preparing the nanoparticle suspension in filtered river water using SP-ICP-MS mode. The dissolved detection limits are higher than those obtained by conventional ICP-MS measurements due to the short integration times used: 100 µs in this work vs. 1 second or longer (typically) by conventional ICP-MS measurements. The particle size detection limit for TiO_2 is greater than that for Au and Ag due to the particle composition: while Au and Ag particles are pure metal, TiO_2 particles are only 60% Ti. Additionally, $^{47}Ti^+$ was used for titanium measurements, even though it is only 7.4% abundant. The reason for selecting this mass instead of the most abundant titanium isotope ($^{48}Ti^+$ = 73.8% abundant) is that Ca also has an isotope at m/z 48. Since Ca is present at elevated levels in drinking waters, it would interfere with Ti at this mass. Therefore, $^{47}Ti^+$ was chosen for analysis.

Table 3. Detection Limits.

Element	Dissolved (µg/L)	Particle (nm)
Ag	0.10	23-25
Au	0.10	28-30
TiO_2	0.75	65-70

To evaluate the effectiveness of the water treatment process in the treatment plants for Au, Ag, and TiO_2 nanoparticles, water samples were collected both pre- and post-treatment at three water treatment plants. None of the six waters contained measureable amounts of Ag or Au, either as particles or dissolved. However, all source water samples contained TiO_2, as shown in Table 4. Plants 1 and 2 effectively removed both dissolved Ti and TiO_2 particles, as evidenced by the lower amounts present in the post-treatment waters than the pre-treatment ones. The results from Plant 3 differed from the first two plants in that Ti-containing particles could still be detected after treatment, although significantly fewer than pre-treatment. However, all the dissolved Ti was removed.

Table 4. Effectiveness of Three Water Treatment Plants Removing TiO_2 Particles and Dissolved Ti.

Plant	Pre/ Post Treatment	Most Frequent Size (nm)	Particle Concentration (particles/mL)	Dissolved Concentration (µg/L)
1	Pre Post	170 < MDL	432,000 < MDL	17.9 1.21
2	Pre Post	156 < MDL	451,000 < MDL	11.7 1.17
3	Pre Post	153 76	425,000 17,237	10.6 < MDL

Table 5. Spike Recovery Studies in Drinking Waters.

Sample	Au			Ag			TiO_2		
	Most Freq Size (nm)	Part Conc. Spike Recovery	Diss Conc. Spike Recovery	Most Freq Size (nm)	Part Conc. Spike Recovery	Diss Conc. Spike Recovery	Most Freq Size (nm)	Part Conc. Spike Recovery	Diss Conc. Spike Recovery
1	98	97%	80%	98	97%	80%	102	9%	84%
2	97	88%	84%	97	88%	84%	87	6%	88%
3	101	94%	89%	101	94%	89%	87	6%	112%

To check the accuracy, spike recovery tests were performed for all metals, both as dissolved and nanoparticles. Three samples were spiked with 2 µg/L of the dissolved metals and 100 nm nanoparticles at a concentration ≈ 1 x 10^5 particles/mL. Table 5 shows the results of these spike recovery studies, which indicate accurate recoveries, except for the concentration of TiO_2 nanoparticles, which recovered below 10% for each sample. Low recovery for TiO_2 particles was due to aggregation in the standards and in the water matrix. Without the addition of a surfactant, these uncapped TiO_2 particles tended to aggregate, which resulted in particle loss between dilutions and in the water matrix where they had the opportunity to react and form new species and/or aggregate further and fall out of solution. The highest recovery obtained for these particles in ultra-pure water and in water matrix were 24% and 9%, respectively.

Conclusions

This work has demonstrated the ability of the NexION 350 ICP-MS running in Single Particle mode to accurately detect Au, Ag, and TiO_2 nanoparticles in drinking water systems. Real samples analyzed both pre- and post-treatment showed that drinking water treatment processes of the studied water treatment plants effectively remove both dissolved and Ti-containing nanoparticles. (Neither Au nor Ag were detected in these water samples.)

The use of the Syngistix Nano Application Module with the NexION 350 running in Single Particle mode is an ideal tool for nanoparticle analysis in real samples to be able to measure rapidly and continually, very important when analyzing samples with low particle concentrations.

PerkinElmer, Inc.
940 Winter Street
Waltham, MA 02451 USA
P: (800) 762-4000 or
(+1) 203-925-4602
www.perkinelmer.com

PerkinElmer®

012176_01 PKI

APPLICATION NOTE

ICP - Mass Spectrometry

Authors:

Ariel R. Donovan[1,2]

Honglan Shi[1,2]

Craig D. Adams[2,3]

Chady Stephan[4]

[1]Department of Chemistry and Environmental Research Center, Missouri University of Science and Technology
Rolla, Missouri, 65409, United States

[2]Center for Single Nanoparticle, Single Cell, and Single Molecule Monitoring (CS^{3}M)
Rolla, Missouri 65409, United States

[3]Department of Civil and Environmental Engineering, Utah State University
Logan, Utah, 84321, United States

[4]PerkinElmer, Inc., 501 Rowntree Dairy Rd, Woodbridge, On, Canada, L4L 8H1

Monitoring Cerium Dioxide and Zinc Oxide Nanoparticles through Drinking Water Treatments using Single Particle ICP-MS

Introduction

With the increasing use of nanoparticles (NPs) in industrial processes and consumer products, it is inevitable that nanoparticles will make their way into environmental systems, including drinking water. As a result, removal of these nanoparticles from drinking water is important, and the effectiveness of various water treatment processes for removing the nanoparticles needs to be understood.

Two commonly and widely used nanoparticles are zinc oxide (ZnO) and cerium dioxide (CeO_2), which have a global production of 550 t/year and 55 t/year, respectively.[1] Both of these nanoparticles cause acute toxicity that results in oxidative stress and oxidative damage to mammalian cells.[2-5]

Although a variety of techniques are available to measure nanoparticles, single particle ICP-MS (SP-ICP-MS) has become increasingly important due to its speed and ability to measure environmentally relevant low nanoparticle concentrations, surpassing the limitations of light-based technologies.[6-7]

PerkinElmer®
For the Better

This work focuses on the use of SP-ICP-MS to analyze samples simulating real-world systems to measure ZnO and CeO_2 NP size, size distribution, particle concentration, and ionic concentration in the various steps of drinking water treatment processes. Using SP-ICP-MS, the fate and transformation of ZnO and CeO_2 NPs was assessed without any laborious sample preparation steps or extensive data processing using PerkinElmer's NexION® 350D ICP-MS with Syngistix™ Nano Application Software Module. More detailed information about this work was recently published in *Analytical and Bioanalytical Chemistry.*[8]

Experimental

Standard and Sample Preparation

Water samples were collected from the Missouri River in polypropylene bottles. To understand the effects of the various processing steps, river water samples without added nanoparticles and river water spiked with ZnO (80-200 nm) and CeO_2 (30-50 nm) nanoparticles (US Research Nanomaterials, Inc., Houston, Texas, USA) were subjected to the various water treatment processes by simulating the general drinking water treatment process (Figure 1) using a six-gang stirrer system. Before treatment and after each process, the samples were collected and analyzed by SP-ICP-MS to understand the effect of treatment on the ZnO and CeO_2 nanoparticles.

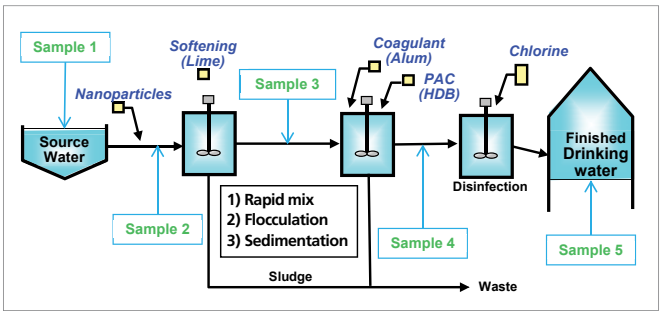

Figure 1. Diagram of simulated drinking water treatment process using the six-gang stirrer system.

Instrumentation and Methodology

All SP-ICP-MS measurements were carried out with a NexION 350D ICP-MS (PerkinElmer Inc., Shelton CT) using the parameters in Table 1. Although Zn at m/z 67 has a lower natural abundance than the other Zn isotopes, it has the fewest potential interferences, so was chosen for this work. In future work, Zn at m/z 66 will be examined in Reaction mode to remove interferences, allowing smaller particles to be measured. Nevertheless, Zn at m/z 67 proved adequate for this work.

Size calibration and transport efficiency studies were carried out with gold nanoparticles (citrate-capped; 50, 80, 100 nm) in 2 mM sodium citrate (nanoComposix™, San Diego, California, USA). Aqueous Ce and Zn calibration standards were made by dilution of 1000 mg/L stock standards (PerkinElmer Inc., Shelton CT).

Table 1. SP-ICP-MS Instrumental and Method Parameters.

Instrument Parameter	Value
Nebulizer	Glass Meinhard Type C
Spray Chamber	Glass Cyclonic
Sample & Skimmer Cones	Platinum
RF Power (W)	1600
Sample Uptake Rate (mL/min)	0.26 -0.29
Dwell Time (ms)	0.1
Sampling Time (s)	100
Transport Efficiency (%)	7.5-8.5

Method Parameter	Zn	Ce
Isotope (amu)	67	140
Density (g/cm^3)	5.61	7.13
Mass Fraction (%)	80.31	81.41
Ionization Efficiency (%)	100	100

Results and Discussion

Before measuring water samples, the CeO_2 and ZnO nanoparticles were first characterized in deionized water to gauge the performance of the methodology; the resulting size distributions are shown in Figures 2a and 2c. The ZnO size distribution is inconsistent, which reflects the wide range stated by the manufacturer (80-200 nm, measured by scanning electron microscopy [SEM] as indicated on the certificate of analysis). The CeO_2 size distribution has a clear maximum at about 25 nm with a wide distribution to larger sizes, which corresponds to the certificate value supplied with the particles. To confirm the inhomogeneity, we also examined these NPs with SEM. The resulting images are shown in Figures 2b and 2d and clearly illustrate the inhomogeneity of both particles, with the ZnO being much more inhomogeneous and irregularly shaped than the CeO_2 particles, which confirms the SP-ICP-MS results.

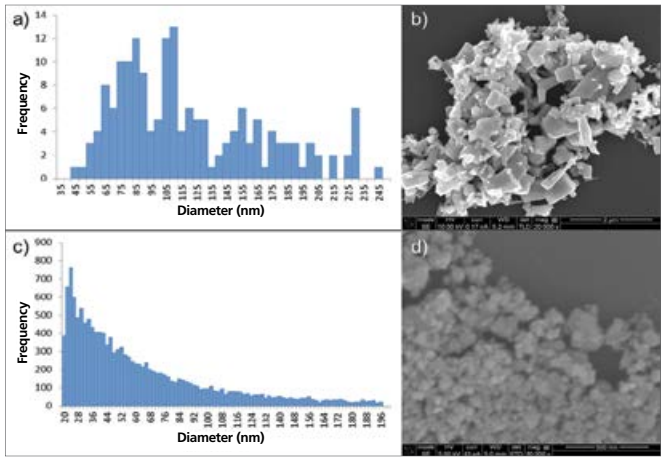

Figure 2. SP-ICP-MS and SEM characterization of ZnO (a and b) and CeO_2 (c and d) NPs.

The NP size detection limits were determined by five times the standard deviation above the background when measuring ultrapure water by SP-ICP-MS. The size detection limits are shown in Table 2. The larger ZnO detection limit is most likely due to the use of $^{67}Zn^{+}$ as the analyte; smaller particles could be detected using a more abundant Zn isotope, although the actual results may be less accurate due to potential interferences.

Table 2. CeO_2 and ZnO NP Size Detection Limits

Nanoparticle	Size Detection Limit (nm)	Dissolved Ion Detection Limit (µg/L)
CeO_2	18-20	0.10
ZnO	35-40	0.20

Next, an untreated river water sample was subjected to each of the treatment steps typically used in water treatment plants: lime softening, alum coagulation with PAC sorption, and disinfection with free chlorine, as shown in Figure 1. Prior to treatment and after each treatment step, the sample was analyzed for CeO_2 and ZnO NPs, as well as their dissolved ions. The same tests were also repeated after spiking the sample with CeO_2 and ZnO NPs at 1×10^6 particles/mL corresponding to mass concentration of 7 µg/L ZnO and 4 µg/L CeO_2.

Table 3 shows the results for ZnO particle size, particle concentration, and dissolved Zn concentration for both the unspiked and spiked sample after each stage of treatment. The results for the unspiked sample indicate that lime softening removes the large ZnO particles, reducing the average size from 75 to 35 nm, and decreases the particle number concentration by 38%. At such particle concentrations (10^6 particles/mL), monitoring the change in the dissolved Zn concentration will not reveal much about the fate of ZnO particles, as they are too small to cause a significant increase in the ionic fraction. Assuming an average particle size of 75 nm, 0.47 µg/L of ZnO would be removed during lime softening. Furthermore, the dissolved Zn concentration also decreased following the lime softening treatment/precipitation process that is causing Zn to drop out of solution. The subsequent water treatment steps did not affect the ZnO particle size or dissolved Zn concentration, but significantly decreased the particle concentration.

Next, the river water was spiked with ZnO NPs, and the same experimental steps were repeated. The results (Table 3) follow the same trends as the unspiked river water. Such observations may suggest that the Zn pulse signals detected in the unspiked river water are ZnO NPs. However, the size is at the detection limit of the NP.

Table 3. Effect of Treatment Steps on ZnO NPs in River Water.

Sample	Parameter	Untreated	Lime	Alum	Chlorine
River Water	Particle Size (nm)	75	35	35	35
	Change in Particle Conc	---	↓38%	↓74% (36%)	↓77% (3%)
	Dissolved Conc (µg/L)	1.11	0.43	0.48	0.52
River Water with ZnO NP Addition (1 x 10^6 parts/mL)	Particle Size (nm)	120	50	50	50
	Change in Particle Conc	---	↓53%	↓79% (26%)	79%
	Dissolved Conc (µg/L)	16.5	0.36	0.46	0.46

The same tests performed with ZnO NPs in the river water samples were repeated with CeO_2 NPs; the results are shown in Table 4. The obtained results demonstrate that the CeO_2 NPs were completely removed during the lime softening treatment, and that no further treatment is needed. It should also be pointed out that CeO_2 NPs are stable in environmental aqueous media and no signs of dissolution were noticed during an up-to-12-hour treatment process.

Table 4. Effect of Treatment Steps on CeO_2 NPs in River Water.

Sample	Parameter	Untreated	Lime	Alum	Chlorine
River Water	Particle Size (nm)	24	---	---	---
	Change in Particle Conc	---	↓> 99%	---	---
	Dissolved Conc (µg/L)	< DL	< DL	< DL	< DL
River Water with CeO_2 NP Addition (1 x 10^6 parts/mL)	Particle Size (nm)	38	---	---	---
	Change in Particle Conc	---	↓> 99%	---	---
	Dissolved Conc (µg/L)	< DL	< DL	< DL	< DL

DL = Detection Limit

A graphical representation of the results from all four sets of experiments appears in Figure 3.

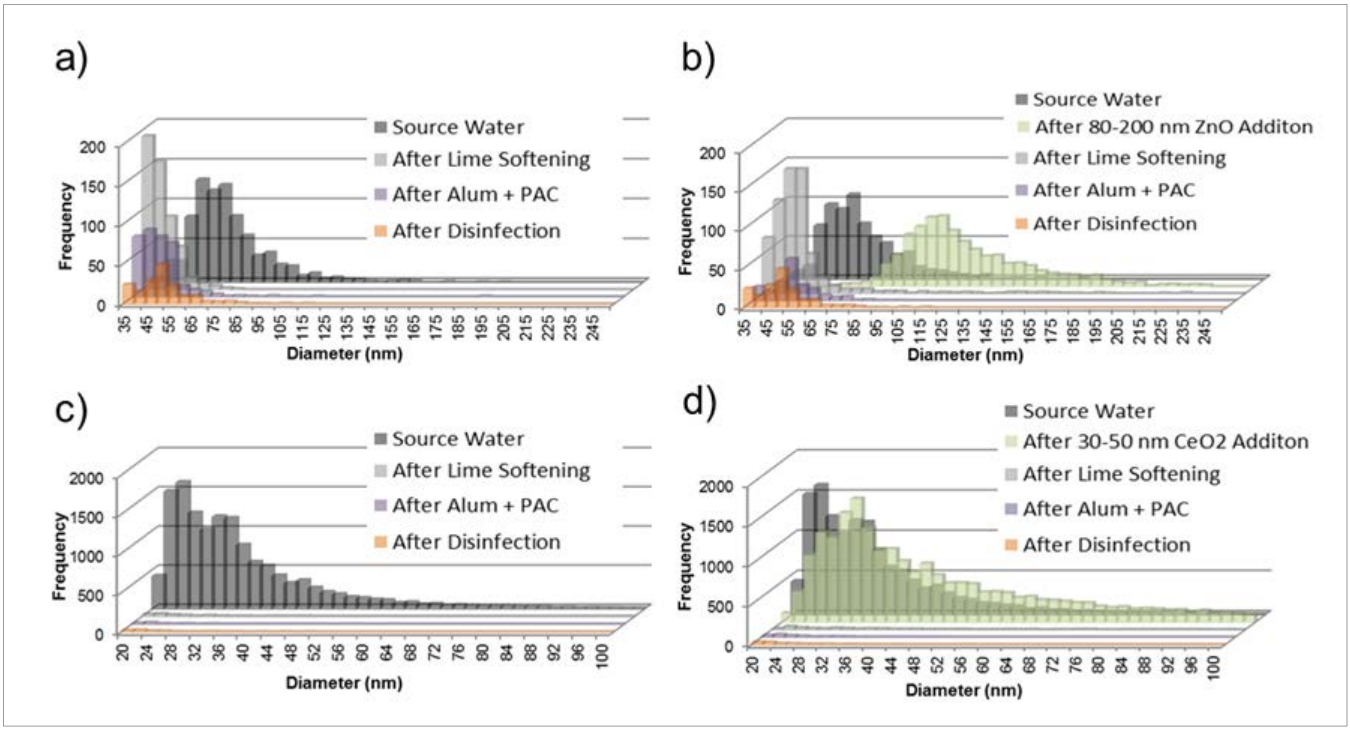

Figure 3. Change in size distribution histograms after sequential drinking water treatments for a) ZnO without NP addition (n=2), b) ZnO with 80-200 nm ZnO addition (n=2), c) CeO_2 without NP addition (n=2), and d) CeO_2 with 30-50 nm CeO_2 addition (n=2).

Conclusion

This work serves as a proof of concept demonstrating the applicability and superiority of SP-ICP-MS as a routine technique in monitoring the efficiency of drinking water treatment process for removal, transformation, and transportation of environmental relevant levels of ZnO and CeO_2 nanoparticles. The results show that the conventional drinking water treatment procedures can reduce up to 80% of ZnO particles and virtually eliminate the presence of CeO_2 nanoparticles. As more complex nanoparticles are being used and introduced in various consumer products, there is an increased need for pilot studies to further investigate the impact of these emerging chemicals on the environment and, subsequently, human health. SP-ICP-MS can serve not only for the pilot research, it may also serve as a rapid tracking technology as part of routine water quality testing for nanoparticles.

References

1. Piccinno, F., Gottschalk, F., Seeger, S., & Nowack, B. (2012) "Industrial production quantities and uses of ten engineered nanomaterials in Europe and the world", *Journal of Nanoparticle Research,* 14(9), 1-11.
2. Weisheng Lin, Yue-wern Huang, Xiao-Dong Zhou, Yinfa Ma. Toxicity of Cerium Oxide Nanoparticles in Human Lung Cancer Cells. *International Journal of Toxicology,* 2006: 25:451–457.
3. Weisheng Lin, Yi Xu, Chuan-Chin Huang, Yinfa Ma, Katie B. Shannon, Da-Ren Chen, Yue-Wern Huang. Toxicity of nano- and micro-sized ZnO particles in human lung epithelial cells. J Nanopart Res. 2009, 11: 25-39.
4. Qingbo Yang and Yinfa Ma. Irradiation-Enhanced Cytotoxicity of Zinc Oxide Nanoparticles, International Journal of Toxicology, 2014, 33(3): 187-203.
5. Xia T, Kovochich M, Long M, Mädler L, Gilbert B, Shi H, Yeh JI, Zink JI, Nel AE (2008) Comparison of the mechanism of toxicity of zinc oxide and cerium oxide nanoparticles based on dissolution and oxidative stress properties. ACS Nano 2 (10):2121-2134. DOI:10.1021/nn800511k.
6. Stephan, C., Neubauer, K. "Single Particle Inductively Coupled Plasma Mass Spectrometry: Understanding How and Why", PerkinElmer White Paper, 2014.7. Hineman, A., Stephan, C. "Effect of dwell time on single particle inductively coupled plasma mass spectrometry data acquisition quality", *JAAS,* 29 (2014), 1252.
8. Ariel R. Donovan, Craig D. Adams, Yinfa Ma, Chady Stephan, Todd Eichholz, Honglan Shi, "Single Particle ICP-MS Characterization of Zinc Oxide and Cerium Dioxide Nanoparticles during Drinking Water Treatment", *Analytical and Bioanalytical Chemistry,* 2016. DOI: 10.1007/s00216-016-9432-0.

Consumables Used

Component	Part Number
50 nm Gold Nanoparticles	N8142302
80 nm Gold Nanoparticles	N8142305
100 nm Gold Nanoparticles	N8142307
1000 ppm Cerium Standard	N9303765 (125 mL) N9300110 (500 mL)
1000 ppm Zinc Standard	N9300178 (125 mL) N9300168 (500 mL)
0.38 mm ID (Green/Green) Flared Peristaltic Pump Tubing for Sample Uptake	N0777042
1.30 mm ID (Gray/Gray) Santoprene Peristaltic Pump Tubing for Drain	N0777444

PerkinElmer, Inc.
940 Winter Street
Waltham, MA 02451 USA
P: (800) 762-4000 or
(+1) 203-925-4602
www.perkinelmer.com

PerkinElmer®

For a complete listing of our global offices, visit www.perkinelmer.com/ContactUs

012724_01 PKI

APPLICATION NOTE

ICP – Mass Spectrometry

Authors:

Mehrnoosh Azodi

Subhasis Ghoshal

McGill University
Montreal, Canada

Chady Stephan

PerkinElmer, Inc.
Shelton, CT

Measurement and Analysis of Silver Nanoparticles in Wastewaters with Single Particle ICP-MS

Introduction

The drastic increase in production and consumption of engineered nanoparticles (ENPs) has raised the concern and questions about their release into the environment and potential harm to aquatic and terrestrial species. The characteristic properties of nanoparticles, such as small size and high specific surface area and reactivity, make them desirable for their use in various products.

Silver (Ag) nanoparticles are among the most commonly used nanoparticles in consumer products due to their antimicrobial properties. Therefore, it is expected that Ag ENPs will find their way into the environment, necessitating a way to accurately and rapidly detect and characterize them in a variety of environmental matrices. Work has already been performed demonstrating the ability to successfully characterize Ag ENPs in a variety of water samples[1-3] and biological media which may be exposed to Ag ENPs in the environment[4].

PerkinElmer®
For the Better

A major source of environmental release is wastewaters, a complex matrix which must be evaluated for the fate of Ag ENPs. The complexity and variety of the wastewater matrices can make the analysis of ENPs challenging.

This work evaluates the ability of SP-ICP-MS to characterize Ag NPs in a dissolved organic solution containing alginate (a common wastewater component) and two wastewater matrices: mixed liquor and effluent.

Experimental

Samples and Sample Preparation

The water samples were collected from a wastewater treatment plant near Montreal, Quebec, Canada. The effluent wastewater was collected after the secondary settling tank, while the mixed liquor was collected from the secondary aeration tank. Both water types were collected in acid-washed, dark glass bottles and sealed. Effluent wastewater is the ultimate treated wastewater which is discharged to the river from this treatment plant, while the mixed liquor is the wastewater which leaves the aeration tank after biological treatment to the secondary settling tank for the suspended solids to sediment. As a result, the mixed liquor has much higher levels of suspended solids and relatively higher dissolved carbon content compared to the effluent wastewater.

Alginate is a polysaccharide which is detected in wastewaters at ppm levels and comprises the dissolved organic carbon fraction of wastewaters. The alginate solution was used as a known control/surrogate for comparison with the wastewater samples. The alginate solutions were prepared from alginic acid sodium salt from brown algae (Sigma-Aldrich, St. Louis, Missouri, USA) at 6 ppm in deionized water by shaking end-over-end for an hour.

Ag ENPs capped with polyvinylpyrrolidone (PVP) with a mean diameter of 67.8±7.6 nm (as determined with transmission electron microscopy [TEM], nanoComposix™ Inc., San Diego, California, USA) were spiked into 10 mL of all samples at a concentration of 10 ppb (5 million particles/mL). The samples were then diluted 10-1000x with deionized water and sonicated for five minutes prior to analysis. All samples were prepared in triplicate.

Instrumental Conditions

All analyses were carried out on a PerkinElmer NexION® 300D/350D ICP-MS operating in SP-ICP-MS mode using the Syngistix™ Nano Application Software Module. Instrumental parameters are shown in Table 1. With these parameters, a transport efficiency of 8.3% was determined.

Table 1. NexION 300D/350D ICP-MS Instrumental Parameters

Parameter	Value
Sample Uptake Rate	0.3 mL/min
Nebulizer	Glass Concentric
Spray Chamber	Glass Cyclonic
RF Power	1600 W
Analyte	Ag107
Analysis Time	100 sec
Dwell Time	100 µsec

Results and Discussion

To determine the accuracy of SP-ICP-MS, the Ag ENPs were added to deionized (DI) water at a concentration of 0.1 ppb (50,000 particles/mL). SP-ICP-MS measurement determined the mean size of the Ag ENPs to be 63.2±0.2 nm (which agrees with the TEM measurements), and the concentration to be 53,758±1363 particles/mL, thus validating the accuracy of the measurements. The values and standard deviations are from the mean of three replicate analyses.

Next, the Ag ENPs were measured in a 6 ppm alginate solution. Figure 1 shows the Ag particle size distribution for 0.1 ppb (50,000 particles/mL), which corresponds to a mean particle size of 66.1±0.1 nm, with a concentration of 52,302±2102 particles/mL. The agreement between the measured and TEM-determined particle sizes indicates that the alginate matrix does not affect the measurement accuracy.

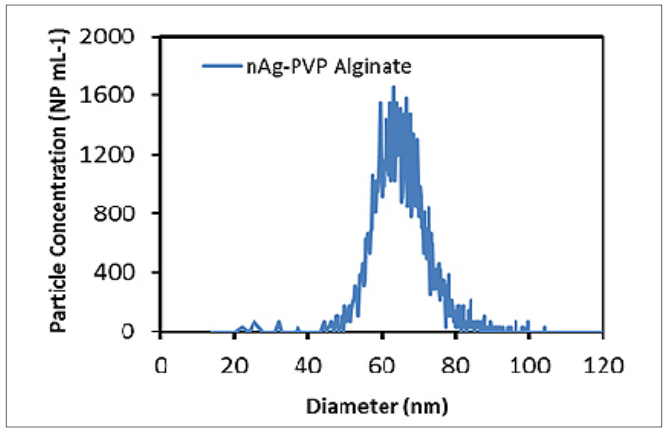

Figure 1. Measured Ag particle size distribution in 6 ppm alginate solution.

With the accuracy of the technique established in the alginate solution, the effluent wastewater and mixed liquor samples were measured next. First, the total Ag concentration was measured in both wastewater samples and was found to range from 25-40 ppt, a level which should not inhibit the determination of Ag ENPs. Figures 2 and 3 show the measured particle size distributions for the effluent and mixed liquor, respectively. The samples were diluted 100x prior to analysis, with Table 2 showing both the measured particle sizes and particle concentrations. Again, the mean particle size agrees with the certificate value, and the particle concentration is close to the calculated value, indicating that neither of the wastewater matrices affects the measurement. These results indicate that Ag ENPs can be successfully measured in wastewater samples.

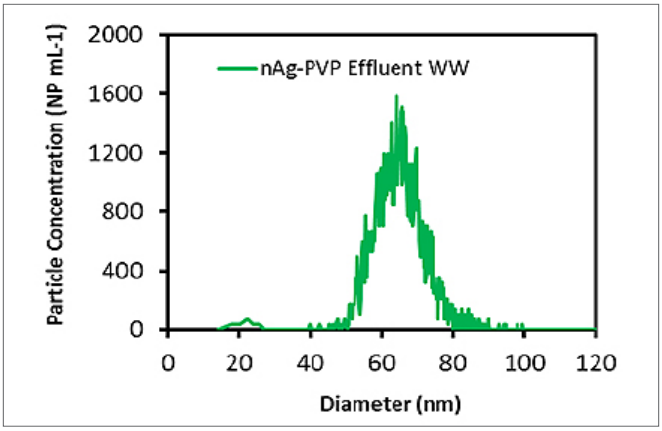

Figure 2. Measured Ag particle size distribution in effluent wastewater diluted 1000 times.

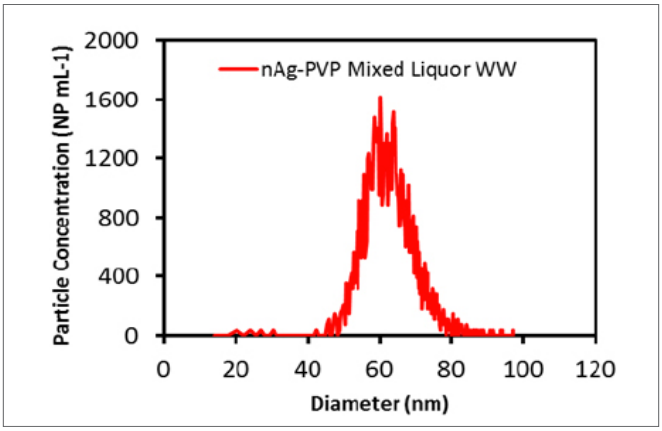

Figure 3. Measured Ag particle size distribution in mixed liquor wastewater diluted 1000 times.

Table 2. Results from Analysis of Wastewater Samples Spiked with Ag NPs.

Sample	Mean Particle Size (nm)	Spiked Particle Conc. (particles/mL)	Measured Particle Conc. (particles/mL)
Effluent Wastewater	66.3±0.2	50,000	54,691±1185
Mixed Liquor Wastewater	63.7±0.4	50,000	53,123±1216

The detection limits for both the Ag particle size and concentrations in the wastewaters were determined. For the determination of particle size detection limits, the diluted samples were analyzed without any Ag ENPs being added. The detection limit was determined by running the unspiked wastewater matrices and observing the particle size which corresponded to the smallest peak recorded in the Syngistix Nano Application Module. For the effluent, the detection limit is about 18 nm, while for the mixed liquor, it is about 12 nm.

To determine the lowest concentration of Ag ENPs which could be detected, Ag ENPs were spiked into DI water and diluted multiple times. The measured particle concentration was then recorded for each concentration. The particle concentration detection limit was determined to be the spiked particle concentration where the measured concentration did not change when the sample was diluted. In this work, the Ag ENP particle concentration detection limit was determined to be 25 ppt (12,500 particles/mL). Since the wastewater matrices did not affect the results, the detection limit was only measured in DI water.

Conclusion

This work has demonstrated the ability of SP-ICP-MS to accurately detect and measure silver nanoparticles in three different types of wastewater samples. Although wastewater matrices are complex, they do not inhibit the ability of SP-ICP-MS to accurately measure the size and nanoparticle concentration.

References

1. Mitrano, D., Ranville, J.F., Stephan, C., "Quantitative Evaluation of Nanoparticle Dissolution Kinetics using Single Particle ICP-MS: A Case Study with Silver Nanoparticle", PerkinElmer Application Note, 2014.
2. Hadioui, M., Wilkinson, K. "Assessing the Fate of Silver Nanoparticles in Surface Waters using Single Particle ICP-MS", PerkinElmer Application Note, 2014.
3. Dan, Y., Zhang, W., Xingmao, M., Shi, H., Stephan, C. "Gold Nanoparticle Uptake by Tomato Plants Characterized by Single Particle ICP-MS", PerkinElmer Application Note, 2015.
4. Gray, E., Higgins, C. P., Ranville, J.F. "Analysis of Nanoparticles in Biological Tissues using SP-ICP-MS", PerkinElmer Application Note, 2014.

Consumables Used

Component	Part Number
Green/Orange (0.38 mm id) PVC Sample Uptake Tubing	N0777110
Gray/Gray (1.30 mm id) Santoprene Drain Tubing	N0777444
Sample Tubes	B0193233 (15 mL) B0193234 (50 mL)

PerkinElmer, Inc.
940 Winter Street
Waltham, MA 02451 USA
P: (800) 762-4000 or
(+1) 203-925-4602
www.perkinelmer.com

PerkinElmer®

012402_01 PKI

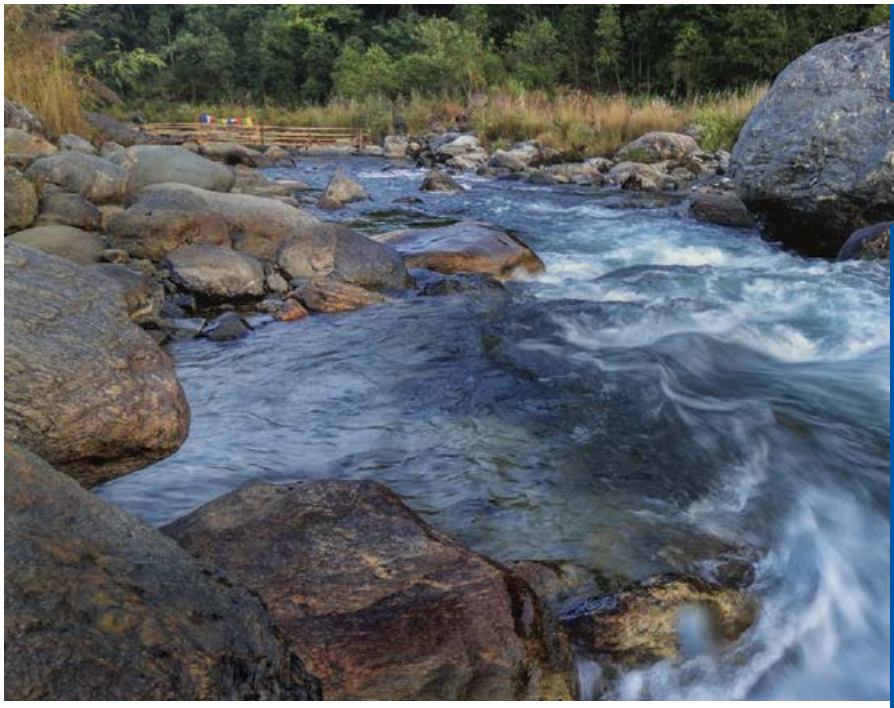

APPLICATION NOTE

ICP - Mass Spectrometry

Authors:

Madjid Hadioui, Ph.D.
Université de Montréal

Kevin Wilkinson, Ph.D.
Université de Montréal

Chady Stephan, Ph.D.
PerkinElmer, Inc.

Assessing the Fate of Silver Nanoparticles in Surface Water using Single Particle ICP-MS

Introduction

During the last decade, the production and use of engineered nanomaterials (ENMs) have experienced a drastic increase, resulting in a potential risk of their release into the environment. Therefore, the study of their impact on the environment becomes crucial. The appropriate ecological risk assessment and management of ENMs in the environment requires quantitative measurements of both exposure and effects[1] that should, ideally, be performed by in situ analysis and give physicochemical characterization. However, most analytical techniques are not suitable for environmental matrices since nanoparticle concentrations are typically very low[2].

Some studies on the persistence, aggregation and dissolution of metal nanoparticles in natural freshwaters and synthetic complex waters were recently published[3-7]. Historically, particle size has been measured by dispersive light scatter (DLS) and tunneling electron microscopy (TEM), while dissolved content has been measured by ultrafiltration. These common techniques have known limitations for measuring low concentrations in the presence of colloidal species in complex waters.

PerkinElmer®
For the Better

Alternatively, single particle inductively coupled plasma mass spectrometry (SP-ICP-MS) has been found to be a promising technique for detecting and characterizing metal nanoparticles at very low concentrations[8-10]. SP-ICP-MS is fast and efficient and can provide more information than other currently available techniques. It can lead to the determination of particle size distribution, particle number concentration, and the proportion of dissolved metal. Moreover, it can distinguish between particles of different elements. The principle of SP-ICP-MS is based on the measurement of the signal intensity produced by a single particle. The suspension of nanoparticles must be sufficiently diluted to make sure that only a single particle reaches the plasma at a time, where it is atomized and ionized, producing a signal of relatively high intensity which is measured as one pulse. If the suspension contains dissolved metal of the same element as in the particles, a constant, continuous signal of that element will be produced as a result of its homogeneous distribution. The recorded signal intensity as a function of time can be processed using a theoretical approach first developed by Duegeldre et al.[11-15] for natural metal colloids and then supported by other authors such as Laborda et al.[16, 17].

Ag, ZnO and TiO_2 are among the most frequently studied nanoparticles[18]. In the case of Ag, this is most probably due to the fact that nanosilver is among the most common nanomaterials found in consumer products and tends to release free Ag^+, especially at low concentration[19]. The aim of this work is to investigate the efficiency of SP-ICP-MS for the detection and characterization of metal nanoparticles in environmental waters where they can be involved in various physicochemical processes as shown by Figure 1. Dissolved silver, including released free ions (Figure 1C) and soluble complexes (Figure 1E), can easily and instantly be measured by SP-ICP-MS. These dissolved species can also be determined by ultrafiltration followed by total metal quantification using ICP-MS or AAS, but this procedure is time consuming since it requires the pre-equilibration of the membrane for at least three cycles of centrifugation, generally 20 min each[19]. Aggregates (Figure 1B) and remaining stable silver nanoparticles (Figure 1G) can be counted and measured by other commonly used techniques (DLS, NTA, TEM) but SP-ICP-MS is the only method that can distinguish between nAg and other colloids in surface water.

Experimental

A PerkinElmer NexION® 350X Inductively Coupled Plasma Mass Spectrometer (ICP-MS) was used for data acquisition using the Nano Application Module within Syngistix™ for ICP-MS software (SP-ICP-MS instrumental parameters are given in Table 1). The sample introduction system consisted of a quartz cyclonic spray chamber, type C0.5 concentric glass nebulizer and a 2 mm bore quartz injector.

Commercially available suspensions of gold and silver nanoparticles were used in this work. A NIST reference material (RM 8013) consisting of a suspension of gold nanoparticles (60 nm nominal diameter, 50 mg/L total mass concentration and stabilized in a citrate buffer) was used to determine the nebulization efficiency. Suspensions of silver nanoparticles were purchased from Ted Pella Inc.: citrate coated (40 and 80 nm nominal diameter) and bare (80 nm nominal diameter) nanosilver suspensions (product numbers. 84050-40, 84050-80 and 15710-20SC, respectively).

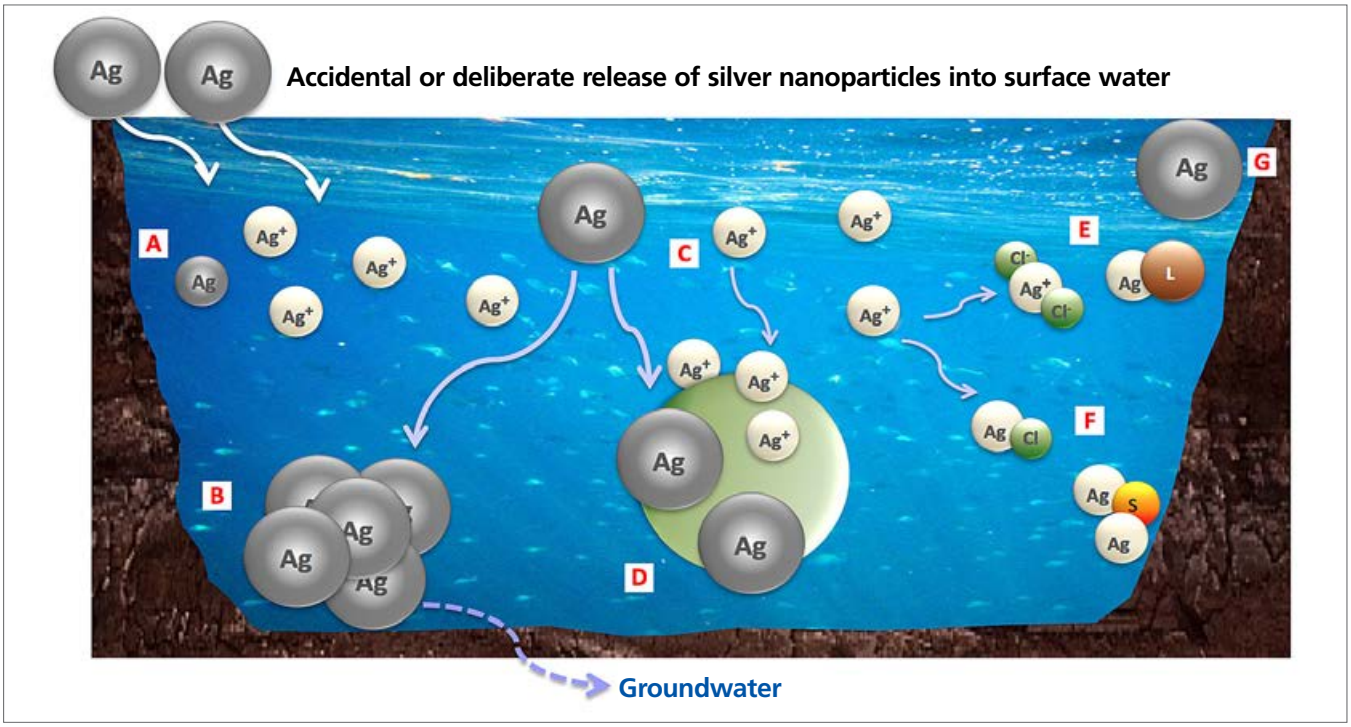

Figure 1. Possible fates of silver nanoparticles in surface waters: (A) Dissolution process leading to free ions release and smaller particles; (B) Aggregation into larger particles, which may settle out of the water, depending on the aggregate size; (C, D) Adsorption of released Ag^+ and nAg, respectively, onto other solids present in the water; (E) Formation of soluble complexes; (F) Reaction with other components in the water, which may result in precipitation; (G) nAg remaining stable.

The surface water was sampled in Rivière des Prairies, Montreal, Canada and filtered with 0.2 µm filter paper prior to spiking with silver nanoparticles. Nano-Ag suspensions were added to water samples with concentrations ranging from 2.5 to 33.1 µg Ag L^{-1} and left to equilibrate under continuous and gentle shaking. Prior to SP-ICP-MS analysis, small aliquots of the samples were diluted to below 0.2 µg Ag L^{-1}.

Data acquisition was performed in triplicate measurements for each sample, and deionized (DI) water was analyzed between replicates to check memory effects. As shown by Figure 2, Syngistix Nano App Module generates frequency vs. size (nm) plots with an interactive focusing window, eliminating the need for any subsequent data processing using theoretical equations[11-17].

SP-ICP-MS data processing is based on distinguishing between the signal of dissolved metal and that of nanoparticles, counting the pulses (or events) corresponding to individual nanoparticles and converting their intensities to particle size. Indeed, the frequency of the events (pulses) provides particle number concentration, and the intensity of each pulse is proportional to the mass of analyte. The latter was converted to volume and then into size knowing the density and the geometry of the particle using the Syngistix Nano Application Module, which provides automated data treatment, so no subsequent manual data processing is required.

Results

Even after filtration of surface waters at 0.2 µm, Nanoparticle Tracking Analysis (NTA), using an LM14 instrument (NanoSight Ltd. – Amesbury, Wiltshire, UK) with a green laser at 532 nm, showed the presence of non-negligible amounts of colloidal particles with an average diameter of ca. 110 nm. Thus, the addition of metal nanoparticles to this complex matrix will make their detection and characterization very difficult, if not impossible, with commonly used techniques (DLS, TEM, etc.).

Table 1. Instrumental parameters for SP-ICP-MS data acquisition.

Parameter	Value
Instrument	NexION 350X ICP-MS
Nebulizer	Concentric
Spray Chamber	Cyclonic
Torch and Injector	Quartz Torch and Quartz 2.0 mm bore injector
Power (W)	1600
Plasma Gas (L/min)	18
Aux Gas (L/min)	1.2
Neb Gas (L/min)	0.97
Sample Uptake Rate (mL/min)	0.5
Sample Tubing	Black/Black
Dwell Time (µs)	100
Sampling Time (s)	60

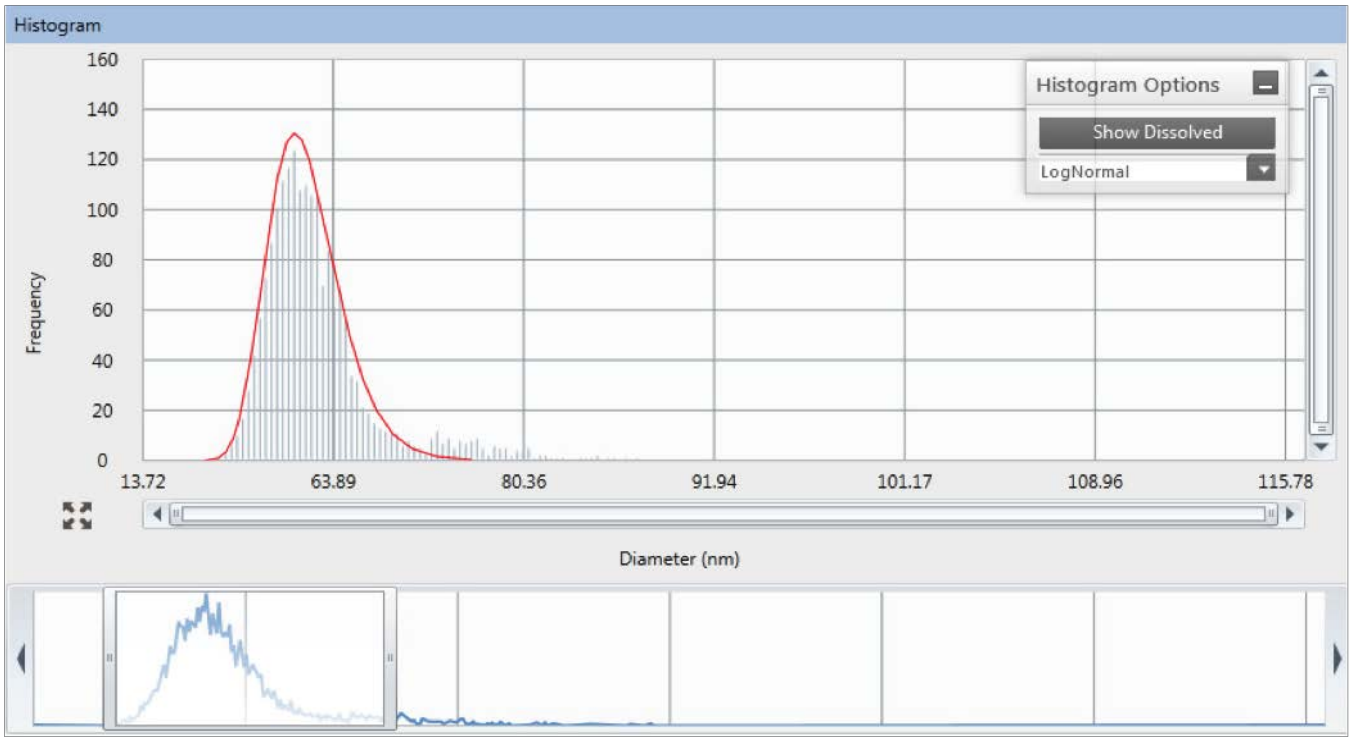

Figure 2. Interactive view of data acquisition with Syngistix for ICP-MS software: signal intensity as a function of acquisition time for silver nanoparticles (bare nAg, 60 nm nominal diameter, total metal concentration 200.8 ng/L) in surface water.

Furthermore, even the determination of the dissolved fraction that is usually performed by ultrafiltration may be inadequate because silver ions may adsorb on the surface of the colloids and, therefore, will be retained by the filtration membrane. Consequently, the proportion of dissolved metal will be underestimated. SP-ICP-MS measurements were found to be more effective and to have fewer limitations than other techniques. Indeed, the presence of other insoluble particles does not interfere with the analysis of silver nanoparticles, as the signal of Ag is recorded independently of the other constituent elements of the colloids.

Figures 3-5 show the evolution of the average particle diameter and the percentage of dissolved metal over time in both pure and river water. In all cases, the average particle size of the persistent nanoparticles remains substantially constant (Figures 3a, 4a and 5a). For suspensions of particles with a nominal diameter greater than 40 nm, between 50 and 80% of the particles persist for at least five days of equilibration in pure and surface water (Figures 3b and 4b). Under the experimental conditions of this work, the coating appears to have no significant effect on the dissolution of nanoparticles over time, as both citrate-coated and bare nAg (80 nm) suspensions showed a slight decrease of particulate silver by ca. 20% during five days. In the meantime, for the same size and equilibration time, the proportion of dissolved silver was found higher in the case of citrate-coated nAg. This does not necessarily mean that bare nanosilver is more stable than citrate-coated nAg. In fact, the release of silver ions may be due to oxidation and/or to residual Ag^+ adsorbed on the surface of nAg or bonded to the coating. Thus, we believe that the stability and behavior of nanoparticles in any medium will depend on the synthesis procedure. According to Figure 5b, smaller particles with a nominal diameter below 40 nm tend to dissolve in greater quantities, but caution should be taken here due to the limitation of the technique to the detection of particles under 20 nm.

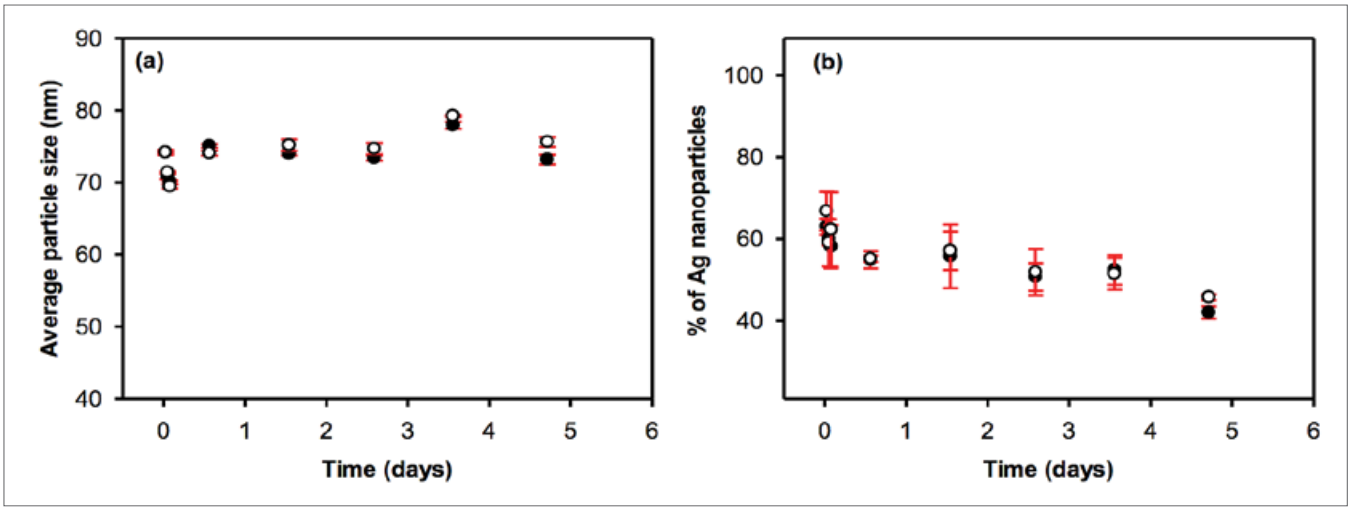

Figure 3. Evolution of (a) the average particle size and (b) the proportion of particulate silver as a function of equilibration time in pure (•) and surface (o) waters. Waters were spiked with 80 nm citrate-coated nAg, and the total metal concentrations were equal to 72.2 and 72.4 ng L^{-1} in DI water and surface water, respectively.

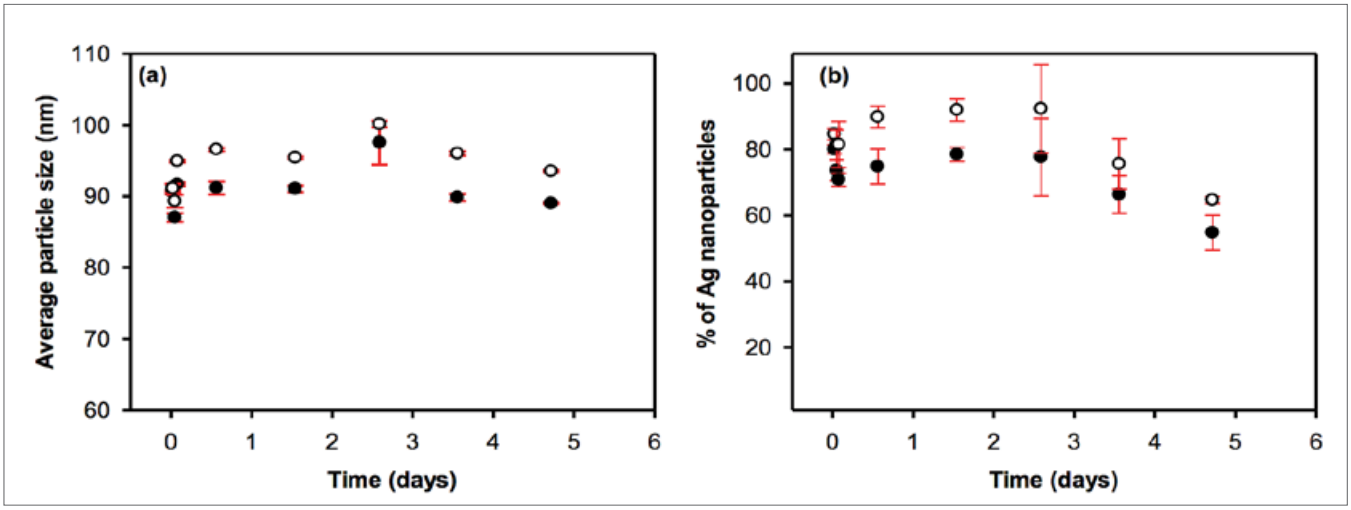

Figure 4. Evolution of (a) the average particle size and (b) the proportion of particulate silver as a function of equilibration time in pure (•) and surface (o) waters. Waters were spiked with uncoated 80 nm nAg, and the total metal concentrations were equal to 196.4 and 200.8 ng L^{-1} in DI water and surface water, respectively.

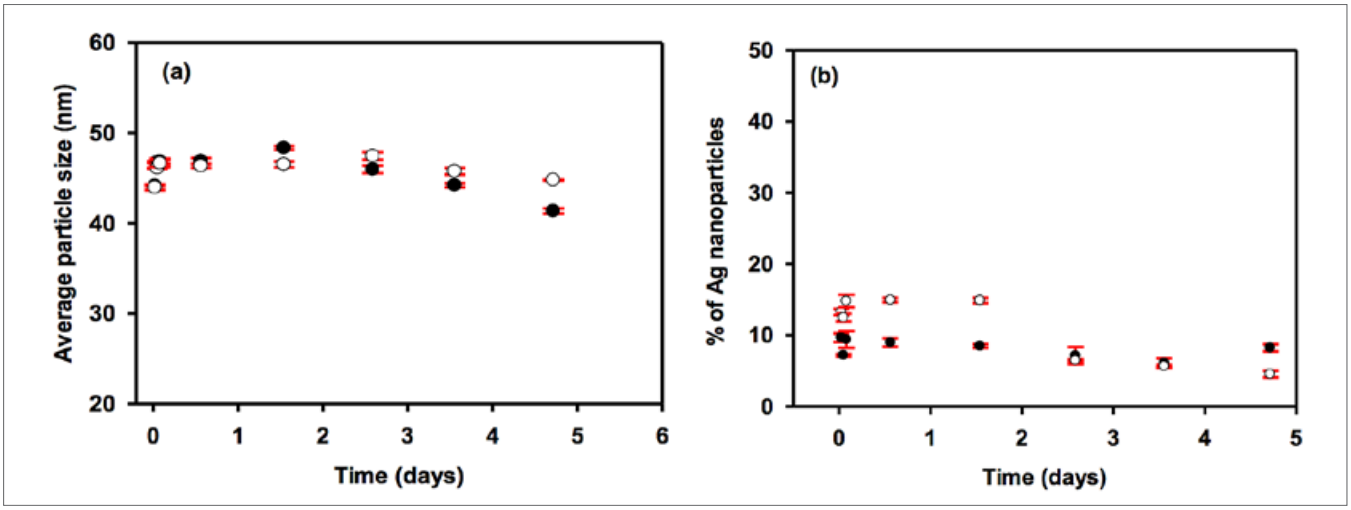

Figure 5. Evolution of (a) the average particle size and (b) the proportion of particulate silver as a function of equilibration time in pure (•) and surface (o) waters. Waters were spiked with 40 nm citrate-coated nAg, and the total metal concentrations were equal to 135.8 and 133.7 ng L^{-1} in DI water and surface water, respectively.

Indeed, the signal intensity of such small nanoparticles is very low and overlaps with the background noise – therefore, all particles smaller than ca. 15 nm will be erroneously counted as dissolved metal. In the case of bare 80 nm nAg, both average particle size and percentage of particles were found higher in surface water compared to DI water (Figure 4). In the case of citrate-coated nAg, no noticeable difference in behavior was found in either aqueous media. This can be explained by the fact that bare nanoparticles are more favorable to aggregation than citrate-stabilized ones. But overall, no significant aggregation was observed.

Conclusion

Using the Nano App Module in the Syngistix for ICP-MS software, it was possible to study the behavior of silver nanoparticles in surface water without using any subsequent manual data processing. The technique has allowed the effective and selective measurement of changing particle size, aggregation and dissolution over time at low concentration. SP-ICP-MS is practically the only suitable technique that can provide such information on the fate of metal nanoparticles at very low concentrations in environmental waters. Although this study only showed the effectiveness of the technique in the particular case of nAg in river water, it is, without any doubt, applicable to other types of metal and metal oxide nanoparticles in a variety of complex matrices form wastewater, effluents to biological fluids and culture media.

References

1. Klaine, S.J., et al., N*anomaterials in the environment: Behavior, fate, bioavailability, and effects.* Environmental Toxicology and Chemistry, 2008. 27(9): p. 1825-1851.
2. Domingos, R.F., et al., *Characterizing Manufactured Nanoparticles in the Environment: Multimethod Determination of Particle Sizes.* Environmental Science & Technology, 2009. 43(19): p. 7277-7284.
3. Chinnapongse, S.L., R.I. MacCuspie, and V.A. Hackley, *Persistence of singly dispersed silver nanoparticles in natural freshwaters, synthetic seawater, and simulated estuarine waters.* Science of the Total Environment, 2011. 409(12): p. 2443-2450.
4. Weinberg, H., A. Galyean, and M. Leopold, *Evaluating engineered nanoparticles in natural waters.* Trac-Trends in Analytical Chemistry, 2011. 30(1): p. 72-83.
5. Van Hoecke, K., et al., *Aggregation and ecotoxicity of CeO_2 nanoparticles in synthetic and natural waters with variable pH, organic matter concentration and ionic strength.* Environmental Pollution, 2011. 159(4): p. 970-976.
6. Badireddy, A.R., M.R. Wiesner, and J. Liu, *Detection, Characterization, and Abundance of Engineered Nanoparticles in Complex Waters by Hyperspectral Imagery with Enhanced Darkfield Microscopy.* Environmental Science & Technology, 2012. 46(18): p. 10081-10088.
7. Li, X. and J.J. Lenhart, *Aggregation and Dissolution of Silver Nanoparticles in Natural Surface Water.* Environmental Science & Technology, 2012. 46(10): p. 5378-5386.
8. Krystek, P., et al., *Application of plasma spectrometry for the analysis of engineered nanoparticles in suspensions and products.* Journal of Analytical Atomic Spectrometry, 2011. 26(9): p. 1701-1721.
9. Tuoriniemi, J., G. Cornelis, and M. Hassellov, *Size Discrimination and Detection Capabilities of Single-Particle ICPMS for Environmental Analysis of Silver Nanoparticles.* Analytical Chemistry, 2012. 84(9): p. 3965-3972.
10. Pace, H.E., et al., *Single Particle Inductively Coupled Plasma-Mass Spectrometry: A Performance Evaluation and Method Comparison in the Determination of Nanoparticle Size.* Environmental Science & Technology, 2012. 46(22): p. 12272-12280.

11. Degueldre, C. and P.Y. Favarger, *Colloid analysis by single particle inductively coupled plasma-mass spectroscopy: a feasibility study.* Colloids and Surfaces a-Physicochemical and Engineering Aspects, 2003. 217(1-3): p. 137-142.

12. Degueldre, C., P.Y. Favarger, and S. Wold, *Gold colloid analysis by inductively coupled plasma-mass spectrometry in a single particle mode.* Analytica Chimica Acta, 2006. 555(2): p. 263-268.

13. Degueldre, C. and P.Y. Favarger, *Thorium colloid analysis by single particle inductively coupled plasma-mass spectrometry.* Talanta, 2004. 62(5): p. 1051-1054.

14. Degueldre, C., P.Y. Favarger, and C. Bitea, *Zirconia colloid analysis by single particle inductively coupled plasma-mass spectrometry.* Analytica Chimica Acta, 2004. 518(1-2): p. 137-142.

15. Degueldre, C., et al., *Uranium colloid analysis by single particle inductively coupled plasma-mass spectrometry.* Talanta, 2006. 68(3): p. 623-628.

16. Laborda, F., et al., *Selective identification, characterization and determination of dissolved silver(I) and silver nanoparticles based on single particle detection by inductively coupled plasma mass spectrometry.* Journal of Analytical Atomic Spectrometry, 2011. 26(7): p. 1362-1371.

17. Laborda, F., et al., *Critical considerations for the determination of nanoparticle number concentrations, size and number size distributions by single particle ICP-MS.* Journal of Analytical Atomic Spectrometry, 2013. 28(8): p. 1220-1232.

18. Baun, A., et al., *Setting the limits for engineered nanoparticles in European surface waters - are current approaches appropriate?* Journal of Environmental Monitoring, 2009. 11(10): p. 1774-1781.

19. Hadioui, M., S. Leclerc, and K.J. Wilkinson, *Multimethod quantification of Ag+ release from nanosilver.* Talanta, 2013. 105(0): p. 15-19.

PerkinElmer, Inc.
940 Winter Street
Waltham, MA 02451 USA
P: (800) 762-4000 or
(+1) 203-925-4602
www.perkinelmer.com

PerkinElmer®

For a complete listing of our global offices, visit www.perkinelmer.com/ContactUs

011646_01

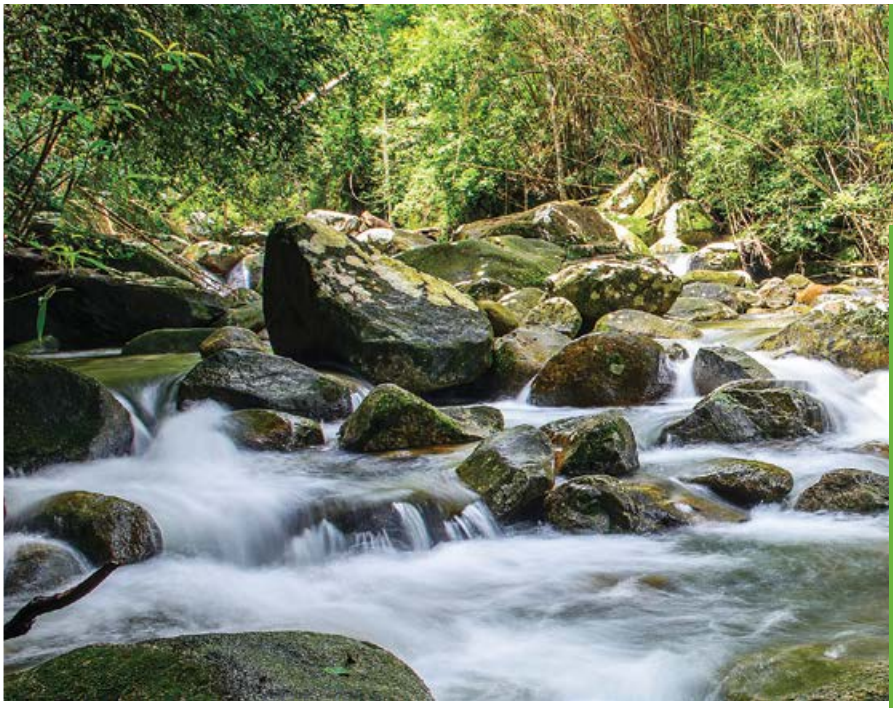

APPLICATION NOTE

ICP - Mass Spectrometry

Authors:

Denise Mitrano

James F. Ranville

Department of Chemistry and Geochemistry
Colorado School of Mines
Golden, CO USA

Chady Stephan

PerkinElmer, Inc.
Shelton, CT

Quantitative Evaluation of Nanoparticle Dissolution Kinetics using Single Particle ICP-MS: A Case Study with Silver Nanoparticles

Introduction

Accurate data on engineered nanoparticle (ENP) environmental behavior and the interplay between ENP size, dissolution rate, agglomeration, and interaction with the sample matrix is critical to appropriately characterize the risks these novel materials may pose to environmental health. The advancement of the single particle ICP-MS (SP-ICP-MS) technique is a great benefit for the study of ENPs in natural systems at environmentally relevant (ng/L) concentrations. Previous studies may have obscured environmentally-relevant transformations because of artificially high ENP concentrations used in the experiments[1]. Therefore, the SP-ICP-MS method is at the forefront to garner the type of information most relevant for environmental risk assessments, namely the precise tracking of changes in ENP size, associated dissolved metal concentration, and determining polydispersity of an ENP sample, all at dilute concentrations in complex solutions. Because dissolution rate is surface-area controlled, the time to complete dissolution is highly dependent on the initial and (potentially stable) intermediate particle sizes. By measuring the change in particle size, as well as the evolution of Ag^+(aq) in solution, using SP-ICP-MS, potential pitfalls related to loss of Ag^+ to experimental materials and to other environmental surfaces, such as suspended sediments or biota in the case of complex matrices, may be avoided.

PerkinElmer®
For the Better

SP-ICP-MS Technique

The theoretical basis of detecting and measuring single particles by SP-ICP-MS has been well-studied in recent years[1-8]. This basis relies on the assumption that at sufficiently short dwell times and low particle number concentrations, detected pulses represent individual particle events. As a result, analysis in single particle mode uses thousands of fast, individual readings with the goal of capturing one (or a slice of one) ENP event. The particle mass can then be determined by the intensity of the ICP-MS response. If the ENP's element is also present as a dissolved species (i.e. dissolved silver vs. a silver nanoparticle), an increase of the baseline is observed in single particle mode. This increase is directly proportional to the instrument's calibration curve of the dissolved species.

In this study, we used the Syngistix™ Nano Application Module for particle measurement/detection and automated data treatment. Determination of the transport efficiency (i.e. the percentage of particles in solution that are detected) is critical to determining the ENP size when using calibrations based on dissolved standards. To avoid coincidence (i.e. two particles being detected in the same pulse), particle concentrations were adjusted so that no more than 1500 particles were detected in 60 s acquisition time[2,6].

Experimental

Materials

Ag ENPs (100 nm diameter, NanoXact, NanoComposix, USA) with polyvinylpyrrolidone (PVP) as a capping agent were examined. ENP suspensions were made by diluting stock solutions (20 mg/L Ag ENPs) with water to yield a final concentration of 50 ng/L Ag ENPs. To match the peak intensities observed by SP-ICP-MS, dissolved Ag standards (High-Purity Standards; QC-7-M) were used for calibration and diluted in 2% HNO_3 (Optima grade) for final concentrations ranging from 0.1-1 µg/L. For determination of nebulization efficiency, 100 nm Au NPs were obtained from BBI™ Solutions (Cardiff, UK) and prepared daily as a 100 ng/L ENP solution in distilled (DI) water.

Water samples analyzed included deionized water (DI, 18.3 M-ohm cm Nanopure), tap water (Colorado School of Mines campus, Golden CO) and surface water. The surface water sample, collected in June 2012 from Clear Creek in Golden, CO, was taken just beneath the water surface, approximately 1 m from the creek bank, and passed through a 0.45-micron filter. The sample was stored in a polyethylene bottle at 20 °C prior to use. The tap water contained approximately 1 mg/L free chlorine, as tested by the Golden, Colorado water treatment facility.

Instrumentation

A PerkinElmer NexION® 350Q ICP-MS was used for analysis. Operating conditions were optimized to produce maximum $^{107}Ag^+$ intensity. Data was collected for 120 seconds, using a dwell time of 100 µs. Aqueous calibration standards included a blank and four dissolved Ag solutions (0-1 µg/L). SP-ICP-MS dissolved standards were made both in 2% HNO_3 and matrix matched to the water chemistry. Acidified samples served as a check standard and a measure of instrument sensitivity, where the latter calibration curve was used for particle sizing. To monitor instrumental drift over time, a single 100 ng/L Ag dissolved calibration check standard was analyzed in SP-ICP-MS mode after every ten ENP samples. All data collection and analysis was done in SP-ICP-MS mode using the Syngistix Nano Application Module.

Analytical Results

Data Collection and Interpretation

Data demonstrating the dissolution of 100 nm PVP Ag ENPs (50 ng/L) in DI are provided in Figure 1, with the decrease in raw pulse intensities being direct evidence of size reduction over time. The corresponding dissolved Ag^+ increase over time was also observed by the elevated background counts (i.e. in the region below 50 counts, in this analysis).

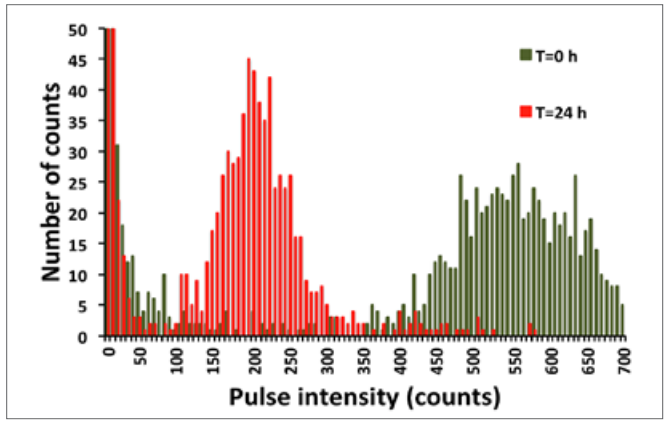

Figure 1. Raw data of 100 nm PVP capped Ag ENPs suspended in DI water, analyzed at 0 h (start of experiment) and after 24 h. Note decreased pulse intensity of main particle distribution histogram and increased background counts in the 24 h sample, indicating increased Ag^+ in solution.

Comparison of Dissolution in Various Water Chemistries

The dissolution of Ag particles was studied over 24 h in deionized (DI) water, tap water, and creek water. Particle distribution histograms were generated for each of the waters (Figure 2). The evolution of particle size and relative distribution can be noted both 1) within a given dissolution set and 2) across water chemistries by comparing diagrams. The average size was computed so the speed of dissolution could be more easily visualized (Figure 3). Dissolution in chlorine-containing tap water was faster than all other solutions examined. This result is expected since chlorine can act as an oxidizing agent, expediting dissolution in this system. Very little change in particle size was observed in the creek water. Natural systems are inherently complex, and thus difficulties arise in pointing to the factors which contribute to particle stability. However, the results from this study suggest dissolved organic carbon in the creek water may be one of the most relevant predictors of dissolution in natural waters, either by acting as a sink for oxidants in the system or physically protecting particle surface from oxidation/dissolution.

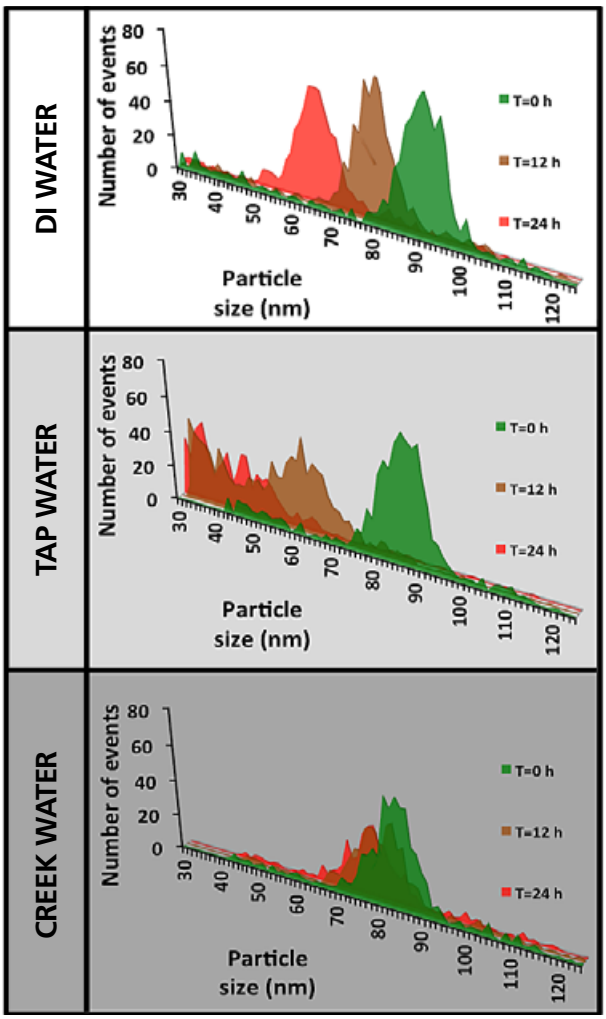

Figure 2. Particle size distribution of Ag ENP suspended in various water chemistries (DI, tap, and creek waters) over 24 h. Evidence of decreasing particle diameter with time through particle oxidation and dissolution in some samples (e.g. DI and tap waters) with less change in particle size observed in other samples, (e.g. creek water).

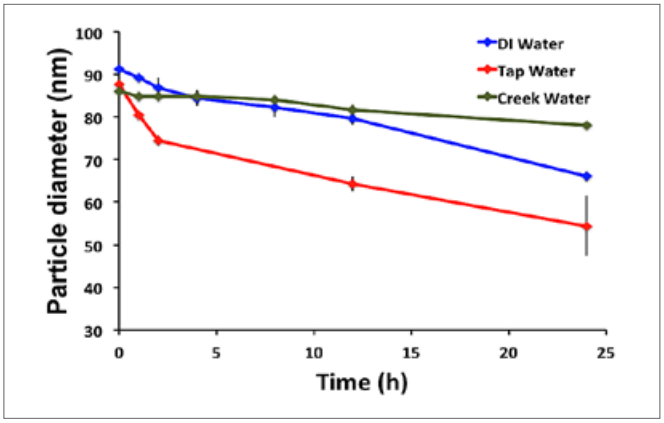

Figure 3. Comparison of Ag ENP dissolution in various waters over 24 hours. Error bars represent standard deviation from triplicate experiments.

Calculating Dissolution Rate Kinetics

Computation of dissolution rates is possible with the information that was collected using SP-ICP-MS. Using the instantaneous average particle diameter, the mass of Ag lost from the original particle can be calculated. After normalizing by calculated geometric surface area for that size particle (assuming spherical particles), the mass of Ag lost per surface area (mol/cm^2) versus time can be examined to obtain the dissolution rate constant. As shown in Figure 3, Ag ENP dissolution follows the first-order kinetics under the studied conditions. However, an inspection of the resultant data indicated that the dissolution rate was not necessarily constant for all time points – two rates were calculated for longer (up to 168 h) experiments: one rate for the < 24 h and one for time points > 24 h. For a more detailed description, see Mitrano et. al[1].

Conclusions

Dissolution potential could be a key component of the screening process for categorizing ENPs with common hazard potential based on their release of ionic species. This study demonstrates the utility of SP-ICP-MS to quantitatively evaluate dissolution kinetics for Ag ENPs under a wide range of conditions. This is particularly important in that only a limited number of methods can be directly applied to aqueous samples, especially considering expected ENP concentrations. Two specific highlights of the benefits of using the SP-ICP-MS technique to measure dissolution in complex samples include:

1) The measurement of primary particle size as the metric of dissolution is more direct than attempting to measure the increase of Ag^+ in solution and

2) This is possible even when known sinks in the system for Ag^+ exist (e.g. sediments, biota, sampling container).

References

1. Mitrano, D. M.; Ranville, J.; Bednar, A.; Kazor, K.; Hering, A. S.; Higgins, C., Tracking dissolution of silver nanoparticles at environmentally relevant concentrations in laboratory, natural and processed waters using single particle ICP-MS (spICP-MS). Environmental Science: Nano 2014.
2. Mitrano, D. M.; Barber, A.; Bednar, A.; Westerhoff, P.; Higgins, C.; Ranville, J., Silver nanoparticle characterization using single particle ICP-MS (SP-ICP-MS) and asymmetrical flow field flow fractionation ICP-MS (AF4-ICP-MS). J. Anal. At. Spectrom. 2012, 27, 1131-1142.
3. Mitrano, D. M.; Lesher, E. K.; Bednar, A. J.; Monserud, J.; Higgins, C. P.; Ranville, J. F., Detection of nano-Ag using single particle inductively coupled plasma mass spectrometry. Environ Toxicol Chem 2012, 31, 115-121.
4. Laborda, F.; Jimenez-Lamana, J.; Bolea, E.; Castillo, J. R., Selective identification, characterization and determination of dissolved silver (I) and silver nanoparticles based on single particle detection by inductively coupled plasma mass spectrometry. J. Anal. At. Spectrom. 2011, 26, (7), 1362-1371.
5. Degueldre, C.; Favarger, P.; Wold, S., Gold colloid analysis by inductively coupled plasma-mass spectrometry in a single particle mode. Analytica Chimica Acta 2006, 555, (2), 263-268.
6. Reed, R.; Higgins, C.; Westerhoff, P.; Tadjiki, S.; Ranville, J., Overcoming challenges in analysis of polydisperse metal-containing nanoparticles by single particle inductively coupled plasma mass spectrometry. J. Anal. At. Spectrom. 2012.
7. Pace, H. E.; Rogers, N. J.; Jarolimek, C.; Coleman, V. A.; Higgins, C. P.; Ranville, J. F., Determining transport efficiency for the purpose of counting and sizing nanoparticles via single particle inductively coupled plasma mass spectrometry. Analytical Chemistry 2011, 83, (24), 9361-9369.
8. Tuoriniemi, J.; Cornelis, G.; Hassellöv, M. Size Discrimination and Detection Capabilities of Single-Particle ICPMS for Environmental Analysis of Silver Nanoparticles. Analytical Chemistry 2012, 84, 3965-3972.

PerkinElmer, Inc.
940 Winter Street
Waltham, MA 02451 USA
P: (800) 762-4000 or
(+1) 203-925-4602
www.perkinelmer.com

PerkinElmer®

011750_01

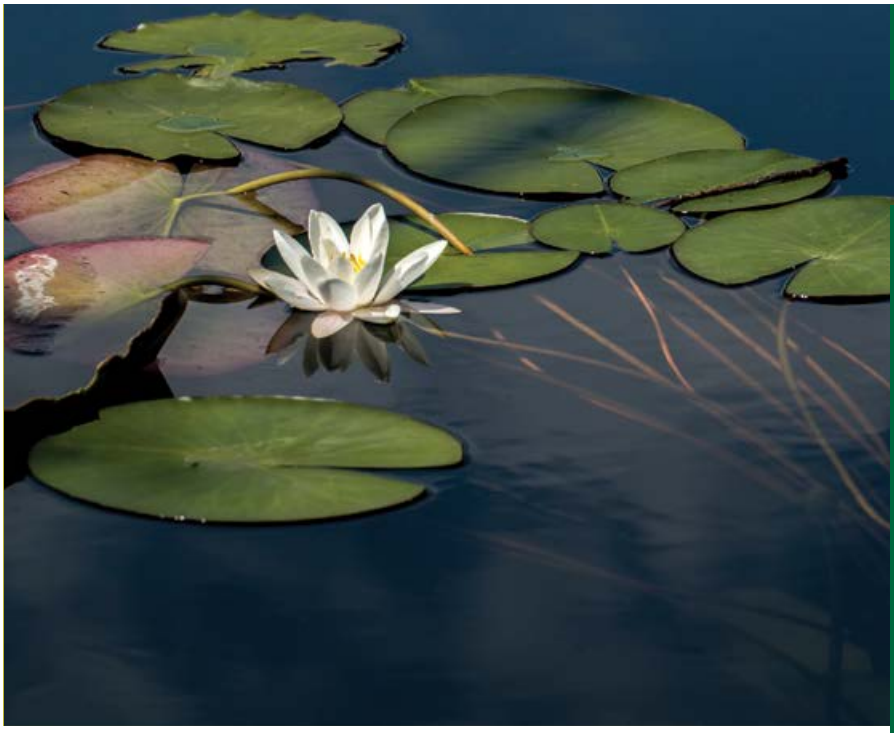

APPLICATION NOTE

ICP - Mass Spectrometry

Authors:

Ruth Merrifield

Jamie Lead

Center for Environmental NanoScience and Risk (CENR)
Arnold School of Public Health
University of South Carolina

Chady Stephan
PerkinElmer, Inc.

Transformations of Gold-Silver Core-shell Nanoparticles in Exposure Media Measured by SP-ICP-MS

Introduction

Engineered nanoparticles (ENPs) are widely used in both industrial processes and consumer products, and, therefore, have well-controlled properties and characteristics for their specific applications. Through their use, ENPs will inevitably make their way into the environment. However, it can be expected that that ENP concentrations in the environment will be much lower than those produced and used in industry. The fate and behavior of ENPs in the environment is largely unknown, mostly due to a combination of the complexity of environmental systems along with the tailored characteristics of ENPs. However, ENPs can undergo numerous transformations: aggregation, dissolution, chemical interactions with salts/metals in the media, and physical interactions are just a few of the possibilities.

PerkinElmer®
For the Better

Current research into environmentally-induced ENP transformations is limited by analytical instrumentation capabilities, including detection limits, sample preparation, and/or time required for data acquisition/analysis. As a result, a multi-method approach is usually required to measure size, aggregation/dissolution kinetics, and chemical alterations; commonly-used techniques include electron microscopy, optical microscopy/spectroscopy, and separation of particulate sizes and ionic fractions. Most of these methodologies require ENP concentrations of at least 25 - 50 µg/L, with the majority of studies being done at 100 - 1000 µg/L. These concentrations are much greater than those typically predicted to be in environmental systems, which for most ENPs is less than 1 µg/L.

Studying ENPs at higher concentrations drastically alters factors that affect transformations, including increased probability of ENP-ENP interactions, lower ENP-to-salt ratios (ENP:salt), and lower ENP-to-natural-organic-matter ratios (ENP:NOM). In fact, previous studies have shown that ENP transformations at 1000 µg/L are different to those at 100 µg/L.[1, 2]

This work shows that single particle inductively coupled plasma mass spectrometry (SP-ICP-MS) is able to overcome the particle concentration limitations of other techniques, almost eliminate sample preparation, and dramatically reduce the acquisition time required to accurately measure the size, size distribution, and particle number concentration (part/mL) of ENPs at more environmentally relevant concentrations (less than 1 µg/L).

SP-ICP-MS is used to study the transformations of ENPs under controlled conditions (meant to mimic toxicological and environmental systems) at time points over a 48-hour period (a typical acute exposure period). This fundamental understanding and methodology can be applied to real-world samples.

Silver (Ag) ENPs were chosen for this case study due to their use in many commercial products, increasing their likelihood of entering environmental systems. They have been shown to be highly toxic, especially in smaller organisms such as bacteria and algae.[3, 4] They are known to react in the presence of sulfide, NOM, chloride, and exposure to natural light. Recently, it has also been shown that Ag NPs can be formed in solutions containing ionic Ag and NOM when exposed to light and heat,[5, 6] thus adding extra complications to the measurement of Ag ENP transformations. Because of the speed and complexity of these transformations, it was decided to use core-shell particles consisting of a less reactive core material (Au) with an Ag shell.

Experimental

Standards, Samples, and Sample Preparation

All exposures were performed with gold-silver core-shell nanoparticles (denoted as Au@Ag) which consist of a 30 nm gold (Au) core and a 15 nm silver (Ag) shell to give a final particle diameter of about 60 nm (Nanocomposix™, San Diego, California, USA). These particles were chosen so that the internal Au NP could be used to monitor the complicated Ag transformations. This difference in reactivity allows a more accurate characterization of the processes occurring in solution.

Transport efficiencies were determined with 30 nm Au nanoparticles (NIST™ 8012, Gaithersburg, Maryland, USA) at a concentration of 100,000 particles/mL. Dissolved calibration standards for both Au and Ag (1, 2, 3 µg/L) were made by serial dilutions of 1000 mg/L stock solutions (Fisher Scientific™). All standards and blanks were made fresh before use and were matrix matched with the exposure samples.

Exposure studies were carried out in three different media: deionized water (DIW), moderately hard water (MHW), and MHW with the addition of 2.5 mg/L fulvic acid (FA); the specific characteristics of these waters are shown in Table 1. The MHW was synthetically produced using EPA guidelines (all chemicals from Fisher Scientific™). These matrices were chosen to cover a variety of situations: a control (DIW), a typical drinking water (MWH), and a sample which more closely mimics environmental surface waters (MHW-FA).

To ensure no particle carryover, a three-minute wash cycle followed each sample: 2 minutes of 1 % aqua regia (to dissolve any remaining ENPs) and 1 minute of ultrapure water to wash out the acid. The size and concentration of freshly made Au@Ag solutions and Au 30 nm NIST particles were measured before and after each time point and periodically between exposure samples to ensure that standard solutions were still returning the correct results.

Table 1. Characteristics of Water Samples.

Media	Acronym	pH	Composition
Deionized Water	DIW	5.3	---
Moderately Hard Water	MHW	7.4 - 7.8	Sodium hydrogen carbonate (96 mg/L)
			Magnesium sulfate (60 mg /L)
			Calcium bicarbonate (60 mg /L)
			Potassium chloride (4 mg /L)
Moderately Hard Water with Fulvic Acid	MHW-FA	7.4 - 7.8	Sodium hydrogen carbonate (96 mg/L)
			Magnesium sulfate (60 mg/L)
			Calcium bicarbonate (60 mg/L)
			Potassium chloride (4 mg/L)
			Suwannee River fulvic acid (2.5 mg/L)

The studies were carried out with particle concentrations between 10 thousand (K) and 44 million (M) parts/mL (0.01 – 46 µg/L of Ag). Solutions were subjected to different conditions (as shown in Table 2) for 48 hours. Conditions were controlled using an Innova® 44 incubator shaker (New Brunswick Scientific™), fitted with a broad spectrum UV/Vis (Ultra Violet/Visible) lamp. Aliquots of the samples were removed at time intervals of 0, 12, 24, and 48 hours during the exposure and analyzed immediately without any extra sample preparation to ensure as little change as possible from the original sample. The Ag signal was measured, followed by the Au signal as the Ag component of the ENP is more susceptible to changes than the Au.

Analytical Conditions

All SP-ICP-MS data was acquired with a PerkinElmer NexION® 350D ICP-MS operating in single particle mode with the Syngistix™ Nano Application Software Module using the conditions specified in Table 3. All samples were run twice: once while monitoring Ag and once for Au. Each analysis provided the following information: particle size, particle concentration, most frequent size, mean size, and dissolved (ionic) concentration.

A core-shell particle in SP-ICP-MS will be measured as two different diameters (one for the Ag signal and one for the Au signal), neither of which will read as the expected total size of the ENP. In this case, the Au particle size will be seen as about 30 nm, as expected from the manufacturer. But the particle size of the Ag layer will be seen as smaller than 60 nm. A simple calculation can be performed to determine the number of atoms[7] expected in the 15 nm Ag shell, which is equivalent to a diameter of 57 nm. An important fact to keep in mind is that by removing 3 nm of Ag atoms from the surface of a 60 nm particle, there are enough atoms to make a 30 nm Ag ENP. This fact can imply that an increase in particle number concentration is possible, indicating the dissolution and re-precipitation of silver in the studied media.

Table 2. Exposure Test Conditions.

Set	Test	Media	Particle Concentration	Temperature (°C)	Light Exposure Time (hours)	Exposure Duration
1	1	DIW, MHW, FA	100 K	15	0	48
	2	DIW, MHW, FA	100 K	15	16	48
	3	DIW, MHW, FA	100 K	22	0	48
	4	DIW, MHW, FA	100 K	22	16	48
2	5	MHW	10 K, 50 K, 100 K, 250 K, 22 M, 44 M	22	16	48
	6	FA	10 K, 50 K, 100 K, 250 K, 22 M, 44 M	22	16	48

K=thousand; M=million

Table 3. NexION 350D ICP-MS Instrumental Conditions.

Parameter	Value
Sample Uptake Rate	0.31 mL/min
Nebulizer	Meinhard™ glass concentric
Spray Chamber	Glass cyclonic
Injector	2 mm ID, quartz
RF Power	1600 W
Dwell Time	100 µs
Electronics Settling Time	0 µs
Data Acquisition Time	60 – 300 sec
Transport Efficiency	9-11 %
Analytes	^{107}Ag, ^{197}Au
Tubing	Orange/green (0.38 mm id)
Spray Chamber	Cyclonic
Cones	Platinum
RF Power (W)	1400

Results and Discussion

In all studies, the ENPs were maintained in controlled environments for 48 hours, with aliquots withdrawn at 0, 12, 24, and 48 hours for analysis. By monitoring the particle size and number concentration (for both Ag and Au) over time, the degree of ENP transformation (aggregation, dissolution, and dissolution/re-precipitation) can be observed. An increase in both Au and Ag particle size, with corresponding decrease in particle number, indicates aggregation, while a decrease in Ag particle size and stable Au particle size indicates dissolution. An increase in Ag diameter while the Au diameter remains unchanged, but a decrease in Ag and Au particle numbers indicates a more complicated transformation, such as ENP aggregation alongside Ag dissolution and reprecipitation onto the NPs in suspension.

Two sets of conditions were used. The first (experiments 1-4 in Table 2) were chosen to simulate some standard toxicological test conditions[3, 8] and synthetic surface waters, which includes temperature, UV exposure, and the presence of natural organic matter (NOM). The second set looked at the effect of ENP concentration on transformations (Table 2, experiments 5-6). The highest concentration is similar to that used in recent ENP transformation exposures,[1] and the lower end is in the range expected to be found in the environment.[9]

The first study revealed that the different conditions affected which processes were most prevalent in Ag ENP transformations. Figure 1 A-D (A: 15 °C no light exposure; B: 15 °C 16 hrs light exposure; C: 22 °C no light exposure; and D: 22 °C 16 hrs light exposure) displays the % change of the ENP diameter from 0 to 48 hours. (The results at 12 and 24 hours are trending in the same direction as those for 48 hours, and are not included here for clarity). A negative change indicates the particle decreasing in diameter, while a positive change indicates an increase in particle diameter.

Figure 1 shows the % change in particle diameter after 48 hours for a high and low concentration of the NP suspensions in all three media and under four different conditions (described in Table 2). At low temperatures (Figure 1 A and B), there is very little difference in the ENP between the light and dark conditions, with the exception of FA at the lower concentration when exposed to light. In general, there is a reduction in Ag size, while there is no significant change in the Au size for both light and dark. There is also no significant change in the particle number from 0 to 48 hours for both the Ag and Au signals. The evidence suggests dissolution of the outer Ag shell. In the FA suspensions, the same trends are observed for both the concentrations in the dark and the higher concentration when exposed to light. But there is a slight increase in both the Ag and Au size for the lower concentration with light, suggesting that the light is causing an interaction with the ENPs and resulting in increased stability, although some aggregation is still observed.

More drastic changes were observed at a higher temperature, both at low and high concentrations. Figure 1C shows the changes seen at 22 °C with no light exposure. For the higher concentration, a positive % change can be seen for both the Ag and Au NP diameter (there is a corresponding negative change in the particle number for both Ag and Au signals) for the DIW and MHW media. This suggests that aggregation is occurring in both of these suspensions. For the high concentration FA suspension and all the suspensions for the low concentrations, there is a positive change for the Ag size and no real change for the Au size. Along with this observation, the Ag particle numbers are also increasing, while the Au particle number remains stable. This suggests a complicated process is occurring, where dissolution is taking place, and the ions are either reprecipitating (i.e forming new Ag particles) or causing a ripening effect on the outside of existing particles in suspension, causing an Ostwald ripening effect.

At 22 °C, the presence of light (Figure 1 D) causes a dramatic change. At the higher concentrations, there is an increase in ENP diameter for all three suspensions in both the Ag and Au case. There is also a decrease in particle number for these suspensions with the most significant decrease occurring in the DIW experiment. Thus, aggregation is occurring in all samples to some extent. However, there is a "protective" effect occurring in both the MHW and FA cases. For the lower concentrations, there is no significant % change in the Au NP diameter but a % decrease in the Ag diameter. However, there is an increase in the number of Ag particles / mL with the least amount of change for the DIW suspension. This suggests that the heat and light are causing the ENPs to dissolve rapidly, but in the presence of MHW and FA, there is some reprecipitation occurring.

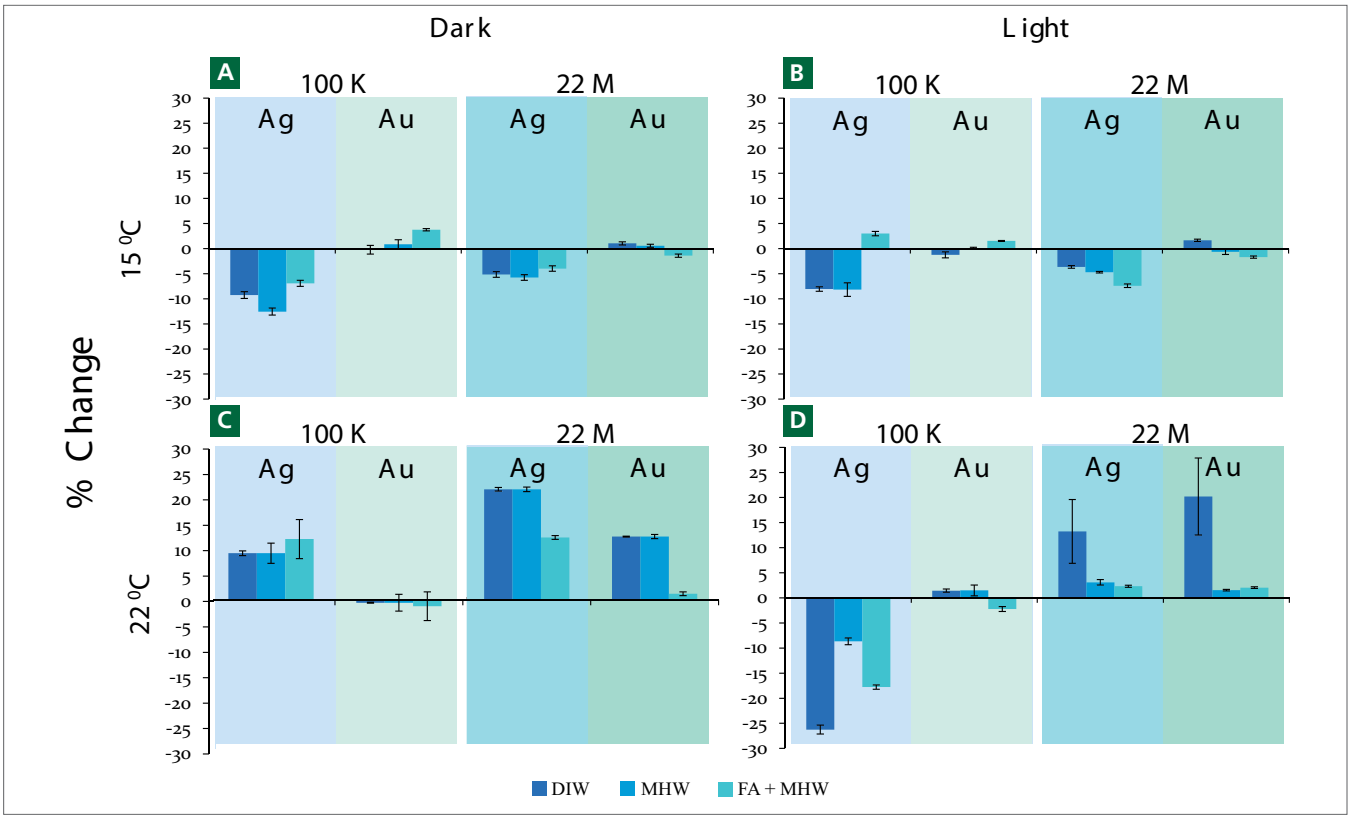

Figure 1. Effect of light, particle concentration, matrix, time, and temperature on ENP transformations for A) 15 °C no light exposure, B) 15 °C 16 hrs light exposure, C) 22 °C no light exposure and D) 22 °C 16 hrs light exposure.

From this study, we can see that temperature, exposure to light, presence of NOM, and ENP concentration all have a significant effect on the types of ENP transformations. At both temperatures, ENPs in all waters behave similarly in the dark, whereas there is a significant difference between the high and low concentrations at 22 °C with light exposure.

The second set of studies (Experiments 5-6 in Table 1) explored the effect of particle concentration on ENP transformations at 22 °C, with 16 hours of UV exposure over 48 hours. Figure 2 shows the % change from 0 to 48 hours for (A) the particle diameter and (B) part /mL for the ENPs in MHW (for comparisons, the actual measured values can be seen in the corresponding Table, C). The graphs show the results for six concentrations ranging from 44 M to 10 K part / mL.

It can be seen that at 44 M and 22 M, there is an increase in both the Ag and Au particle diameter and a corresponding decrease in part/mL. The number of part/mL drops at the same rate for both the Ag and Au signals; since these are core-shell particles, it can be assumed that the particles are undergoing aggregation due to their equivalent loss. At concentrations of 250 K and below, the Ag ENP size decreases, while their concentration increases. For these sample conditions, the Au particle diameter and number do not change significantly over 48 hours. These observations suggest that the Ag layer is not only dissolving from the particle, but also reprecipitating as other particles, possibly as a silver complex (sulfide, oxide or chloride). The % change in Ag particle diameter and part/mL becomes larger as the original concentration of particles in suspension is decreased, meaning that the drop in original concentration causes the dissolution and reprecipitation rate to increase over 48 hours.

Figure 3 shows the % change after 48 hours for the particle diameter (A) and ENP concentration (B) along with the measured values (C) for original concentrations between 44 M to 10 K part/mL in FA media. The highest concentrations of 44 M and 22 M part/mL show a positive change in particle diameter for the Ag signal only with a corresponding negative change in particle number for both Ag and Au. The stability in the Au particle diameter along with the growth in Ag diameter suggests that the Ag layer is growing due to the deposition of Ag ions onto the surface or onto fulvic acid molecules that are bound to the ENP surface. This, along with the decrease in part/mL for both Ag and Au signals, implies that not only are the particles aggregating and settling out of the suspension, but they are also dissolving, and the excess Ag ions are depositing onto the suspended particles. This highlights the necessity of the core-shell particle, as just looking at the Ag data would lead to the conclusion that the particles are aggregating.

At concentrations below 250 K, the Au particle diameter and particle number are stable. But there is a decrease in the Ag particles size and increase in the Ag particle number suggesting dissolution and precipitation of the ENPs that is increasing in rate as a function of particle number.

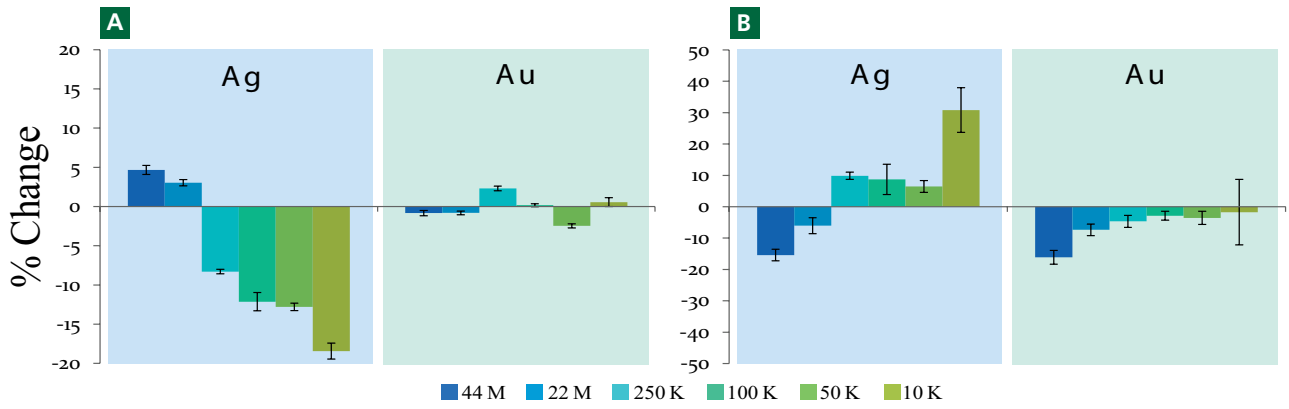

C

		Original Particle	44 M	22 M	250 K	100 K	50 K	10 K
Measured Au size (nm)		31.0	33.2	32.0	31.1	31.3	31.1	31.0
Measured Ag size (nm)		57.7	62.7	61.0	55.3	54.7	54.1	52.6
Calculated total particle size (nm)		60.6	65.7	63.8	58.4	58.0	57.4	56.0
Particle Conc (part/mL)	Ag	---	32.3 M	17.6 M	259 K	115 K	62.1 K	21.1 K
	Au	---	31.1 M	19.0 M	232 K	102 K	49.9 K	9.7 K

Figure 2. The % change of A) particle diameter and B) particle number concentration of ENPs in MHW after 48 hours. The corresponding table (C), shows the actual measured values for the particle diameter and concentration, as well as the calculated total diameter of the ENP.

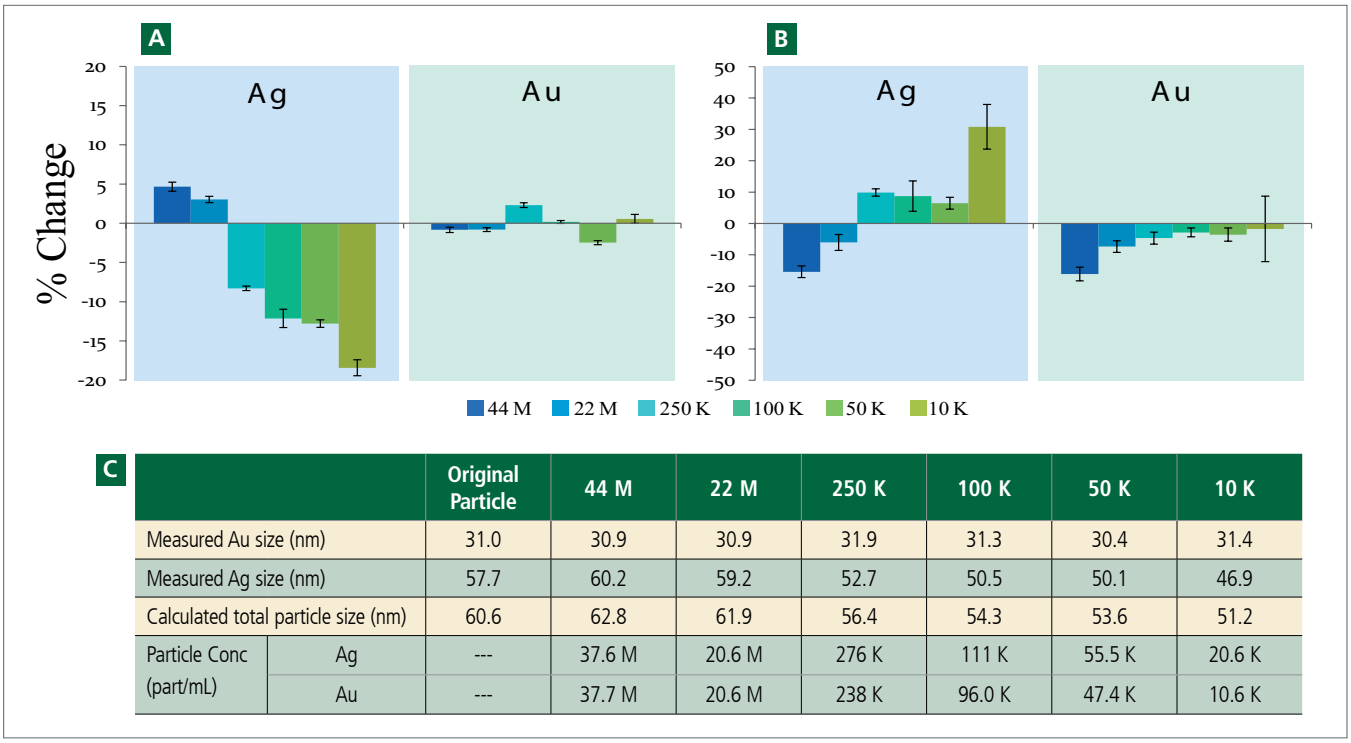

C

		Original Particle	44 M	22 M	250 K	100 K	50 K	10 K
Measured Au size (nm)		31.0	30.9	30.9	31.9	31.3	30.4	31.4
Measured Ag size (nm)		57.7	60.2	59.2	52.7	50.5	50.1	46.9
Calculated total particle size (nm)		60.6	62.8	61.9	56.4	54.3	53.6	51.2
Particle Conc (part/mL)	Ag	---	37.6 M	20.6 M	276 K	111 K	55.5 K	20.6 K
	Au	---	37.7 M	20.6 M	238 K	96.0 K	47.4 K	10.6 K

Figure 3. The % change of A) particle diameter and B) particle number concentration of ENPs in FA after 48 hours. The corresponding table (C) shows the actual measured values for the particle diameter and concentration as well as the calculated total diameter of the ENP.

Table 4. Number of Fulvic Acid Molecules per Nanoparticle.

Particle Concentration			Number of FA Molecules	
Particles/mL	Ag (µg/L)	Au (µg/L)	Molecules/nm^2 of Particle Surface Area	Number of FA Molecules / NP
22,000 M	23,000	6,000	8	85,511
44 M	46	12	3,780	4.28E+7
22 M	23	6	7,561	8.55E+7
250 K	0.261	0.068	665,355	7.53E+9
100 K	0.104	0.027	1,663,386	1.88E+10
50 K	0.052	0.014	3,326,773	3.76E+10
10 K	0.010	0.003	16,633,863	7.88E+11

It is important, when thinking about interactions of ENPs with NOM, to consider the ratio of ENP surface area to NOM molecule concentration. For the calculations made in Table 4, we have assumed the molecular mass to be between 800 – 1000 Da taken from several papers as the most frequent size of Suwannee River fulvic acid in surface waters (which can change with pH and ionic concentration)[10, 11] and a concentration of 2.5 mg/L of FA.

In Table 4, it can be seen that the number of available molecules of FA per nm^2 of particle is dramatically different from the stock suspension (8 molecules/nm^2) for the concentrations studied. At the most dilute suspension in this study (10K particles / mL), there are over 16,000,000 FA molecules available per nm^2 of ENP. We have shown here that when the ENP concentration is decreased with respect to a simulated surface water containing a fixed amount of FA, there is a dramatic effect on the ENP transformations going from a stabilizing effect at higher concentrations to accelerating dissolution at lower concentrations. This ratio is an important factor to consider when conducting transformation experiments.

Conclusions

SP-ICP-MS has been used to help understand ENP transformations in exposure and environmental media. Using this methodology, it is possible to obtain information on ENP size and particle number concentration, among other properties, at environmentally relevant concentrations, about 100 times less concentrated than in previous studies. In addition, SP-ICP-MS can acquire this information in 1 - 5 minutes per sample, rather than hours/days to obtain the same data using a combination of electron microscopy and optical spectroscopy techniques. However, for very complex transformations such as particle shape and whether complexes are formed with sulfides, oxides, and/or chlorides, additional data are needed.

This work has demonstrated that FA helps stabilize higher concentrations of ENPs at lower temperatures in the presence of light. However, it appears that at lower ENP concentrations, light and higher temperatures seemingly accelerate dissolution and some re-precipitation. There are differences between all high and low ENP concentrations pointing towards ENP:salt concentration and ENP:NOM concentration being key ratios when looking at NP transformations.

The advantages of SP-ICP-MS are obvious, and incorporating core-shell particles (where the core is stable and less likely to dissolve than the coating) makes analysis of the more reactive outer shell transformations easier to interpret. It is difficult to point out the nature of the silver species formed (sulfides, oxides, chlorides, among others) without a multi-method approach in which ICP-MS and SP-ICP-MS are essential parts.

References

1. Baalousha, M.; Sikder, M.; Prasad, A.; Lead, J.; Merrifield, R.; Chandler, G. T., The concentration-dependent behaviour of nanoparticles. Environmental Chemistry 2015.
2. Zou, X.; Shi, J.; Zhang, H., Morphological evolution and reconstruction of silver nanoparticles in aquatic environments: The roles of natural organic matter and light irradiation. Journal of Hazardous Materials 2015, 292, 61-69.
3. Romer, I.; Gavin, A. J.; White, T. A.; Merrifield, R. C.; Chipman, J. K.; Viant, M. R.; Lead, J. R., The critical importance of defined media conditions in Daphnia magna nanotoxicity studies. Toxicol. Lett. 2013, 223, (1), 103-108.
4. Bondarenko, O.; Ivask, A.; Kakinen, A.; Kurvet, I.; Kahru, A., Particle-Cell Contact Enhances Antibacterial Activity of Silver Nanoparticles. Plos One 2013, 8, (5).
5. Hou, W. C.; Stuart, B.; Howes, R.; Zepp, R. G., Sunlight-Driven Reduction of Silver Ions by Natural Organic Matter: Formation and Transformation of Silver Nanoparticles. Environmental Science & Technology 2013, 47, (14), 7713-7721.
6. Yin, Y. G.; Shen, M. H.; Zhou, X. X.; Yu, S. J.; Chao, J. B.; Liu, J. F.; Jiang, G. B., Photoreduction and Stabilization Capability of Molecular Weight Fractionated Natural Organic Matter in Transformation of Silver Ion to Metallic Nanoparticle. Environmental Science & Technology 2014, 48, (16), 9366-9373.
7. Lu, Y.; Wang, L.; Chen, D.; Wang, G., Determination of the Concentration and the Average Number of Gold Atoms in a Gold Nanoparticle by Osmotic Pressure. Langmuir 2012, 28, (25), 9282-9287.
8. Croteau, M. N.; Misra, S. K.; Luoma, S. N.; Valsami-Jones, E., Bioaccumulation and Toxicity of CuO Nanoparticles by a Freshwater Invertebrate after Waterborne and Dietborne Exposures. Environmental Science & Technology 2014, 48, (18), 10929-10937.
9. Gottschalk, F.; Sun, T.; Nowack, B., Environmental concentrations of engineered nanomaterials: Review of modeling and analytical studies. Environmental Pollution 2013, 181, 287-300.
10. Beckett, R.; Jue, Z.; Giddings, J. C., Determination of Molecular-Weight Distributions of Fulvic and Humic Aacids Using Flow Field-Flow Fractionation. Environmental Science & Technology 1987, 21, (3), 289-295.
11. Schafer, A. I.; Mauch, R.; Waite, T. D.; Fane, A. G., Charge effects in the fractionation of natural organics using ultrafiltration. Environmental Science & Technology 2002, 36, (12), 2572-2580.

Consumables Used

Component	Description	Part Number
Sample Uptake Tubing	Green/orange (0.38 mm id) flared PVC	N0777042
Drain Tubing	Grey/grey (1.30 mm id) Santoprene	N0777444
Gold Nanoparticles	30 nm spherical gold nanoparticles in water	N8142300
Gold Standard	1000 mg/L aqueous gold standard, 125 mL	N9303759
Silver Standard	1000 mg/L aqueous gold standard, 125 mL	N9300171

PerkinElmer, Inc.
940 Winter Street
Waltham, MA 02451 USA
P: (800) 762-4000 or
(+1) 203-925-4602
www.perkinelmer.com

PerkinElmer®

For a complete listing of our global offices, visit www.perkinelmer.com/ContactUs

012511_01 PKI

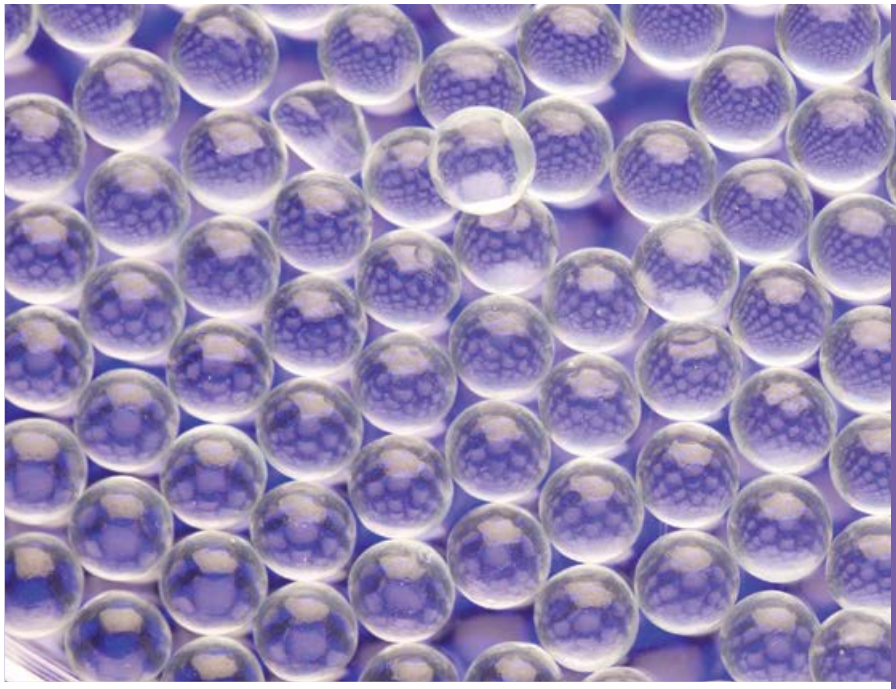

APPLICATION NOTE

ICP – Mass Spectrometry

Authors:

Ruth C. Merrifield

Jamie R. Lead

Center for Environmental NanoScience and Risk (CENR), Arnold School of Public Health
University of South Carolina, SC

Chady Stephan

PerkinElmer, Inc.
Shelton, CT

SP-ICP-MS Analysis of Size and Number Concentration in Mixtures of Monometallic and Bimetallic (Core-shell) Nanoparticles

Introduction

It is challenging to separate and measure the physical and chemical properties of monometallic and bimetallic engineered nanoparticles (NPs), especially when mixtures of NPs consist of particles of similar size, composition, and especially when present at low concentrations. Fully characterizing suspensions of NPs usually requires a multimethod approach to yield the most reliable results[1,2]. This process becomes increasingly difficult for more complex bimetallic NPs used in some applications or for those that require a mixture of different NPs, since differentiating between NPs can be a slow and arduous task. There are a variety of techniques that have been used for the determination of particle diameter, composition, and particle number concentration (part. mL^{-1}) of engineered NPs, including dynamic light scattering (DLS), field flow fractionation (FFF), ultraviolet/visible spectroscopy (UV/Vis), multi-angle light scattering (MALS), and, more recently, single particle inductively coupled plasma mass spectrometry (SP-ICP-MS)[3]. All these techniques have their own strengths and weaknesses as well as measuring size and/or composition in different ways.

PerkinElmer®
For the Better

Both DLS and FFF measure the particles' hydrodynamic diameter; however, FFF has the advantage of separating particles on the basis of their hydrodynamic size, making it unbiased to particle size, unlike DLS. While FFF separates particles by size, it must be coupled to a detector, traditionally UV/Vis, MALS, DLS, or fluorescence, all light source techniques that lack the required sensitivity for environmental-type research. For that, FFF has been coupled to ICP-MS, a more sensitive detector, which allows for lower detection limits of metal-based engineered nanomaterials than the above-mentioned detectors[4]. However, when dealing with a mixture of monometallic and bimetallic particles, simulating a random environmental sample, all these detection techniques will suffer to provide the particle number concentration.

One of the most difficult properties to routinely measure in a NP suspension is particle number concentration[3,5], which can be measured directly using techniques like nanoparticle tracking analysis (NTA)[6] or by a complex, multimethod approach[7]. However, these techniques have limitations when dealing with mixtures of NPs, as they do not offer compositional information.

As a standalone technique, Single Particle ICP-MS (SP-ICP-MS) has emerged as the technique of choice for the detection of metallic NPs at environmental levels, providing particle size, size distribution, and particle number concentration all on particle per particle basis[8]. In this work, we demonstrate the use of SP-ICP-MS as a stand-alone technique to measure complex suspensions of NPs and discriminate between mixtures of monometallic gold (Au) and silver (Ag) NPs and bimetallic Au@Ag (core-shell) NPs, yielding particle-size and particle-number concentrations for each constituent.

Experimental

Field flow fractionation (FFF)

An Eclipse DualTech FFF separation system from Wyatt (Wyatt Technology, Santa Barbara, California, USA) was used and equipped with a 10 KDa polyethersulfone (PES) hollow fiber (diameter of 0.8 mm and length of 17 cm, purchased from Wyatt) which was used as a separation channel. A detector flow of 0.5 mL/min and focus flow of 0.2 mL/min were used to focus the particles in the channel. These conditions were allowed to reach equilibrium for 2 minutes before injecting the sample, and then focusing for 10 minutes. The particle elution followed by ramping the cross flow from 0.15-0.6 mL/min over a 10-minute period (the particles eluted between 0.1 and 0.6 mL/min cross flow). A 5-minute post elution with no cross flow was used to clear the channel of any residual particles, resulting in a total analysis time of 27 minutes. Injection volumes of 2-20 µL were used. The carrier solution was 0.2 mM sodium citrate, and the separation was measured using a UV detector at 400 nm.

Inductively coupled plasma mass spectrometry (ICP-MS)

A PerkinElmer NexION® 350D ICP-MS equipped with the Syngistix™ Nano Application Software Module, operating under the conditions outlined in Table 1, was used.

Nanoparticles (NPs)

NP suspensions for this study were purchased from Nanocomposix™ (San Diego, California, USA) and the National Institute of Standards Technology (NIST™, Gaithersburg, Maryland, USA).

Table 1. NexION 350D ICP-MS operating conditions.

Parameter	Value
Nebulizer	Meinhard®
Spray Chamber	Cyclonic
Power (W)	1600
Plasma Gas (L/min)	16
Aux Gas (L/min)	1.2
Neb Gas (L/min)	1.12
Sample Flow Rate (mL/min)	0.5 – 1
Dwell Time (µs)	50
Sampling Time (s)	60

The following particles were used for this study: 60 nm Ag, 60 nm Au, 60 nm Au@Ag (Au core size 30 nm, Ag shell thickness 15 nm), 80 nm Ag, 80 nm Ag, and 80 nm Au@Ag (Au core size 50 nm, Ag shell thickness 15 nm). The particle concentrations provided by the manufacturer are shown in Figure 1B and were diluted to between 10,000 and 100,000 particles (part.) mL^{-1} for SP-ICP-MS analysis, based on the manufacturers' data. For FFF analysis, the particles were used at the nominal concentrations of the stocks (Figure 1B) or diluted to 1,000,000 part. mL^{-1}, depending on injection volume used.

Standards

For SP-ICP-MS work, ionic Au and Ag standards at 1, 2, 3, and 4 ppb were used as ionic calibrations and made from 1000 mg/L stock standards. NIST™ Au NP standards of 30 nm and 60 nm were used for Au particle calibrations at concentrations of 100,000 part. mL^{-1}. The NIST™ 60 nm Au particles were used to determine the transport efficiency of the system.

Results and Discussion

NIST™ 30 and 60 nm certified reference materials (CRMs) were used to quantify the accuracy of the SP-ICP-MS measurements. The certified diameter and size distribution measured by TEM for the nominally 30 and 60 nm standards are 27.6 (± 2.1) and 56.3 (± 1.5) nm, respectively. Diameters of the same NPs measured by SP-ICP-MS are 26.9 (± 0.3) nm and 57.3 (± 0.1) nm, which is in excellent agreement with the certified values. Additionally, the measured particle number concentrations of the CRMs were within 3% of the certified values, validating the accuracy of SP-ICP-MS.

With the accuracy of SP-ICP-MS established, six test NP suspensions purchased from commercial sources (details shown in Table 2) were analyzed by SP-ICP-MS to determine particle size and concentration of each individual suspension for later reference. The commercial NPs have a higher degree of dispersity compared to the NIST reference standards, sometimes showing bimodal distributions, an example of which is shown in Figure 1A, where the Au 80 nm suspension has a peak at 60.4 (± 0.1) (dotted line) and at 78.1 (±4.0) (dashed line). In addition, the commercial NPs showed an offset in particle number, an example of which is Ag 60 nm, showing a measured concentration that is 1.7 times lower than expected (Figure 1D). To simplify data analysis, we fitted a Gaussian curve to the size distributions (dot-dash line) and used these fits for data interpretation.

Table 2. NP suspensions used in this study.

Element	Description	Nominal Size (nm)
Ag	Pure Ag	60
	Pure Ag	80
Au	Pure Au	60
	Pure Au	80
Au@Ag	30 nm Au core, 15 nm Ag shell	60
	50 nm Au core, 15 nm Ag shell	80

Figures 1B and 1C show the measured particle diameters and measured particle number concentrations for the individual NP suspensions, respectively. The total particle diameters for the separate Ag or Au NPs are 73.5 (3.9) nm, 76.2 (0.2) nm, 54.7 (0.2) nm, and 55.5 (0.3) nm for the nominally Au 80 nm, Ag 80 nm, Au 60 nm, and Ag 60 nm particles, respectively. The actual stated values from the manufacturers are 81.2 (10.5) nm, 78.9 (10.5) nm, 60.6 (5.9) nm, and 59.6 (5.8) nm, suggesting the information supplied by the manufacturer is accurate, but SP-ICP-MS is capable of greater precision. This supports the ability of SP-ICP-MS to easily identify bimodal distributions when they exist, as shown in Figure 1A.

SP-ICP-MS is a mass-based technique, thus particle size is determined from the total number of ions detected as individual particles. When analyzing core-shell structures, the converted size for silver in an Au@Ag 60 nm particle is 57.8 (±0.3) nm and 74.3 (±0.5) nm for an Au@Ag 80 nm particle. These calculated sizes can be directly compared to the manufacturer's (TEM) measurements of 60.8 (±6.3) nm and 78.2 (±8.8) nm. Figure 1C shows the particle number concentrations for each of the particle suspensions. All of the suspensions were diluted so that their concentration was expected to be 100,000 part. mL^{-1}.

It is evident that the manufacturer's data for most suspensions is accurate. However, the manufacturer's data for the Au 80 and Ag 60 were not in agreement with SP-ICP-MS, with the Au 80 nm sample containing significantly more particles and the Ag 60 nm sample containing significantly fewer particles than expected. Figure 1D compares the manufacturer's particle concentration with those measured by SP-ICP-MS, where the final column contains a correction factor which converts the accurate measured value to the manufacturer's value. As all samples were diluted per the manufacturer's data, this correction factor was applied to all measured particle numbers to make the analysis easier. For the core-shell NPs, the concentrations for both Ag and Au signals were identical, confirming that we do not have mixtures of Ag and Au samples.

Mixtures of Au@Ag, Au, and Ag NPs in SP-ICP-MS provide an extremely challenging test of the selectivity of SP-ICP-MS. Typical SP-ICP-MS data for mixtures of the 80 nm particles and 60 nm particles are shown in Figure 2. The Au and Ag signals for the 80 nm mixtures are shown in Figures 2A and 2B, respectively, and the Au and Ag signals for the 60 nm mixtures are shown in Figures 2C and 2D, respectively. The Gaussian fits for the single NP suspensions are shown. The dotted black lines represent the Gaussian fit for the monometallic NPs, while the dashed lines are for the bimetallic NPs. Figures 2A and 2C show a good separation of the signal from the Au core particles at 46.0 nm (A dashed line) and 29.5 nm (C dashed line), and the Au monometallic particles at 76.2 nm (A dotted line) and 54.7 nm (C dotted line). This separation allows the size and concentration of the core particles (from the Au@Ag NPs) to be differentiated from the monometallic Au NPs.

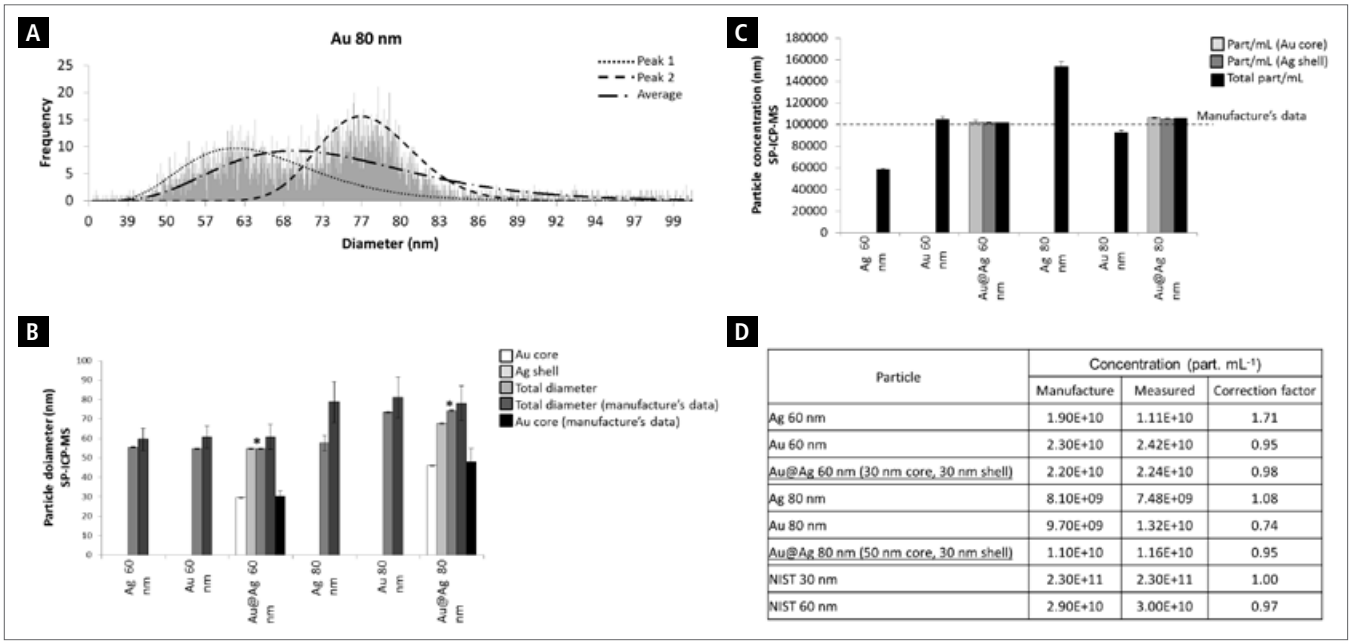

Particle	Concentration (part. mL^{-1})		
	Manufacture	Measured	Correction factor
Ag 60 nm	1.90E+10	1.11E+10	1.71
Au 60 nm	2.30E+10	2.42E+10	0.95
Au@Ag 60 nm (30 nm core, 30 nm shell)	2.20E+10	2.24E+10	0.98
Ag 80 nm	8.10E+09	7.48E+09	1.08
Au 80 nm	9.70E+09	1.32E+10	0.74
Au@Ag 80 nm (50 nm core, 30 nm shell)	1.10E+10	1.16E+10	0.95
NIST 30 nm	2.30E+11	2.30E+11	1.00
NIST 60 nm	2.90E+10	3.00E+10	0.97

Figure 1. A) Bimodal distribution measured for Au 80 nm NP suspension; B) and C) Particle diameters (B) and concentrations (C) for six nanoparticles; and D) Measured versus nominal concentrations of the particles along with the correction factor, as measured by SP-ICP-MS. All particles suspensions were diluted to 100,000 part. mL^{-1} based on the data provided by the manufacturer. The 'total diameter' is SP-ICP-MS data collected in this study, accounting for the core-shell geometry. Manufacturer's data is from transmission electron microscopy, although no data on sample preparation was provided. Figure 1D shows the measured particle numbers from SP-ICP-MS.

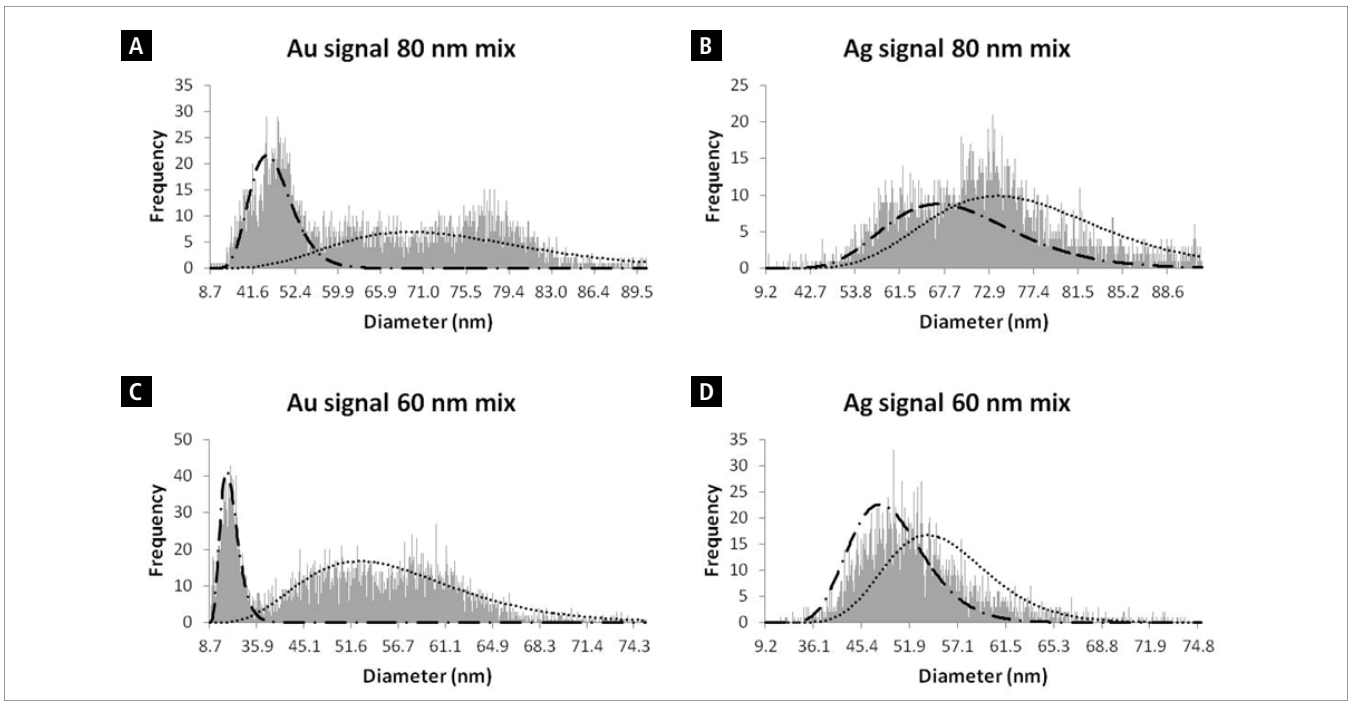

Figure 2. SP-ICP-MS particle size distribution for (A) Au from a mixture of 80 nm Au and 80 nm Au@Ag particles; (B) Ag from a mixture of 80 nm Ag and 80 nm Au@Ag particles; (C) Au from a mixture of 60 nm Au and 60 nm Au@Ag particles; (D) Ag from a mixture of 60 nm Ag and 60 nm Au@Ag particles The dotted black curve corresponds to the expected signal from the monometallic particles, and the dashed black curve shows the Gaussian curve from the bimetallic (core-shell) particles.

Figures 2B and 2D are the Ag signals for the 80 nm mixture and 60 nm mixture, respectively. In contrast to the Au signals, the Ag shell signal (dashed lines) and Ag monometallic NP (dotted lines) overlap, meaning they cannot be distinguished on the basis of SP-ICP-MS alone. (The peak separation needs to be twice of the average of the full width half maxima of each peak to accurately measure size and particle number concentration counts).

There is enough separation in the Au signal to determine the particle number concentration for both the Au monometallic particle and the Au core from the bimetallic NP. Despite the lack of separation in the Ag signal, it is still possible to calculate the particle number concentrations for all three NPs in the suspension. The Ag signal contains the particle numbers for both the Ag monometallic and Ag shell (from the Au@Ag NP). Since we know the particle number of the bimetallic NPs from the Au signal, we can subtract this from the total Ag signal to obtain a particle number concentration for the Ag monometallic NP. Thus, it is possible to calculate the concentrations of all the NPs.

Subsequent to this initial analysis, five mixtures of these NP suspensions were produced (Table 3). The particle diameters and particle number concentrations for the three mixtures containing Au 80 nm and Au@Ag 80 nm NPs (mixtures 1-3, Table 3) are shown in Figures 3A and 3B, respectively. For these samples, the Au signal contained information for both the Au core and Au monometallic NPs, while the Ag signal only contained information from the Ag shell. The total measured particle number concentration was used as a check to ensure that the particles were not being over- or under-represented. In all three mixtures, the total number of particles per mL measured for the Au signal is within 0.5% of the particles per mL measured for the smaller and larger peak combined. This means that all particles are only counted once, verifying that the methodology is truly a single particle analysis at these concentrations.

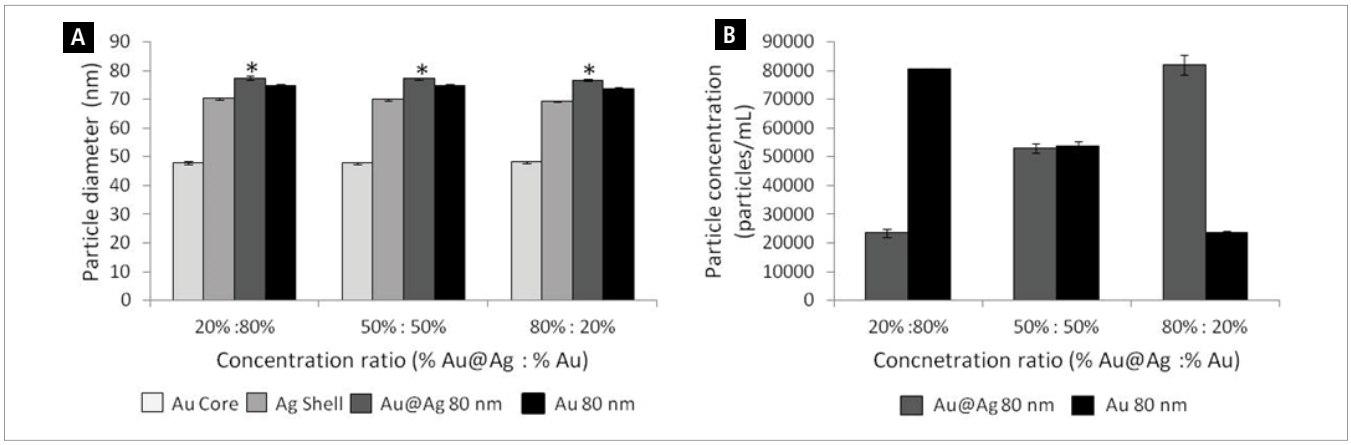

Figure 3. Particle diameters (A) and particle number concentrations (B) for three particle suspensions as measured from SP-ICP-MS. All three suspensions contain Au@Ag 80 nm and Au 80 nm particles with different ratios of particle number concentrations: 1:4 (20,000:80,000), 1:1 (50,000:50,000) and 4:1 (80,000:20,000) part/mL (Au@Ag:Au). The total particle diameter for the Au@Ag 80 nm particle was calculated from the measured Au and Ag signal and is marked with an *.

Table 3. Mixtures of particles.

Mixture	Concentration (part. mL^{-1})		
	Au	Ag	Au@Ag
1. Au 80 and Au@Ag 80	80,000	-	20,000
2. Au 80 and Au@Ag 80	50,000	-	50,000
3. Au 80 and Au@Ag 80	20,000	-	80,000
4. Au 80, Ag 80, and Au@Ag 80	64,600	53,900	73,000
5. Au 60, Ag 60, and Au@Ag 60	100,000	66,000	40,000

Figure 3 shows that in all three mixtures of the Au and Au@Ag NPs, the correct particle sizes can be measured despite the relative mixture composition, and the particle number concentration changes with mixture composition in the expected manner. The total number of Au particles in each mixture is between 5 and 16% of the amount expected. In Figure 3A, the particle diameters for the Au 80 nm, Au-core, and Ag shell were all measured within 3% of those measured for the individual NPs. The particle number concentrations of the mixtures were not significantly different from their expected values, based on Figures 1 and 2, and the mixture ratios used. The challenge in back calculating the true individual values from a mixture becomes more pronounced where the mixture ratios are high (or low) and where the NP samples are polydisperse. For these bimodal suspensions and at these mixture ratios, the actual and expected values are in good agreement, with < 20% difference in size and number concentration. However, criteria must be worked out on a case by case basis.

Figure 4 shows the measured sizes (Figure 4A) and calculated particle numbers (Figure 4B) for the 80 nm and 60 nm mixed NP suspensions of a three component mixture of the Ag, Au and Au@Ag NPs. The Au core and NP can be quantitatively resolved due to their differences in size (Figures 2A and 2C), while the Ag signal cannot be resolved (Figures 2B and 2D). The Ag monometallic NPs and the Ag shell of the Au@Ag NPs are too similar to be resolved, so neither the Ag-monometallic NPs nor the total diameter for the Au@Ag NPs could be distinguished and calculated.

However, the particle number concentrations for all three particles are shown in Figure 4B. These were calculated from the acquired data, where the number of monometallic Au NPs are contained in the large peak of the Au signal (dashed line Figures 2A and 2C), the number of Au@Ag NPs can be found from the number of particles contained in the smaller peak (dotted line, Figure 2A and 2C), and the Ag signal contains the number of particles for both the Au monometallic and Au@Ag bimetallic NP combined, the latter of which can be removed from the Ag signal by subtracting the number measured for the small peak in the Au signal. The measured particle number concentrations for the 80 nm mixture are shown on the left-hand side of the graphs in Figure 4B. The particle number concentrations for the 80 nm mixture were approximately 66,100, 53,400, and 70,000 particles mL^{-1} for the Au, Ag, and Au@Ag particles, respectively. These particle number concentrations are within 5% of the original added amounts (64,600, 53,900, and 73,300 part. mL^{-1}), showing excellent agreement. For the nominally 60 nm particles, concentrations were within 7% of the expected values (107,000, 65,800, 37,800 part. mL^{-1} for the Au 60 nm, Ag 60 nm, and Au@Ag 60 nm particles compared to the expected values of 100,000, 66,000, and 40,000 part. mL^{-1}).

Data from a FFF with a UV detector was collected to show that the components of the 80 nm mixtures were eluting at the same time, confirming that the solution does indeed contain NPs of nominally the same diameter with no smaller particles present in the suspension. In this case, FFF cannot differentiate between monometallic Au or Ag or a bimetallic NP consisting of both Au and Ag. Figure 5 shows the elution of Au 80 nm, Ag 80 nm, Au@Ag 80 nm, and a mixture of all three compared to 40 and 80 nm polystyrene beads. A clear separation of the 40 and 80 nm polystyrene beads is visible, marked as features A (also shown in insert) and B in Figure 5, respectively. The 80 nm polystyrene beads and all the 80 nm metal particles elute close together, marked by features C and D in Figure 5. This shows that the Au@Ag particles and the Au 80 nm particles are of the same size. It is impossible to identify from the UV data if there are core-shell and solid metallic particles present in the suspension.

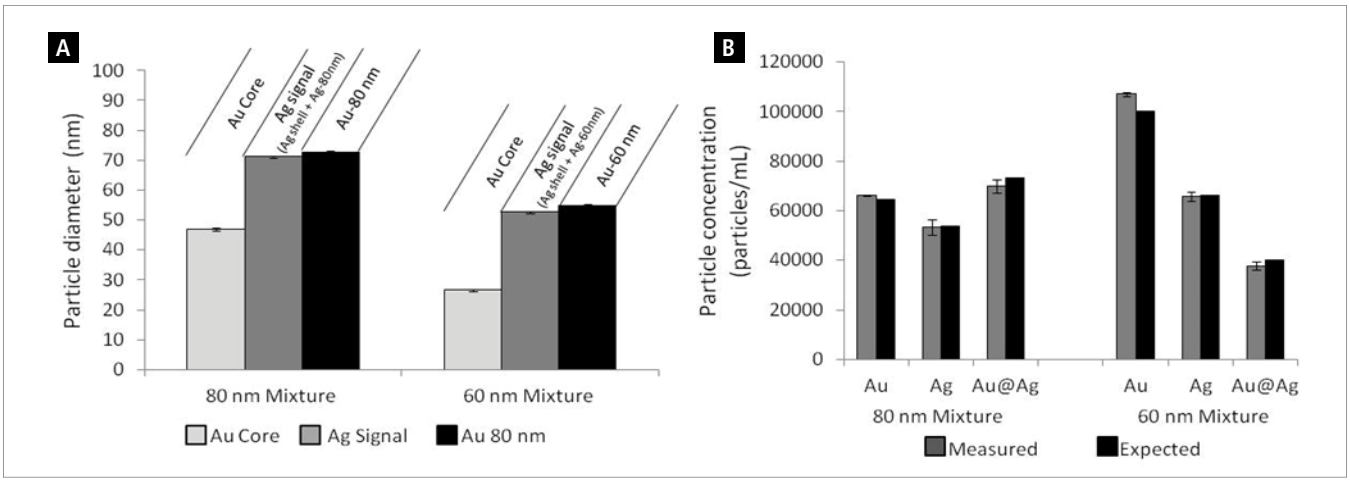

Figure 4. Particle diameters (A) and particle number concentrations (B) for two particle suspensions, as measured from SP-ICP-MS. The first suspension, an 80 nm mixture, contains Au 80 nm, Ag 80 nm and Au@Ag 80 nm NPs; the second mixture contains Au 60 nm, Ag 60 nm and Au@Ag 60 nm NPs. In (A) the diameters of the Au monometallic particles and the Au core from the Au@Ag NPs can be measured accurately, but the Ag signals from the monometallic and bimetallic particles are too close to resolve which signal belongs to which particle. However, from the data collected, all particle numbers can be calculated and can be seen to be close to the expected values in Figure 4B.

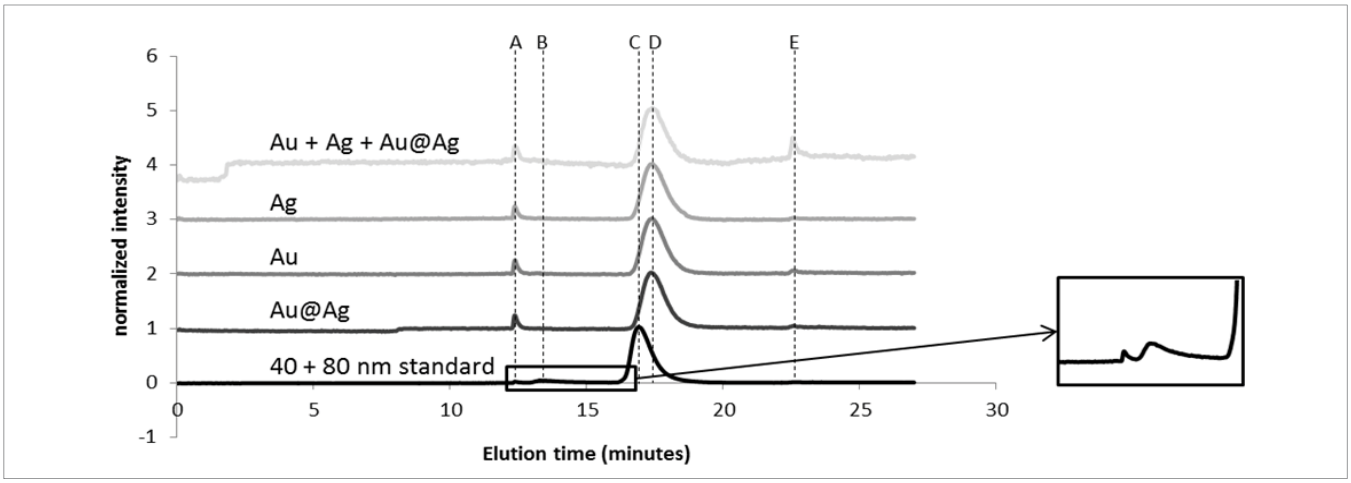

Figure 5 . Fractograms showing elution of a mixture of 40 and 80 nm polystyrene beads, a solution of 80 nm Au@Ag NPs, 80 nm Au NPs, 80 nm Ag NPs, and a mixture of 80 nm Au+Ag+Au@Ag NPs, measured with a UV detector at a wavelength of 400 nm. The insert shows feature B associated with the 40 nm polystyrene beads.

Conclusion

We have shown that PerkinElmer's NexION 350 ICP-MS single particle analyzer is capable of collecting separate data on size and number concentration of complex mixtures of single metal and core-shell metal NPs while also being able to distinguish monometallic from bimetallic particles of the same size. The obtained data resolution shows that this method is an excellent addition to a multi-method approach[9] for NP metrology in complex systems, offering a greater level of precision when it relates to particle number and size distribution.

References

1. Baalousha, M.; Ju-Nam, Y.; Cole, P. A.; Gaiser, B.; Fernandes, T. F.; Hriljac, J. A.; Jepson, M. A.; Stone, V.; Tyler, C. R.; Lead, J. R., Characterization of cerium oxide nanoparticles-Part 1: Size measurements. Environmental Toxicology and Chemistry 2012, 31, (5), 983-993.
2. Baalousha, M.; Ju-Nam, Y.; Cole, P. A.; Hriljac, J. A.; Jones, I. P.; Tyler, C. R.; Stone, V.; Fernandes, T. F.; Jepson, M. A.; Lead, J. R., Characterization of cerium oxide nanoparticles-Part 2: Nonsize measurements. Environmental Toxicology and Chemistry 2012, 31, (5), 994-1003.
3. Shang, J.; Gao, X., Nanoparticle counting: towards accurate determination of the molar concentration. Chemical Society Reviews 2014, 43, (21), 7267-7278.
4. Mitrano, D. M.; Barber, A.; Bednar, A.; Westerhoff, P.; Higgins, C. P.; Ranville, J. F., Silver nanoparticle characterization using single particle ICP-MS (SP-ICP-MS) and asymmetrical flow field flow fractionation ICP-MS (AF4-ICP-MS). Journal of Analytical Atomic Spectrometry 2012, 27, (7), 1131-1142.
5. Li, M.; Guha, S.; Zangmeister, R.; Tarlov, M. J.; Zachariah, M. R., Method for Determining the Absolute Number Concentration of Nanoparticles from Electrospray Sources. Langmuir 2011, 27, (24), 14732-14739.
6. Malloy, A., Count, size and visualize nanoparticles. Materials Today 2011, 14, (4), 170-173.
7. Baalousha, M.; Sikder, M.; Prasad, A.; Lead, J.; Merrifield, R.; Chandler, G. T., The concentration-dependent behaviour of nanoparticles. Environmental Chemistry 2016, 13, (1), 1-3.
8. Laborda, F.; Jimenez-Lamana, J.; Bolea, E.; Castillo, J. R., Critical considerations for the determination of nanoparticle number concentrations, size and number size distributions by single particle ICP-MS. Journal of Analytical Atomic Spectrometry 2013, 28, (8), 1220-1232.
9. Domingos, R. F.; Baalousha, M. A.; Ju-Nam, Y.; Reid, M. M.; Tufenkji, N.; Lead, J. R.; Leppard, G. G.; Wilkinson, K. J., Characterizing Manufactured Nanoparticles in the Environment: Multimethod Determination of Particle Sizes. Environmental Science & Technology 2009, 43, (19), 7277-7284.

Consumables Used

Component	Description	Part Number
Sample Uptake Tubing	Green/orange (0.38 mm id) flared PVC	N0777042
Drain Tubing	Grey/grey (1.30 mm id) Santoprene	N0777444
Gold Standard	1000 mg/L aqueous gold standard, 125 mL	N9303759
Silver Standard	1000 mg/L aqueous silver standard, 125 mL	N9300171

PerkinElmer, Inc.
940 Winter Street
Waltham, MA 02451 USA
P: (800) 762-4000 or
(+1) 203-925-4602
www.perkinelmer.com

PerkinElmer®

012821_01 PKI

APPLICATION NOTE

ICP - Mass Spectrometry

Authors:

Lee Davidowski, Ph.D.

Chady Stephan, Ph.D.

PerkinElmer, Inc.
Shelton, CT

Characterization of Silver Nanoparticles in Dietary Supplements by Single Particle ICP-Mass Spectrometry

Introduction

A nanopartcile is defined as a small object, between 1 and 100 nanometers in size, that behaves as a whole unit with respect to its transport and properties. Because of their small size and large surface area, nanoparticles can exhibit different chemical and physical properties from the bulk material. Nanoparticles have found their way into a large number of consumer products. As of 2013, it is estimated that there are over 1300 different consumer products which feature nanoparticles. Silver nanoparticles (AgNPs) are the most frequently found element in all varieties of consumer products (>23%)[1]. Manufacturers of consumer products use AgNPs due primarily to their known antimicrobial properties. Because of their very small size, AgNPs have high surface areas yielding high reaction rates, increasing the efficacy of silver as an antimicrobial.

The use of colloidal and nano silver is directly marketed to the public in such forms as odorless clothing, mildew-resistant shower curtains, food containers and food cutting boards and are even being promoted for direct human consumption as dietary supplements to fortify one's immune system.

PerkinElmer®
For the Better

Even as silver nanoparticles have become a valuable weapon in microbial warfare, there are increasing concerns over AgNPs release into the environment and their impact on plant and aquatic organisms. Other studies have shown that AgNPs can kill liver and brain cells in laboratory rats. On the nano scale, AgNPs can easily penetrate into organs and cells[2].

To better understand the fate of AgNPs in our environment, several analytical techniques are usually needed to measure the following key characteristics: particle concentration, composition, shape, size, size distribution, as well as dissolution and agglomeration tracking. Inductively coupled plasma mass spectrometry (ICP-MS) is a very sensitive, element-specific technique for studying elements at environmentally relevant concentrations. Recently, the capabilities of this technique have been extended to single particle analysis mode (SP-ICP-MS)[3, 4], a unique operating mode that allows the differentiation between ionic and particulate forms of prescribed elemental composition entering the plasma source. The resulting data allows for the determination of particle concentration, size, size distribution and dissolved concentration at very low levels, making SP-ICP-MS the conventional technique assessing the fate of engineered nanoparticles in diverse environmental matrices.

Experimental

Instrumental Conditions

Silver nanoparticles, which are suspended in aqueous samples, are introduced into the plasma in exactly the same manner as dissolved solutions with a standard nebulizer and spray chamber combination. However, the data acquisition parameters are very different. Each small nanoparticle entering the plasma is ionized into a very short burst of ions. To accurately measure that burst of ions, the quadrupole and measurement electronics of the instrument must be able to acquire data in the double digit µsec range.

Figure 1 shows a real-time signal that is produced from a single nanoparticle's cloud of ions. In this study, the instrument is continuously acquiring data using a 50 µsec dwell time with no settling time between readings; this eliminates the chances of missing a particle or partially integrating a particle signal, improving particle counting and sizing information. The PerkinElmer NexION® 350D ICP-MS in single particle mode routinely generates up to six million data points per minute of analysis time (operated at 10 µsec dwell time).

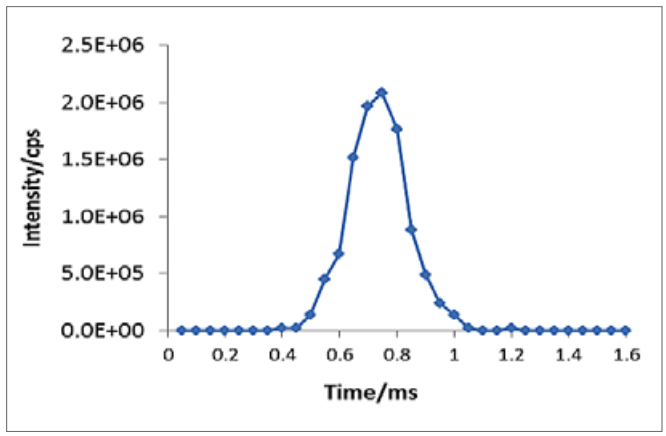

Figure 1. Signal of a single silver nanoparticle captured by SP-ICP-MS. Data acquired at 50 µsec dwell time and zero quadrupole settling time.

SP-ICP-MS data processing is based on the ability to count every particle going through the plasma source, and the ability to distinguish between particles and dissolved metal. When analyzing dissolved elements with an ICP-MS, the resulting signal is essentially a steady-state signal (Figure 2a). When analyzing a dilute suspension of nanoparticles, however, the signal is markedly different, showing ion bursts or plumes from individual nanoparticles (Figure 2b).

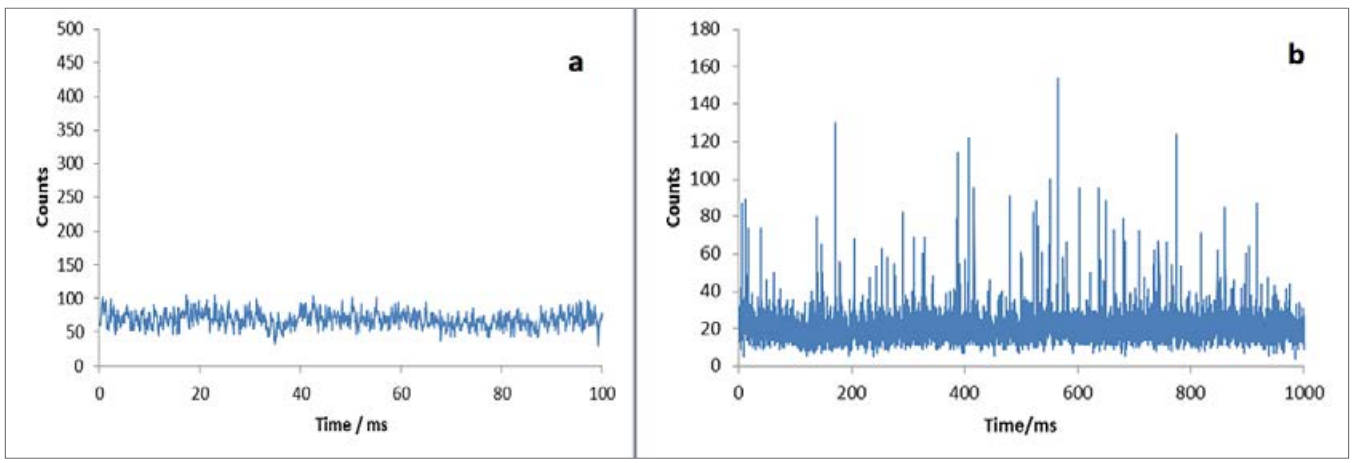

Figure 2. (a) Continous signal from dissolved ionic silver; (b) raw data of sample containing AgNPs.

The Syngistix™ Nano Application Module (PerkinElmer, Shelton, CT), an extension of Syngistix for ICP-MS software, calculates the metal solution concentration (µg/L), the concentration of particles (particles/mL), the size and size distribution of the particles, shows data acquisition in real time, and a size distribution histogram of the sample (Figure 3).

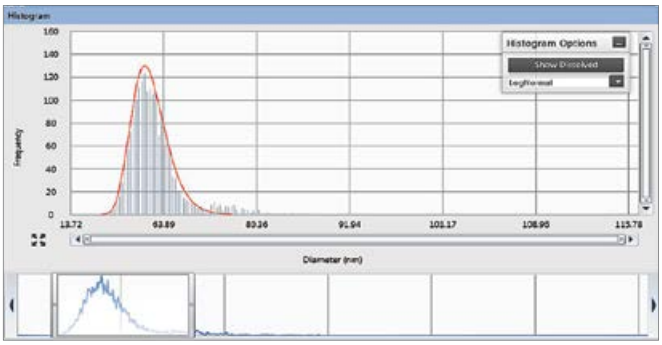

Figure 3. The Results panel of the Syngistix Nano Application Module for SP-ICP-MS, showing size distribution histogram and adjustable integration window at the bottom.

The amount of analyte actually entering the plasma is a fraction of the amount aspirated. This ratio, known as the transport efficiency, is an integral part of particle concentration calculation[5]. AgNP suspensions of known size and concentration are available from several commercial sources. For size and transport efficiency calculations, this work used silver nanoparticle suspensions of 20 nm, 50 nm and 80 nm nominal sizes in citrate buffer from Ted Pella, Inc. (Redding, CA). For the ionic or dissolved silver determinations, a calibration curve from 0.5 to 5 µg/L was constructed from PE Pure (PerkinElmer, Shelton, CT) primary silver standard.

All SP-ICP-MS measurements were made with a NexION 350D ICP-MS (PerkinElmer, Shelton, CT) operating in Standard (no gas) mode and with the Syngistix Nano Application Module. The Syngistix Nano Application Module leads the user through all the components of SP-ICP-MS data collection in an intelligent workflow manner. All measurements were made per the instrumental conditions shown in Table 1.

Table 1. Instrumental Operating Parameters and Conditions

Parameter	Condition
Instrument	NexION 350D ICP-MS in Standard Mode
Nebulizer	ESI PFA Concentric
Spray Chamber	Baffled Cyclonic, Glass
Injector	2.0 mm id Quartz
Power	1600 W
Aux Flow	1.1 L/min
Neb Gas Flow	1.05 L/min
Sample Uptake Rate	0.4 mL/min
Silver Isotope	107 AMU
Dwell Time	50 µsec
Quad Settling Time	Zero
Sampling Time	120 sec

Sample Preparation

Reference silver nanoparticles and the three commercially available dietary supplement samples were placed in an ultrasonic bath for more than five minutes to help ensure that the particles were evenly distributed in the solutions and to minimize agglomeration. The samples were serially diluted with laboratory Type I deionized (DI) water into polyethylene 50 mL sample tubes. The samples and reference solutions were diluted such that the particle concentration was approximately 200,000 particles/mL. This dilution allows measurements to be taken on individual particles and minimizes particle coincidence.

Figure 4. Three commercially available dietary supplements containing silver nanoparticles used in this work.

Results

SP-ICP-MS produces different kinds of information about an unknown sample. While acquiring the data, the ICP-MS signal produced can be viewed in real time. This provides instant information on the sample being analyzed and helps indicate if furthur dilution is necessary to avoid particle coincidence. After the data is collected, it can be reviewed in a number of ways. Graphically, size data are shown as a size distribution histogram. An adjustable integration window with slider bars allows one to choose a slice of the size distribution data for statistical evaluation. Data is also tabulated in a list of scrolling results which shows information on each sample such as: most frequent size, mean size, particle concentration, dissolved concentration and other information about the particle counts. This tabulated data is instantly updated to reflect the slice of data selected with the adjustable window and the type of histogram data fitting used (Gaussian, LogNormal, or Maximum).

Figures 5 and 6 show the size distribution histograms for AgNPs in Sample #1 and Sample #2. Both are using the LogNormal fitting algorithm, as shown by the solid line.

The Sample #1 data show a clear distribution of particles around 15 nm, and the Sample #2 data show a distribution of particles around 33 nm.

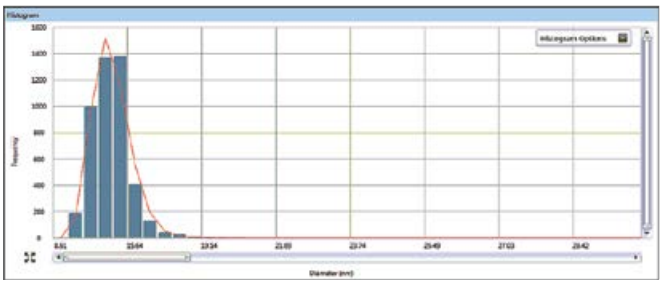

Figure 5. Sample #1 size distribution histogram from Syngistix Nano Application Module.

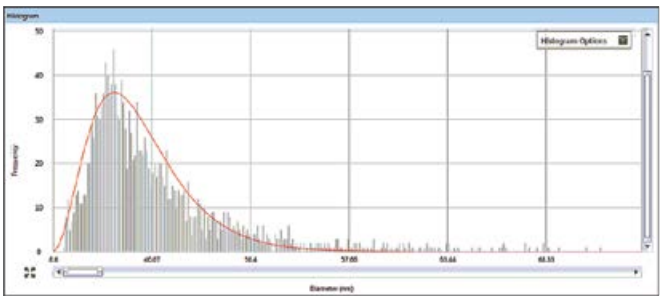

Figure 6. Sample #2 size distribution histogram from Syngistix Nano Aplication Module.

The tabulated data for the samples are given in Table 2. Besides the size distrubution results, the Syngistix Nano Application Module gives the particle concentration and the dissolved concetrations in the samples. The concentration results shown in Table 2 are corrected for the laboratory's dilution. The Ted Pella™ 50 nm AgNP standard was run as control sample check. The most frequent size of 48 nm is in good agreement with the given value of 50 nm, and the measured particle concentration is in good agreement with the value given by the manufacturer of 2.5 E+10 particles/mL.

Table 2. Results for the SP-ICP-MS Analysis of Silver in Dietary Supplement Samples

Sample ID	Mean Size (nm)	Most Frequent Size (nm)	Particle Concentration (particles/mL)	Dissolved Concentration (mg/L)
Sample #1	14	14	3.0 E+10	9.5
Sample #2	39	33	2.1 E+9	21.9
Sample #3	53	59	2.7 E+10	48.1
Ted Pella™ Ag 50 nm	43	48	2.8 E+10	-

Conclusion

Using PerkinElmer's Syngistix Nano Application Module along with the superior ultra-fast data acquisition electronics of the NexION 350 ICP-MS, silver nanoparticles were measured in three commercially available dietary supplements.

Single particle ICP-MS allows for the differentiation and quantitation between the dissolved ionic and particulate fractions of the analyte. In a single analysis, particle composition, concentration, size and size distribution can be directly determined.

The use of the SP-ICP-MS technique has been extended to other elements – and beyond consumer products – into food analyses, biological fluids and to the study of the fate of nanoparticles in the environment.

References

1. Zhang, Hongyin, "Application of Silver Nanoparticles in Drinking Water Purification" (2013) *Open Access Dissertations.* Paper 29. http://digitalcommons.uri.edu/oa_diss/29.
2. S. Prabhu and E. Poulose, *International Nano Letters* 2012, 2:32.
3. F. Labora, J. Jimenez-Lamana, E. Bolea and J. Castillo, "Selective identification, characterization and determination of dissolved silver and silver nanoparticle detection by inductively coupled plasma mass spectrometry", *J. Anal. At. Spectrm.*, 2011, Volume 26, Issue 7, pp 1362-1371.
4. F. Labora, E. Bolea, and J. Jimenez-Lamana, *Analytical Chemistry* 2014, 86 (5) pp 2270-2278.
5. H. Pace, N. Rogers, C. Jarolimek, V. Coleman, C. Higgins and J. Ranville, *Analytical Chemistry* 2011, (83), pp 9361-9369.

PerkinElmer, Inc.
940 Winter Street
Waltham, MA 02451 USA
P: (800) 762-4000 or
(+1) 203-925-4602
www.perkinelmer.com

PerkinElmer®

011800_01

APPLICATION NOTE

ICP – Mass Spectrometry

Authors:

Yongbo Dan[1,2], Weilan Zhang[3], Xingmao Ma[2,3], Honglan Shi[1,2], Chady Stephan[4]

[1] Department of Chemistry, Missouri University of Science and Technology

[2] Center for Single Nanoparticle, Single Cell, and Single Molecule Monitoring (CS[3]M), Missouri University of Science and Technology

[3] Department of Civil and Environmental Engineering, Southern Illinois University

[4] PerkinElmer, Inc.

Gold Nanoparticle Uptake by Tomato Plants Characterized by Single Particle ICP-MS

Introduction

With the increasing use of engineered nanoparticles (ENPs) in a variety of products and processes, there is concern about the release of ENPs into and impact on the environment. One aspect of the environmental impact of ENPs that must be explored is their uptake by plants, as ENPs can make their way to plants via migration through water and/or soil. If ENPs end up in food crops, this is a potential pathway to human exposure.

The challenge arises in how to measure ENPs in plant materials and, more specifically, in sample preparation. To our knowledge, current sample preparation techniques have limited capability to conserve the concentration and characteristics of nanoparticles (NPs) once they enter plant tissues, as they mainly depend on acid digestion. These limitations can be avoided by careful choice of the ENP extraction procedure and performing the analysis with single particle ICP-MS (SP-ICP-MS), the combination of which will preserve the particle size information, allow for rapid analysis of a large number of samples, and yield results on the particle size, concentration, and size distribution.

PerkinElmer®
For the Better

The goals of this work are to develop an extraction procedure for ENPs from plant materials and perform the analysis with SP-ICP-MS. Once these steps have been established, both will be applied to the determination of gold (Au) NP uptake by tomato plants. A more detailed study of the work presented here is available[1].

Experimental

Sample Preparation

Tomato plants were grown from seeds. After developing for 29 days, the seedlings were exposed to 40 nm polyvinylpyrrolidone (PVP)-coated Au NPs (nanoComposix™, San Diego, California, USA) at different concentrations for four days before being harvested for analysis.

After harvesting, plant shoots were washed three times with deionized water, then cut into small pieces and homogenized in 8 mL of the a 2 mM citrate buffer. After homogenization, 2 mL of Macroenzyme R-10 (bioWORLD™, Dublin, Ohio, USA) was added, and the sample then shaken in a 37 °C water bath for 24 hours. The samples were then allowed to settle for one hour. A 0.1 mL aliquot of the supernatant was diluted 100x with deionized water for analysis by SP-ICP-MS. Controls and blanks were prepared the same way. Au NPs were spiked into the plant extract, as appropriate.

Instrumental Conditions

All analyses were performed on a PerkinElmer NexION® 300D/350D ICP-MS using the Nano Application Module (PerkinElmer Part No. N8140309) within Syngistix™ software. Instrumental parameters are shown in Table 1. Both particle and dissolved calibrations were performed. Au nanoparticle calibrations were performed with 30, 50, 80, and 100 nm citrate-stabilized Au nanoparticle (nanoComposix™, San Diego, California, USA). In order to see the smallest particles, the instrument's ion optics and detector were optimized for maximum sensitivity for Au 197.

Table 1. NexION 300/350D Instrumental and Analytical Parameters.

Parameter	Value
Nebulizer	Concentric (glass)
Nebulizer Flow	1.08 L/min
Spray Chamber	Baffled Cyclonic (glass)
ICP RF Power	1600 W
Analyte	Au
Mass	197 amu
Dwell Time	0.1 ms
Settling Time	0 ms
Sampling Time	100 sec
Number of Data Points Acquired	1 million per sample
Au Density	19.3 g/cm^3

Results and Discussion

Fundamental studies performed prior to analyzing plants indicated that 40 nm Au NPs could be accurately measured at concentrations as low as 1000 NPs/mL. It was important to establish the lowest concentration where Au NPs can be accurately measured, since the Au NP concentration in the plant tissues is unknown.

To assess the impact of the digestion enzyme on Au NPs, a solution of 50 nm Au NPs (2.05 x 10^5 NPs/mL) was treated with Macroenzyme R-10. Figure 1 shows the resulting particle size distribution, which indicates that the primary particle size is 50 nm. In addition, the measured particle concentration was 1.81 x 10^5 NPs/mL, an 88.3% recovery of the original concentration. These results indicate that the enzymatic digestion procedure does not affect particle-size distribution.

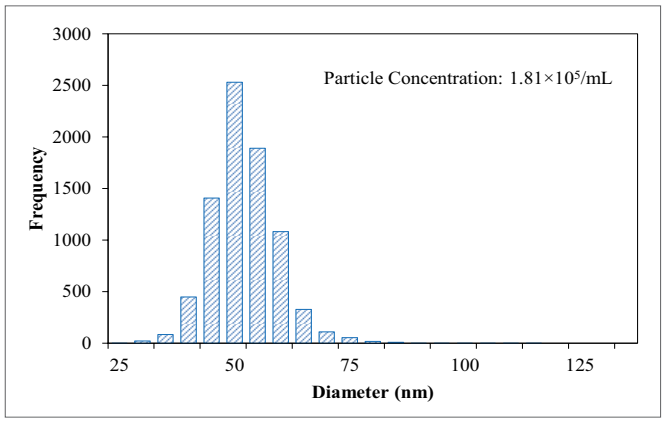

Figure 1. Particle size distribution histogram of enzyme-treated 50 nm AuNP (without plant tissue).

To establish the potential of seeing Au NPs in plants, a series of tests was performed, the results of which are shown in Figure 2. First, a solution of the Macroenzyme R-10 in a 2 mM citrate solution was analyzed for Au NPs. The resulting trace (Figure 2a) shows two random spikes, but no particles, indicating that the digestion medium will not contribute false positives.

Next, a tomato plant which had not been exposed to Au NPs was analyzed. Similar to the reagent blank, only random spikes were observed (Figure 2b). Finally, 100 nm Au NPs were added to the non-exposed digested plant (from Figure 2b) at a concentration of 4.7x10^4 NPs/mL. The resulting trace (Figure 2c) shows that the Au NPs are easily seen, with the resulting particle size distribution (Figure 2d) indicating a size distribution centered at 100 nm. These tests demonstrate that neither the enzyme nor plant material will contribute false positives, while neither inhibits the ability to detect Au NPs.

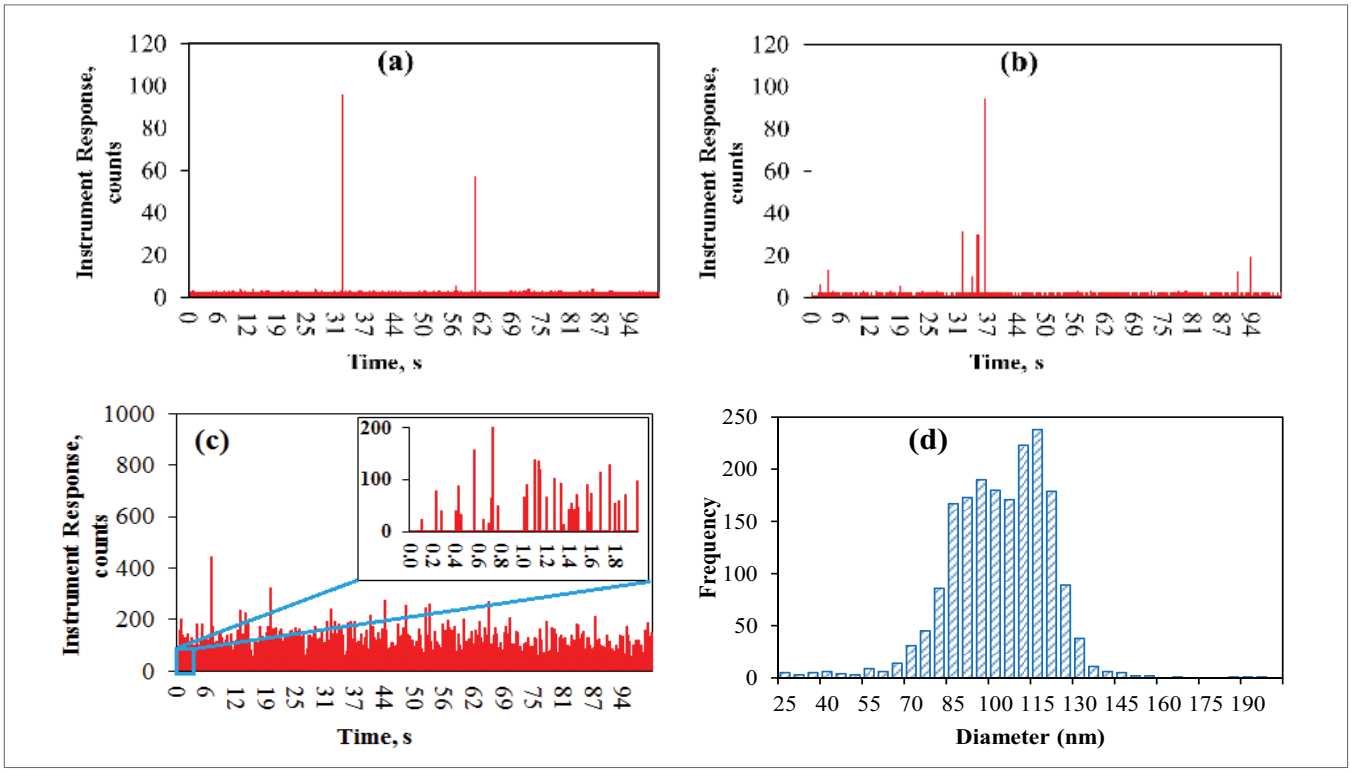

Figure 2. (a) Raw data for reagent blank (reagent blank: enzyme in 2 mM citrate solution, without plant tissues and Au NPs); (b) Raw data for control plant without exposure to Au NPs; (c) Raw data for spiking 4.7×10^4 NPs/mL of 100 nm Au NPs into control plant sample; (d) Size distribution histogram for spiking 4.7×10^4/mL of 100 nm Au NPs into control plant sample.

Next, a tomato plant exposed to 40 nm Au NPs at 0.2 mg/L for four days was digested and analyzed. Figures 3a and 3b show the resulting trace, which indicates uptake of the Au NPs by the plant. Figure 3c shows the resulting particle size distribution, which in centered at 40 nm, indicating the accuracy of the methodology. Finally, the same solution was spiked with 100 nm Au NPs (at $4.7\text{x}10^4$ NPs/mL) and analyzed. The resulting particle size distribution appears in Figure 3d and clearly shows two size distributions centered around 40 and 100 nm, indicating that both particle sizes are seen. In addition, the relative intensities of the distributions indicate that more 100 nm particles are present than 40 nm particles.

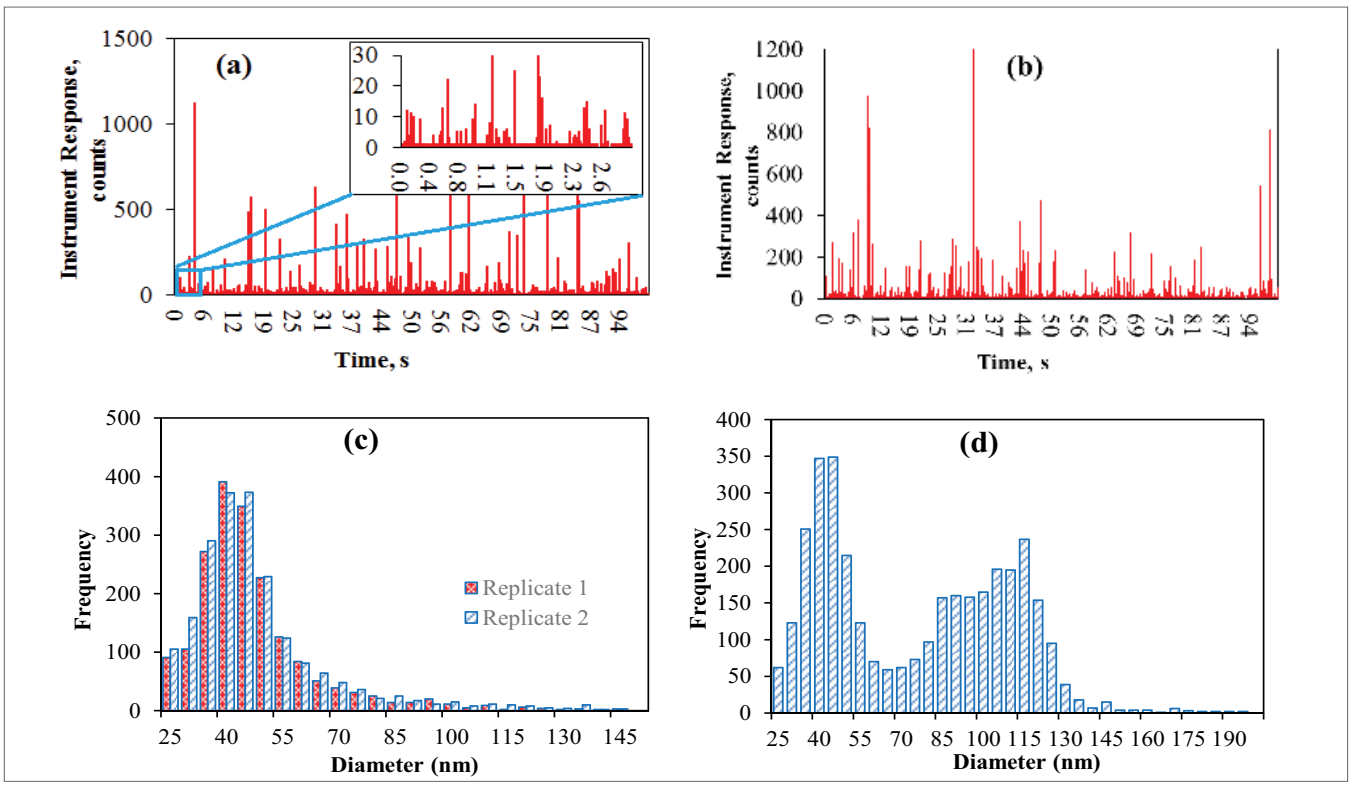

Figure 3. (a)&(b) Raw data of duplicated tomato plants exposed to 5 mg/L of 40 nm Au NPs for 4 days; (c) Size distributions histograms of duplicated tomato plants exposed to 5 mg/L of 40 nm Au NPs from Figure 4(a) and 4(b); (d) Size distribution histogram of spiking 4.7×10^4 particles/mL of 100 nm Au NPs into tomato plants exposed to 5 mg/L of 40 nm Au NPs.

Conclusions

This work has demonstrated uptake of Au NPs by tomato plants and the ability of SP-ICP-MS to detect and accurately size the particles. A digestion procedure was developed which breaks down the plant material, yet does not dissolve the Au NPs, allowing SP-ICP-MS to analyze the resulting solutions. The combination of the enzymatic digestion and SP-ICP-MS permits whole or subsections of plant shoots to be analyzed, allowing ENPs to be quickly and easily measured in plants.

References

1. Yongbo Dan, Weilan Zhang, Runmiao Xue, Xingmao Ma, Chady Stephan, Honglan Shi, 2015, "Characterization of Gold Nanoparticles Uptake by Tomato Plants Using Enzymatic Extraction Followed by Single Particle Inductively Coupled Plasma-Mass Spectrometry Analysis", *Environmental Science and Technology*, 49(5):3007-3014.

Consumables Used

Component	Part Number
Green/Orange Flared Peristaltic Pump Tubing (package of 12)	N0777042
Gold Nanoparticles in Water (30 nm)	N8142300
Gold Nanoparticles in Water (50 nm)	N8142302
Gold Nanoparticles in Water (80 nm)	N8142305
Gold Nanoparticles in Water (100 nm)	N8142307
Autosampler Tubes	B0193233 (15 mL) B0193234 (50 mL)

PerkinElmer, Inc.
940 Winter Street
Waltham, MA 02451 USA
P: (800) 762-4000 or
(+1) 203-925-4602
www.perkinelmer.com

PerkinElmer®

012175_01 PKI

APPLICATION NOTE

ICP - Mass Spectrometry

Authors:

Kenneth Neubauer

Chady Stephan

PerkinElmer, Inc.
Shelton, CT

Determination of Gold and Silver Nanoparticles in Blood Using Single Particle ICP-MS

Introduction

Rapid development of nanotechnologies and their potential applications in clinical research have raised concerns about the adverse effects of nanoparticles (NPs) on human health. The small size of nanoparticles implies enhanced reactivity due to their larger surface area per volume. While these properties may enhance the desired effects, they may also introduce new, unwanted toxic effects[1]. Two metal NPs, gold (Au) and silver (Ag), have been intensively studied – Au NPs, due to their desired intrinsic properties such as high chemical stability, well-controlled size and surface functionalization; while Ag NPs, due to their antibacterial effect, are often applied in wound disinfection, coatings of medical devices and prosthesis, and commercially in textiles, cosmetics and household goods[2]. As a result, concerns have been raised about the migration of Ag NPs from things like bandages or medical devices into open wounds, and thus the blood stream. These concerns emerge from recent publications showing that NPs can directly be taken up by the exposed organs and are able to translocate using the blood stream to secondary organs, such as the central nervous system, potentially affecting the growth characteristics of embryonic neural precursor cells[3].

Therefore, the need exists for researchers to detect and measure NPs in blood. This work explores the ability of single particle ICP-MS (SP-ICP-MS) to detect and measure gold and silver nanoparticles in blood.

PerkinElmer®
For the Better

Experimental

Samples and Sample Preparation

A blood Standard Reference Material (Seronorm™ Trace Elements in Whole Blood, Level I) was diluted 20 times with tetramethylammonium hydroxide (TMAH) + 0.1% Triton-X. Gold and silver nanoparticles (gold - 30 and/or 60 nm, NIST® 8012, 8013; silver - 40 and/or 60 nm, Ted Pella™ Inc.) were added to each blood sample at various concentrations. To break up any agglomerated particles, the stock solutions were sonicated for five minutes prior to spiking in the blood. The blood samples were manually shaken prior to analysis.

Instrumentation

All samples were run on a PerkinElmer NexION® 350D ICP-MS using the Nano Application Module in Syngisitx™ software. Instrumental conditions are shown in Table 1. Calibrations were carried out with both dissolved and particulate gold or silver. Table 2 shows the calibration standards used for each element.

Two rinses were used between samples: 1% HCl + 0.1% Triton-X was aspirated to dissolve/remove any residual gold particles, followed by deionized water to remove traces of the hydrochloric acid. A 1% HNO_3 + 0.1% Triton-X solution was used as a rinse solution for silver particles. This two-solution rinse approach was found essential as residual acid could dissolve particles in the sample. Each rinse solution was aspirated for one minute.

Table 1. NexION 350 ICP-MS Parameters.

Parameter	Value
Nebulizer	Glass concentric
Spray Chamber	Glass cyclonic
RF Power	1600 W
Nebulizer Gas Flow	Optimized for maximum Au signal
Dwell Time	100 µs
Quadrupole Settling Time	0 µs
Data Acquisition Rate	10,000 points/sec
Analysis Time	60 sec

Table 2. Calibration Standards for Au and Ag Nanoparticle Analysis.

Gold				
Particle Standard	Particle Size (nm)	Approx. Particle Concentration (Particles/mL)	Dissolved Standard	Concentration (µg/L)
1	10	100,000	1	1
2	30	100,000	2	1.5
3	60	100,000	3	5
Silver				
Particle Standard	Particle Size (nm)	Approx. Particle Concentration (Particles/mL)	Dissolved Standard	Concentration (µg/L)
1	40	100,000	1	1
2	60	100,000	2	5

Results

Initial tests were performed with gold nanoparticles. Figure 1 shows a blood sample spiked with a mixture of 30 and 60 nm Au NPs (approximately 100,000 particles/mL each). There are clearly two size distributions, indicating that both particle sizes are seen. This sample was analyzed three times consecutively, with the measured particle sizes shown in Table 3. These results demonstrate both accuracy and repeatability.

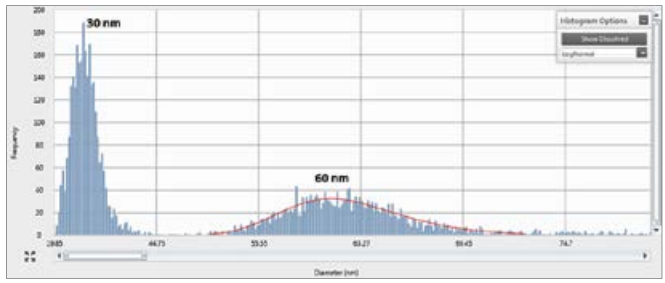

Figure 1. Size distribution of 30 and 60 nm Au nanoparticles (100,000 particles/mL each) in blood (20x dilution).

Table 3. Analysis of 30 and 60 nm Au Nanoparticle Mixture in Blood.

Replicate	Nominal Size (nm)	Most Frequent Size (nm)	Mean Size (nm)	Particle Concentration (Particles/mL)
1	30	30	31	108,710
	60	61	62	107,490
2	30	31	31	102,878
	60	61	62	101,294
3	30	31	32	102,017
	60	61	62	103,467

Next, 40 and 60 nm Ag NPs were added to blood sample so that the final, total particle concentration was about 200,000 particles per milliliter. Figure 2 shows the detected particle distribution, and Table 4 shows the results from three consecutive analyses. From Figure 2, it is evident that there are more 40 nm particles than 60 nm. Despite this difference, the measured size is accurate and reproducible for both size particles.

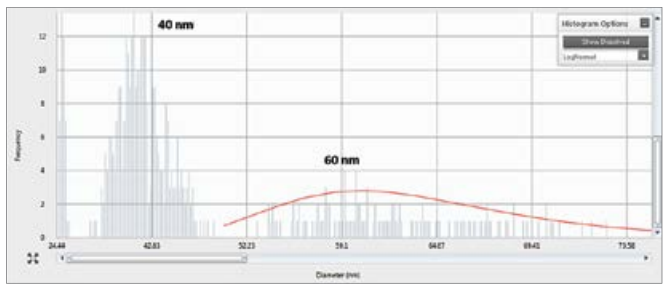

Figure 2. Size distribution of 40 and 60 nm Ag nanoparticles (100,000 particles/mL each) in blood (20x dilution).

Table 4. Analysis of 40 and 60 nm Ag Nanoparticle Mixture in Blood.

Replicate	Nominal Size (nm)	Most Frequent Size (nm)	Mean Size (nm)	Particle Concentration (Particles/mL)
1	40	41	42	100,024
	60	60	63	97,483
2	40	41	42	101,967
	60	61	63	98,957
3	40	41	42	102,263
	60	60	63	99,069

To see if lower particle concentrations could be detected in blood, only 40 nm Ag particles were spiked into the blood samples at a nominal concentration of 50,000 particles per milliliter, half the concentration of the previous analysis. Figure 3 shows that the particles are detected, while the data in Table 5 demonstrate that even at low concentrations, Ag NPs can be accurately and reproducibly measured in blood.

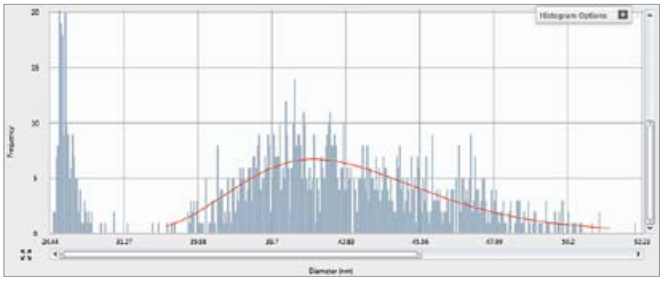

Figure 3. Size distribution of 40 nm Ag nanoparticles in blood, at a concentration of 50,000 particles/mL.

Table 5. Analysis of 40 nm Ag Nanoparticles in Blood at 50,0000 Particles/mL.

Replicate	Nominal Size (nm)	Most Frequent Size (nm)	Mean Size (nm)	Particle Concentration (Particles/mL)
1	40	42	43	50,242
2	40	42	43	50,775
3	40	42	43	50,486

Conclusion

This work demonstrates the ability of SP-ICP-MS to rapidly and accurately detect and measure gold and silver nanoparticles in whole blood, both at low concentrations and in mixtures. These measurements were accomplished with simple sample preparation (requiring only dilution) using PerkinElmer's NexION 350 ICP-MS and Syngistix Nano Application Module, offering continuous data acquisition and instant particle counting and sizing for research applications.

Reference

1. Chen X, Schluesener HJ (2008) Nanosilver: a nanoproduct in medical application. Toxicol Lett 176: 1–12.
2. Sintubin L, Verstraete W, Boon N (2012) Biologically produced nanosilver: Current state and future perspectives. Biotechnol Bioeng 109: 24222–22436.
3. Soderstjerna E, Johansson F, Klefbohm B, Johansson UE (2013) Gold- and Silver Nanoparticles Affect the Growth Characteristics of Human Embryonic Neural Precursor Cells. Plosone 8-3:58211.

Consumables Used

Component	PerkinElmer Part #
Green/orange peristaltic pump tubing	N0777042
Meinhard™ Type C0.5 glass nebulizer	N8145012
Baffled glass cyclonic spray chamber	N8145014
Quartz ball joint injector, 2.0 mm	WE023948
Quartz torch	N8122006
Nickel sampler cone	W1033612
Nickel skimmer cone	W1026356

For research use only. Not intended for diagnostic procedures.

PerkinElmer, Inc.
940 Winter Street
Waltham, MA 02451 USA
P: (800) 762-4000 or
(+1) 203-925-4602
www.perkinelmer.com

PerkinElmer®

011935_01 PKI

APPLICATION NOTE

ICP - Mass Spectrometry

Authors:

Ciprian-Mihai Cirtiu

Normand Fleury

National Public Health Institute of Quebec (INSPQ), Canada

Chady Stephan

PerkinElmer, Inc.
Shelton, CT

Assessing the Fate of Nanoparticles in Biological Fluids using SP-ICP-MS

Introduction

Nanotechnology is growing fast, with currently more than 1600 nanomaterials-based consumer products available on the market, as indicated by Nanotechnology Consumer Products Inventory.[1] Silver and gold are among the most used nanomaterials in consumer products and biomedical applications.[2, 3] Since humans can be exposed through various scenarios (consumer products, environment, workplace) and routes (respiratory, gastrointestinal tract, skin), there is an urgent need for analytical methods that can detect and quantify nanoparticles in biological fluids.

PerkinElmer®
For the Better

Single particle ICP-MS (SP-ICP-MS) is capable of quantitatively differentiating between ionic and particulate fractions, providing the user with several important measurements such as the ionic concentration (µg/mL), the particles' concentration (part/mL), size and size distribution in the same sample analysis. In addition, SP-ICP-MS can detect low concentrations of particles (as might be expected in biological fluids) and can perform rapid analyses (typically 1-2 minutes). With such capabilities, SP-ICP-MS is becoming "The" technique of choice for researchers studying the fate/transformation of nanoparticles in various sample matrices.[4, 5]

The present work explores the ability of SP-ICP-MS to assess the fate of nanoparticles (NPs) in biological fluids, building on the initial work which demonstrated the ability of SP-ICP-MS to detect gold and silver nanoparticles in blood.[6] The transformation (fate) of silver and gold nanoparticles in blood and urine was tracked over 76 hours by following the change in size, the ionic concentration, as well as the aggregation/agglomeration of the nanoparticles.

Experimental

Instrumentation

All samples were analyzed with a PerkinElmer NexION® 300S/350S ICP-MS. The Nano Application Module from Syngisitx™ software was used for data acquisition and automated data treatment. Instrumental conditions used for all measurements are shown in Table 1. Operating conditions were optimized in order to get the maximum Ag^+ and Au^+ intensities. A rinse solution (1% HNO_3 + 1% HCl + 0.1% Triton-X) was aspirated for 1 minute between each sample in order to wash and remove any residual nanoparticles. This rinse solution was followed by deionized water to remove the acid.

Table 1. NexION 300S/350S ICP-MS Parameters.

Parameter	Value
Sample uptake rate	0.44 mL/min
Nebulizer	Quartz concentric
Spray chamber	Quartz cyclonic
RF power	1600 W
Nebulizer gas flow	Optimized for maximum Ag and Au signal
Dwell time	50 µs
Analysis time	60 sec

Materials and Sample Preparation

Blood samples were prepared by diluting 20 times a certain volume of human blood from a non-exposed person with an aqueous solution of 0.5% ammonium hydroxide + 0.1% octylphenol ethoxylate (Triton-X). Urine samples were prepared by diluting 20 times a certain volume of human urine from a non-exposed person with an aqueous solution of 0.5% HNO_3.

Diluted blood and urine were then spiked with a 5-minute sonicated stock solution of Ag or Au NPs (Ag - 40 and 80 nm from Ted Pella Inc., Redding, California, USA; Au - 30 and 60 nm, NIST™ 8012, 8013 from National Institute for Standards and Technology, Gaithersburg, Maryland, USA) to reach a concentration of 250,000 particles/mL. A control sample (blank) was prepared with 40 nm Ag and 30 nm Au NPs following the same procedure, but no matrix (urine or blood) was added. The dilution solutions (ammonium hydroxide for blood and nitric acid for urine) were chosen based on their regular use in research analysis of metals and metalloids in blood and urine respectively. The samples were manually shaken prior to analysis.

Calibration curves for dissolved species (from 0 to 5 ppb) were prepared using a 1000 ppm Au standard solution (VHG Labs, Manchester, New Hampshire, USA) and a 10,000 ppm Ag standard solution (SCP Science, Baie D'Urfé, Quebec, Canada), respectively. Calibration curves for particles were built with 40 and 60 nm Ag NPs and 30 and 60 nm Au NPs respectively, at 250,000 particles/mL.

Results and Discussion

The fate of Ag and Au NPs was studied in blood and urine by following the change in size of the NPs, as well as the concentration of the ionic species which could be generated by partial or complete dissolution of NPs. The NP concentration in each sample was followed over time in order to attempt a correlation with the change in size and increase in concentration of the ionic species. In order to check if a change in size and concentration of NPs is caused by the biological matrix (urine or blood) or by the dilution solution, blank samples were prepared for 40 nm Ag NPs (40 nm Ag blank) and 30 nm Au NPs (30 nm Au blank) following the same procedure as for the other samples but without adding the biological matrix (urine or blood).

As shown in Figure 1, a decrease in NP size is noticed for both 40 and 80 nm Ag NPs in diluted blood after 76 hours. A similar trend is observed for the blank sample with a slightly more pronounced decrease when comparing with samples. This suggests that the decrease in size of the primary distribution is due mainly to the dilution solution and not to the matrix (blood). It seems that blood has a light-protecting role in preventing dissolution of Ag NPs. A very slight increase of the ionic Ag concentration (Ag^+) was found for the blank. From these observations and considering the complex medium in which the NPs are being diluted (blood), it could be hypothesized that smaller-size NPs can undergo, to some extent, dissolution and that ions thus generated can reform smaller-size NPs. Other phenomena can occur, like sedimentation and deposition of NPs in the tubes, giving rise to a non-homogeneous solution, especially in the blank sample where the lack of blood leads to a less stable solution.

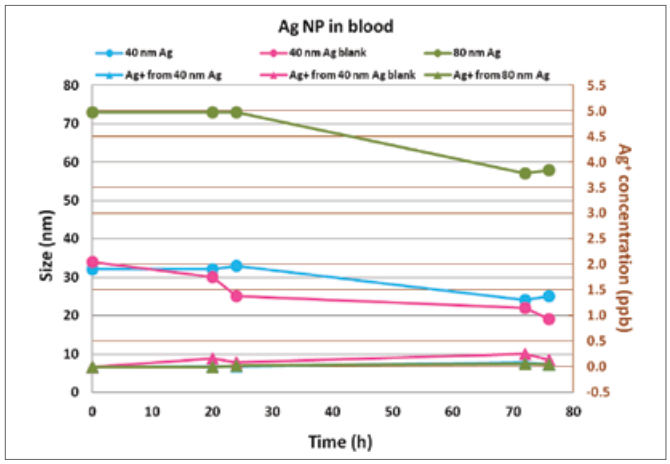

Figure 1. Size change for Ag NPs (40 and 80 nm) and Ag^+ concentration over time in blood. Ag^+ from 40 nm Ag appears under Ag^+ from 80 nm Ag.

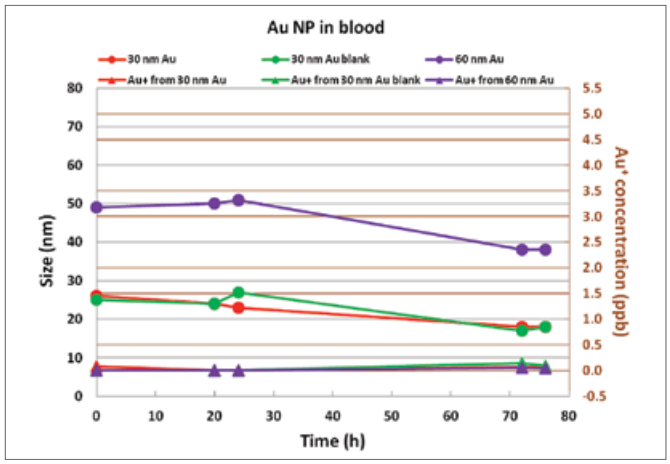

Figure 3. Size change for Au NPs (30 and 60 nm) and Au^+ concentration over time in blood. Au^+ from 30 nm Au and Au^+ from 30 nm Au blank appear under Au^+ from 60 nm Au.

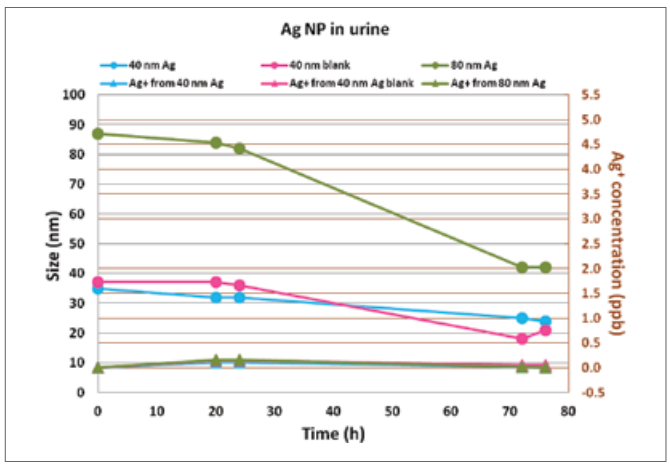

Figure 2. Size change for Ag NPs (40 and 80 nm) and Ag^+ concentration over time in urine. Ag^+ from 40 nm Ag and Ag^+ from 40 nm Ag blank appear under Ag^+ from 80 nm Ag.

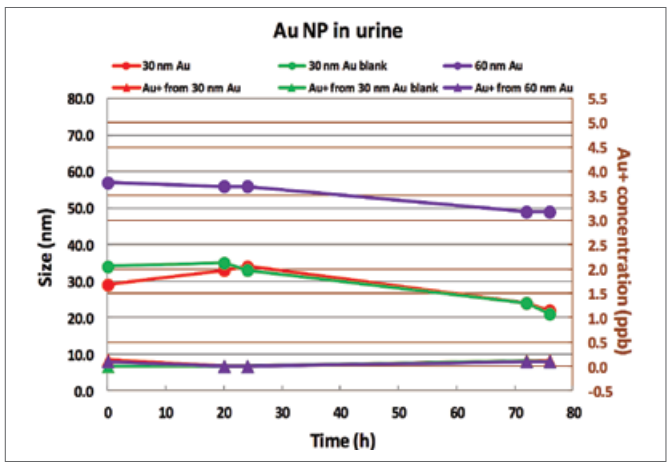

Figure 4. Size change for Au NPs (30 and 60 nm) and Au^+ concentration over time in urine. Au^+ from 30 nm Au and Au^+ from 30 nm Au blank appear under Au^+ from 60 nm Au.

A more pronounced decrease in size was observed for Ag NPs in urine (Figure 2), especially for 80 nm Ag NPs. The blank sample seems to be slightly more affected than the other samples. This can be expected as the acidic solution used to dilute urine (diluted nitric acid) has the potential to dissolve metals. However, the increase in Ag^+ due to dissolution of NPs is negligible.

A linear fit for the curves that show the decrease in NP size over time (Figures 1 and 2) allows us to estimate the dissolution rate of the NPs in a certain matrix. When comparing the slopes of the curves for the same NP, e.g. 80 nm Ag NPs in blood (Figure 1, slope: -0.2414, $R^2 = 0.92$) and urine (Figure 2, slope: -0.6743, $R^2 = 0.96$), it is clear that the dissolution rate is different in both matrices. A three-times-higher dissolution rate is obtained in urine than in blood.

Similar trends were found for Au NPs in blood and urine (Figures 3 and 4). The decrease in NP size is due mainly to the dilution solution, as confirmed by the blank sample in both cases. The increase in Au^+ due to dissolution of NPs is negligible.

Again, when comparing the slopes of the curves for the same NP, e.g. 60 nm Au NPs in blood (Figure 3, slope: -0.182, $R^2 = 0.86$) and urine (Figure 4, slope: -0.118, $R^2 = 0.97$), it can be seen that the dissolution rate is different in both matrices. Actually, the dissolution rate for 60 nm Au NPs is 1.5 times faster in blood than in urine.

Conclusion

The fate/transformation of nanoparticles in biological fluids is of crucial importance to help researchers understand their behavior in the body. The present study demonstrates the capability of SP-ICP-MS to assess the fate of Ag and Au NPs in blood and urine, two important biological fluids from a toxicological point of view. The change in size and the ionic concentration were tracked over 76 hours. A certain decrease in size was noticed for all NPs in blood and urine with a more or less significant increase in the ionic concentration. No significant aggregation/agglomeration was observed. From the results obtained with the blank samples, it is clear that decrease in size occurs because of the dilution solution employed to dilute blood and urine, probably by dissolution. The analysis of blood or urine samples should be done right after dilution to avoid any transformation of NPs.

References

1. http://www.nanotechproject.org/cpi/
2. M. Ahamed, M.S. AlSalhi, M.K. Siddiqui, Silver nanoparticle applications and human health, Clin. Chim. Acta 2010, 411, 1841-1848.
3. L. Dykman, N. Khlebtsov, Gold nanoparticles in biomedical applications: recent advances and perspectives, Chem. Soc. Rev. 2012, 41, 2256-2282.
4. Mitrano, D. M.; Ranville, J.; Bednar, A.; Kazor, K.; Hering, A. S.; Higgins, C., Tracking dissolution of silver nanoparticles at environmentally relevant concentrations in laboratory, natural and processed waters using single particle ICP-MS (spICP-MS) Environmental Science: Nano 2014.
5. Mitrano, D. M.; Ranville, J; Stephan, C., Quantitative Evaluation of Nanoparticle Dissolution Kinetics using Single Particle ICP-MS: A Case Study with Silver Nanoparticles www.perkinelmer.com.
6. Neubaeur, K., Stephan, C., Determination of Gold and Silver Nanoparticles in Blood Using Single Particle ICP-MS www.perkinelmer.com.

For research use only. Not for use in diagnostic procedures.

PerkinElmer, Inc.
940 Winter Street
Waltham, MA 02451 USA
P: (800) 762-4000 or
(+1) 203-925-4602
www.perkinelmer.com

PerkinElmer®

012008_01 PKI

APPLICATION NOTE

ICP - Mass Spectrometry

Authors:

Evan Gray

Christopher P. Higgins

Department of Civil and Environmental Engineering

James F. Ranville

Department of Chemistry and Geochemistry

Colorado School of Mines, Golden, CO USA

Analysis of Nanoparticles in Biological Tissues using SP-ICP-MS

Introduction

The use of engineered nanoparticles (ENPs) in consumer products is well documented and has raised concern of the eventual fate and potential toxicity of these materials at the end of their consumer-product life[1,2]. It is likely that these materials will eventually find their way into environmental systems through food packaging and manufacturing, food products or waste disposal[3]. The analysis of ENPs is focused on three metrics: particle size, particle number, and particle mass distributions. Each of these metrics is very important for assessing environmental effects, and ultimately the risk associated with the use of these materials in consumer products. While established methods exist for the determination of mass distributions of metals in tissue samples, few robust methods have been developed to detect and characterize nanomaterials, especially particle number and size distributions[4].

PerkinElmer®
For the Better

The recent development of the analytical technique single particle inductively coupled plasma mass spectrometry (SP-ICP-MS) has provided an analytical means to directly quantify particle size, mass and number distributions at environmentally relevant concentrations (ng/L). This is the first analytical technique capable of determining all three nano-specific metrics from a single sample. The utility of this technique has been proven in numerous sample matrices including wastewater, EPA moderately hard water and tissue samples, with the aid of tissue digestion[5–8].

The use of SP-ICP-MS to detect ENPs in aqueous samples is straightforward, with sample preparation only consisting of dilution prior to analysis. However, the analysis of ENPs in tissues is more difficult and requires a digestion step prior to analysis. Traditional digestion procedures focus on using strong acids to liberate the desired elements from tissues. However, this type of digestion is incompatible with ENP analysis, as ENPs present would likely dissolve.

Instead, a different approach is to use strong bases or enzymes to digest tissues, ideally liberating ENPs without altering them. The medical community initially developed these non-traditional extractions for analysis of artificial joint wear particles[9,10]. These extractions have been applied in an attempt to extract and analyze ENPs. One approach used for ENP extraction is chemical digestion using the strong base tetramethylammonium hydroxide (TMAH)[5–8]. TMAH extraction has proven to yield high recoveries of both particle number and total mass, as compared to tissue digestion using sonication and water, and is a promising technique for analyzing ENPs in biological samples[5]. This work will describe the process of tissue extraction coupled with SP-ICP-MS analysis using the PerkinElmer NexION® 350Q ICP-MS.

Experimental

Materials

Citrate-coated Ag ENPs (60 and 70 nm) used in this work were purchased from NanoComposix (San Diego, CA). Ground beef was purchased from a local supermarket (Golden, CO) and used as a model mammalian tissue. *Lumbriculus variegatus (L. variegatus, a* species of aquatic worm) were purchased from aquatic foods (Fresno, CA) and were used as an environmentally and toxicologically relevant tissue.

All extracts containing ENPs were diluted in NanoPure™ (NP) water immediately prior to SP-ICP-MS analysis (water or digested tissues).

Instrumentation

Analysis using SP-ICP-MS was conducted following the method described by Pace et al. 2011[11] using the size based efficiency approach. All samples were analyzed using a NexION 350Q ICP-MS (PerkinElmer, Shelton, CT). ICP-MS operating conditions are shown in Table 1. Silver was measured at AMU 107. All data was measured in triplicate, though raw data shown is for one run, while the size distribution is a composite of all three runs.

Sample Preparation

Tissue digestion was conducted using the method described by Gray et al. 2013[5]. Briefly, the organic base (TMAH) was used to digest tissues and liberate ENPs from tissues at a solvent to tissue ratio of 20:1. The TMAH digestion solution was 20 %TMAH w/w. This concentration was selected based on spike recovery optimization tests using model mammalian tissue. Sample digestions were performed over 24 hours at room temperature, the first hour of which all samples were sonicated. Digested tissues were diluted to 1 %TMAH prior to analysis. This TMAH concentration was maintained if further dilution was required.

Table 1. Operating conditions for SP-ICP-MS analysis.

Parameter	Values
SP-ICP-MS Instrument	PerkinElmer NexION 350Q ICP-MS
Plasma Power	1600 W
Nebulizer, Spray Chamber, and Flow	Meinhard, Cyclonic, 1 mL/min
Efficiency Calibration	Particle Size Method
Masses Monitored	^{107}Ag, ^{197}Au
Dwell Time per AMU	50 µs
Readings per Sample	60 sec

Bioaccumulation experiments (70 nm Ag ENPs) were conducted using *L. variegatus.* The exposure period was 24 hours in EPA moderately hard water at a concentration of 5 mg/L. Silica sand was used in each beaker to provide adequate substrate for the worms to live in. The test was conducted in an incubator which was maintained at 20 °C with a 16:8 light/dark photoperiod. At the conclusion of the exposure, all worms were depurated for 24 hours prior to analysis to allow gut-associated ENPs to be cleared.

Results and Discussion

Tissue Spike Recovery

Spike digestion experiments showed that TMAH succesfully decomposed all of the model mamalian tissue prior to analysis. Figure 1 shows the resulting raw data for an Ag ENP standard run in water (A) compared to the same Ag particle spiked and extracted from tissue (B). These two figures clearly show similarites between the number of particles observed, their average intensity, and the background count mean (representing dissolved Ag). The similarity observed between detected pulses is as expected, as each sample was spiked with an identical mass concentration (and particle number concentration) of the same ENP. Further, TMAH digestion does not adversely affect particle stability through aggregation and particle settling (loss of pulses). Finally, the silver background signal did not increase between the water-based standard and the extracted tissues. This indicates that the extraction procedure did not cause any ENP dissolution as compared to the standard in water. It is possible that similar dissolution could have occurred in both the standard and TMAH digestion. However, this has not been observed for particle standards in water[12].

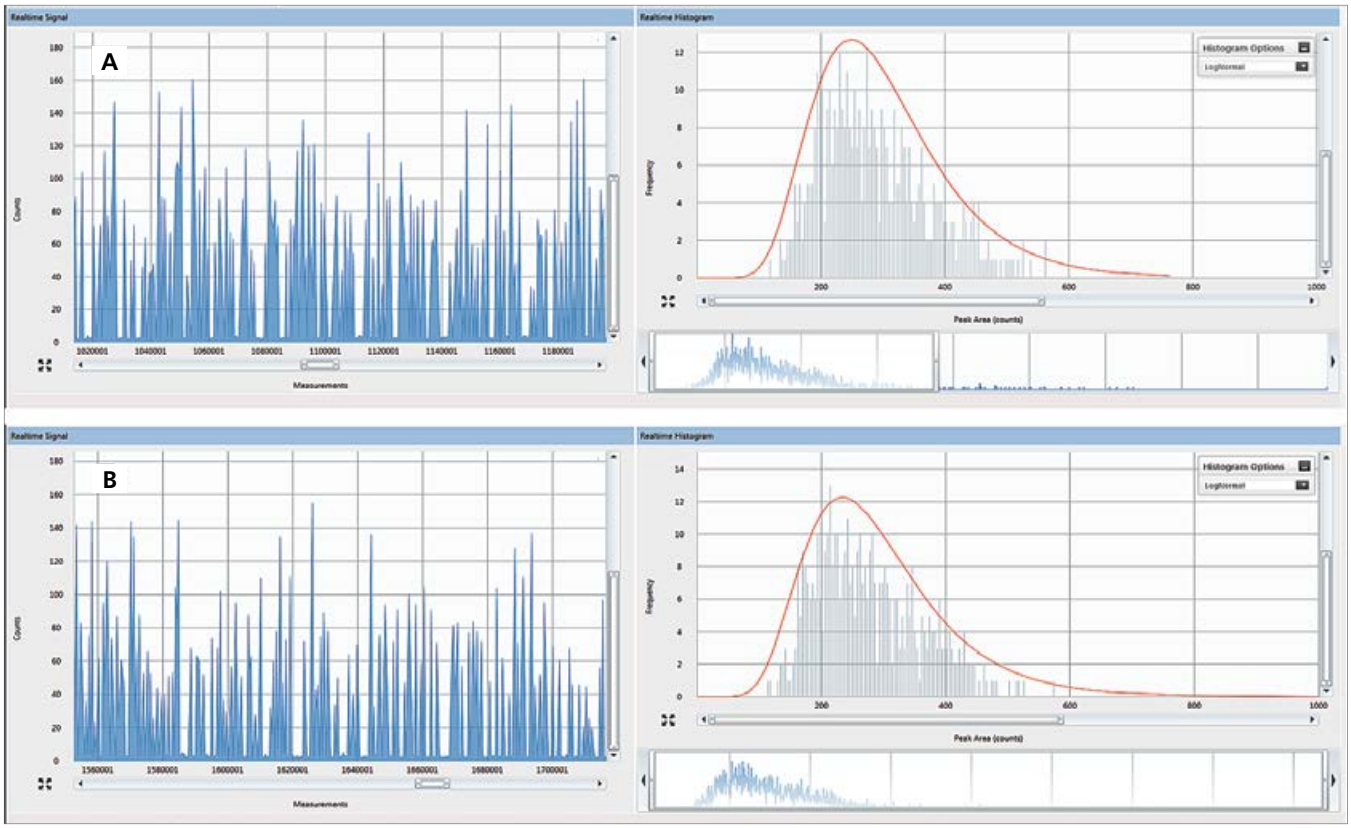

Figure 1. Raw counts for 60 nm Ag ENPs spiked into (A) nanopure water and (B) ground beef at an aqueous concentration of 19 µg/L and a tissue concentration of 19 µg/kg w/w tissue.

Biological Uptake

L. variegatus was readily digested using the TMAH procedure, allowing for SP-ICP-MS analysis of tissues. Ag ENPs were detected in *L. variegatus* after 24 hours of depuration, proving that this technique can be applied to liberate and analyze bioaccumulated ENPs. The pulses observed in Figure 2A, can clearly be observed above a very low Ag^+ background. The observed pulses in Figure 2A were converted to a size distribution (Figure 2B), showing a peak mode of 55 nm. The observed size distribution was slightly smaller than the manufacturer-reported diameter. However, this size distribution is closer to what was observed using TEM analysis (data not shown). The observed tissue concentration was 7.1 µg/kg with essentially all of the Ag present as ENPs.

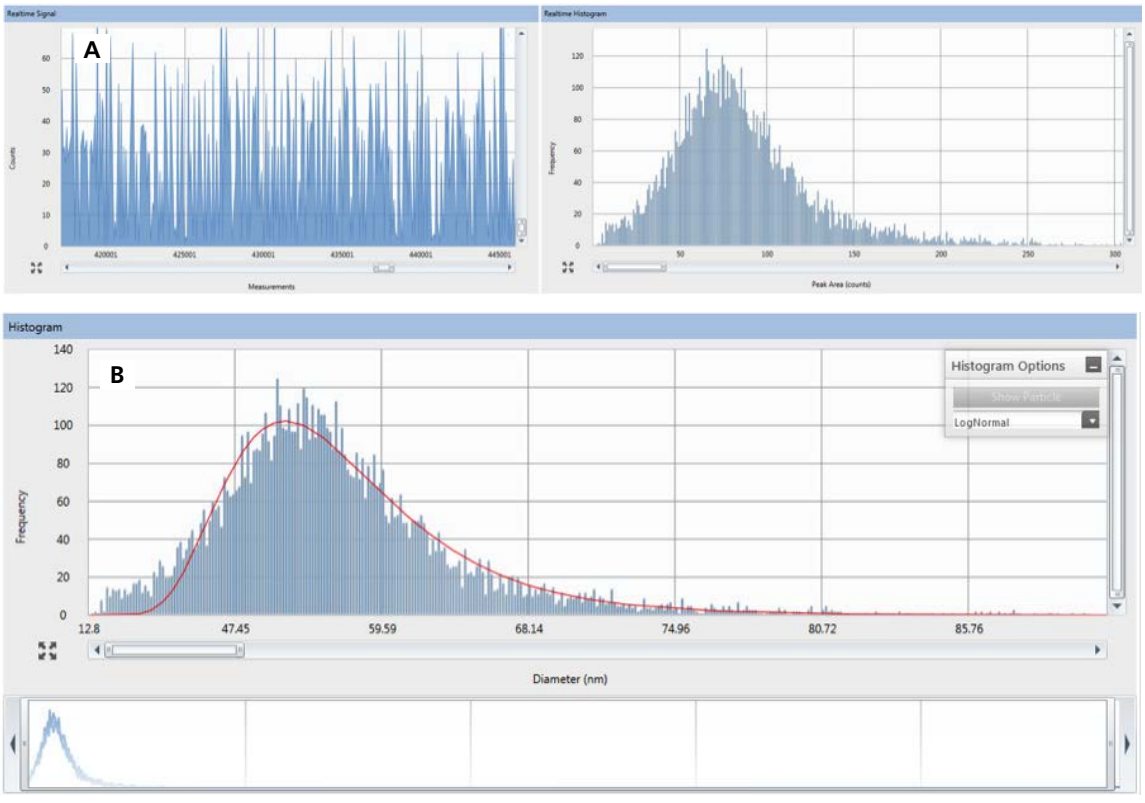

Figure 2. Raw counts (A) and size distribution (B) for ENPs that were acummulated by the aquatic worm, *L. variegatus*. Organism exposure was conducted at 5 µg/L as ENP of 70 nm Ag.

Conclusion

This work has shown that ENPs can be extracted from biological tissues and analyzed using SP-ICP-MS. Further, this approach is valid for ENPs bioaccumulated in tissues at low concentrations due to the senstivity of ICP-MS. The extraction procedure did not visibly change the background for a 60 nm Ag ENP extracted from water compared to ENPs extracted with TMAH from model mamalian tissue. ENPs were also sucessfully extracted from *L. variegatus* exposed to 5 µg/L Ag ENPs in water. These experiments prove that TMAH extraction coupled to SP-ICP-MS can be used to successfully liberate ENPs from tissues. ENP count distributions can ultimately be converted to size distributions, allowing for size, number, and mass distributions to be determined using this analysis technique. The applicability of this digestion technique beyond these tissue matrices is unknown and should be investigated for any new tissue sample.

References

1. Klaine, S. J.; Alvarez, P. J. J.; Batley, G. E.; Fernandes, T. F.; Handy, R. D.; Lyon, D. Y.; Mahendra, S.; McLaughlin, M. J.; Lead, J. R. Nanomaterials in the environment: Behavior, fate, bioavailability, and effects. *Environ. Toxicol. Chem.* 2008, 27, 1825–1851.
2. Nowack, B.; Bucheli, T. D. Occurrence, behavior and effects of nanoparticles in the environment. *Environ. Pollut.* 2007, 150, 5–22.
3. Bednar, A. J.; Poda, A. R.; Mitrano, D. M.; Kennedy, A. J.; Gray, E. P.; Ranville, J. F.; Hayes, C. A.; Crocker, F. H.; Steevens, J. A. Comparison of on-line detectors for field flow fractionation analysis of nanomaterials. *Talanta*. 2013, 104, 140–148, DOI: 10.1016/j.talanta. 2012.11.008.
4. Handy, R. D.; Cornelis, G.; Fernandes, T.; Tsyusko, O.; Decho, A.; Sabo-Attwood, T.; Metcalfe, C.; Steevens, J. A.; Klaine, S. J.; Koelmans, A. A.; et al. Ecotoxicity test methods for engineered nanomaterials: Practical experiences and recommendations from the bench. *Environ. Toxicol. Chem.* 2012, 31, 15–31.
5. Gray, E. P.; Coleman, J. G.; Bednar, A. J.; Kennedy, A. J.; Ranville, J. F.; Higgins, C. P. Extraction and Analysis of Silver and Gold Nanoparticles from Biological Tissues Using Single Particle Inductively Coupled Plasma Mass Spectrometry. *Environ. Sci. Technol.* 2013, 47, 14315–14323.
6. Loeschner, K.; Brabrand, M.; Sloth, J.; Larsen, E. Use of alkaline or enzymatic sample pretreatment prior to characterization of gold nanoparticles in animal tissue by single-particle ICPMS. *Anal. Bioanal. Chem.* 2013, 1–7.
7. Loeschner, K.; Navratilova, J.; Kobler, C.; Molhave, K.; Wagner, S.; Kammer, F.; Larsen, E. Detection and characterization of silver nanoparticles in chicken meat by asymmetric flow field flow fractionation with detection by conventional or single particle ICP-MS. *Anal. Bioanal. Chem.* 2013, 1–11.
8. Schmidt, B.; Loeschner, K.; Hadrup, N.; Mortensen, A.; Sloth, J. J.; Koch, C. B.; Larsen, E. H. Quantitative Characterization of Gold Nanoparticles by Field-Flow Fractionation Coupled Online with Light Scattering Detection and Inductively Coupled Plasma Mass Spectrometry. *Anal. Chem.* 2011, 83, 2461–2468.
9. Campbell, P.; Ma, S.; Schmalzried, T.; Amstutz, H. C. Tissue Digestion For Wear Debris Particle Isolation. J. *Biomed. Mater. Res.* 1994, 28, 523–526.
10. Baxter, R. M.; Steinbeck, M. J.; Tipper, J. L.; Parvizi, J.; Marcolongo, M.; Kurtz, S. M. Comparison of Periprosthetic Tissue Digestion Methods for Ultra-High Molecular Weight Polyethylene Wear Debris Extraction. *J. Biomed. Mater. Res. Part B-Appl. Biomater.* 2009, 91B, 409–418.
11. Pace, H. E.; Rogers, N. J.; Jarolimek, C.; Coleman, V. A.; Higgins, C. P.; Ranville, J. F. Determining Transport Efficiency for the Purpose of Counting and Sizing Nanoparticles via Single Particle Inductively Coupled Plasma Mass Spectrometry. *Anal. Chem.* 2011, 83, 9361–9369.
12. Mitrano, D. M.; Ranville, J. F.; Bednar, A.; Kazor, K.; Heringd, A. S.; and Higgins, C. P. Tracking dissolution of silver nanoparticles at environmentally relevant concentrations in laboratory, natural, and processed waters using single particle ICP-MS (spICP-MS). *Environ. Sci.: Nano,* 2014, 1, 248-259.

PerkinElmer, Inc.
940 Winter Street
Waltham, MA 02451 USA
P: (800) 762-4000 or
(+1) 203-925-4602
www.perkinelmer.com

PerkinElmer®

011803_01

PerkinElmer, Inc.
940 Winter Street
Waltham, MA 02451 USA
P: (800) 762-4000 or
(+1) 203-925-4602
www.perkinelmer.com

For a complete listing of our global offices, visit www.perkinelmer.com/ContactUs

012982_01 PKI